Finite Element Analysis for Fixture Stiffness

by

Yi Zheng

A Ph.D. Dissertation

Submitted to the faculty

of the

WORCESTER POLYTECHNIC INSTITUTE

in partial fulfillment of the requirements for the

Degree of Doctor of Philiosophy

in

Manufacturing Engineering

By

_____

April 2005

APPROVED:

_____

Yiming(Kevin) Rong, Advisor, Professor of Mechanical Engineering

_____

Zhikun Hou, Co-advisor, Professor of Mechanical Engineering

_____

Yiming(Kevin) Rong, Professor of Mechanical Engineering, Associate Director of Manufacturing and Materials Engineering Program

ABSTRACT

With growing demands on improved product quality and shorter time to market, there is need for rigorous but practical tools to support the fixture design and analysis process. Computer-aided fixture design (CAFD), with predictable fixture stiffness, becomes a means to provide an appropriate solution in fixture design. The effectiveness of previous CAFD systems is not fully satisfactory partially because analysis of fixture stiffness has not kept pace with the development of CAFD. The dissertation research provides a model of fixture unit stiffness analysis and an experimental method of identifying contact stiffness parameters. The model and the method offer the potential for a more realistic analysis of fixture stiffness properties of a fixture–workpiece system, based on a fixture unit description.

An FEA model of fixture unit stiffness is developed with contact elements for solving contact problems encountered in the study of fixture unit stiffness. The penalty function method is used to model the contact conditions in the energy equation of the general FEA and to describe the nonlinearity of connection shown in previous experiments. The contact and friction conditions are represented mathematically in the FEA model. The FEA model and the analysis procedure are validated by numerical simulation.

An experimental study on contact parameters is carried out to identify contact stiffness, including normal contact stiffness and tangential contact stiffness, by both static and dynamic approaches. For normal contact stiffness, a static identification procedure is developed to estimate the contact parameters, using experimental data. Four factors - testing environment, contact area, surface finish of the specimen, and normal loads, - are

examined to see how they affect the behavior of the contact interface. A dynamic method is also used to identify normal contact stiffness. A scheme of eigenvalue analysis is developed to test the contact structure to estimate contact stiffness. The dynamic test results are compared with the results of static test under the same experimental condition and a reliable correspondence is presented. Similar to methods devised to identify normal contact stiffness, a frequency–domain identification system is developed to estimate tangential contact stiffness, using FEA and experimental data. A simulation study on vibration data from tangential contact model is presented in this study. The experimental study is carried out and tangential contact stiffness is estimated based on numerical simulation and experimental data.

This research establishes the finite element model of fixture unit stiffness and develops the experimental approaches to identify contact stiffness. Based on this study, the database of fixture stiffness can be built up, and further used in CAFD.

ACKNOWLEDGEMENTS

I would like to take this opportunity to acknowledge people who have tremendously helped me during my dissertation and my study at Worcester Polytechnic Institute.

I would like to express my deepest gratitude to Professor Yiming Rong, my advisor for helping, guiding and encouraging me to finish this dissertation. Without his numerous suggestions, inspiring ideas, patience, and support, this work would have never been completed.

I also would like to express my sincere gratitude to Professor Zhikun Hou, my co-advisor, for his constant inspiration and valuable guidance. His numerous suggestions and immense knowledge have made my dissertation possible.

I also thank Professor Richard Sisson, Professor Mustapha S. Fofana, and Professor Paramasivam Jayachandran for their enthusiastic service on the dissertation committee.

I would like to thank Professor John R. Hall, Mr. Jim Johnston and Mr. Steve Derosier for the use of their equipment, their expertise and many discussions that greatly inspired this work. I appreciate the great help offered by all members in CAM Lab at WPI.

I would like to express my great gratitude to my parents, my sister, her husband, and her lovely son for their endless love and encouragement throughout my studies at WPI.

Special thanks should be given to my husband, Zhonghai Zuo, for his profound love, patience, understanding, and unconditional support throughout the development of this dissertation. I would not have been able to complete this work without his support.

Finally I would like to dedicate my accomplishment to my parents. “With them, all things are possible.”

TABLE OF CONTENTS

LIST OF FIGURES

LIST OF TABLES

Chapter 1 Introduction

This chapter gives an introduction of the research - motivation, objectives and goal, and overall tasks of finite element analysis of fixture stiffness. The organization of the dissertation is also listed at the end of this chapter.

1.1 Motivation

Manufacturing involves tooling-intensive operations, and fixtures are an important aspect of tooling that contributes significantly to the quality, cost, and the cycle time of production. In machining processes, fixtures are used to accurately position and constrain workpieces relative to the cutting tool. Fixturing accuracy and reliability is crucial to the success of machining operations. Poor fixture design is one of the major factors that contribute to dimensioning errors of rejected workpieces, and product quality is often sacrificed when the functional capability of a fixture is not predictable. The time and cost spent on designing and fabricating fixtures is crucial for improving the production cycle of current products and new products (Thompson, 1986).

Fixtures were developed for job, batch, and mass productions; they are widely used in manufacturing operations to locate and hold a part firmly in position so that the required manufacturing processes can be carried out according to design specifications (Hoffman, 1991). In machining processes, the stationary components of the fixture, such as locating pads, buttons, and pins, come into immediate contact with the workpiece when it is loaded. Subsequent clamping (by movable elements) creates preloaded joints between the workpiece and each fixture component. There may also be supporting components and a

fixture base in a fixture. The primary requirements for a fixture are to locate and secure the workpiece in a given position and orientation on a worktable of the machine tool. Many other demands also need to be met, such as ensuring productivity (e.g., ease of loading and unloading the workpiece, use of automated or semi-automated clamping devices, and chip disposal), reducing the deformation of weak-rigidity parts, providing for simple and safe operation (e.g., the use of antimistake components for costly parts), effectively reducing costs (e.g., prioritizing considerations of fixture materials, fabrication processes, and use of standard elements) (Rong, 1999).

The fixture design activity presents many challenges, since it involves a multitude of conflicting criteria and competing objectives; it also requires a great deal of expertise and knowledge, both of which are not easy to model and implement. For example, the automobile industry needs fixtures to hold automobile motor parts in place during machining operation. Because a single setup for multiple operations (even rough and finish machining) is required with a single machining center, the fixture design must consider accuracy and space availability, so that placing fixture components avoids interference and supplies adequate stiffness. The fixtures must fit in a limited space. In addition, they must allow access from all sides of the part being machined. Fixtures also need to achieve a sufficient level of stiffness. In fixture design, a thoughtful, economic fixture-workpiece system maintains uniform maximum joint stiffness throughout machining while also providing the fewest fixture components, most accessible workpiece cutting, and the shortest setup and unloading cycles. Both static and dynamic stiffness in this fixture-workpiece system rely upon the number, layout, and static stiffness of the fixture structure. These affect on fixture performance must be addressed

through appropriate design solutions that integrate the fixture with other process elements to produce a highly rigid system.

Although fixtures can be designed and developed by using Computer-Aided Design (CAD) functions, a lack of scientific tools and systematic approaches for evaluating the design performance makes fixture designs significantly rely on trial-and-error, and results in several problems such as (Rong, 2003):

(1) These may be overdesign in functions, which is very common and sometimes depredates the performance (e.g., unnecessary heavy weight);
(2) The quality of design cannot be ensured in production planning;
(3) The long cycle time of fixture design, fabrication, and testing may take weeks, if not months;
(4) These may also be lack of technical evaluation of fixture design in the production planning stage.

Computer-Aided Fixture Design (CAFD) has become a means of providing solutions to improve production operation. There are three major stages in the CAFD process. (1) Fixture planning, to determine the locating datum surfaces and locating/clamping positions on the workpiece surfaces for totally constrained locating and reliable clamping. (2) Fixture configuration design, to generate a design of the fixture structure as an assembly, according to different production requirements such as production volume and machining conditions. (3) Fixture design verification, to evaluate fixture design performance in satisfying the production requirements such as completeness of locating, tolerance stack-up, accessibility, fixturing stability, and the ease of operation. The development of CAFD tools enhances both the flexibility and performance of the

workholding systems by providing a more systematic and analytic approach to fixture design. Therefore, many advanced techniques and approaches -- group technology (GT) (Grippo, 1987, Rong, 1992); geometric reasoning (Ma, 1998; An, 2000); knowledge-based reasoning (Markus, 1988; Nee, 1991; Nnaji, 1990; Pham, 1990); and case-based reasoning (Kumar, 1995; Sun, 1995) -- have been adopted in the research of CAFD to reduce the cycle time of fixture design and to optimize fixture design.

Although a tremendous effort has been made in developing CAFD systems in the last fifteen years, this has led to limited successes. The effectiveness of these CAFD systems is not fully satisfactory because analysis of the fixture stiffness has not kept pace with the development of CAFD. All the three stages of the CAFD system involve workpiece locating principles, kinematic and force analysis, and fixture stiffness analysis to determine the workpiece location layout and to evaluate the clamping forces required against the cutting forces. Fixture stiffness has the most significant impact on the product quality during fixturing and machining of workpieces. However, several questions in fixture stiffness analysis remain unanswered and many issues must still be resolved.

In order to study fixture stiffness in a general manner, a fixture structure is decomposed into functional units with fixture components and functional surfaces (Rong, 1999). Typical fixture function units are shown in Figure 1.1 (An, 2000). Figure 1.2 shows a sketch of the fixture units in a fixture design.

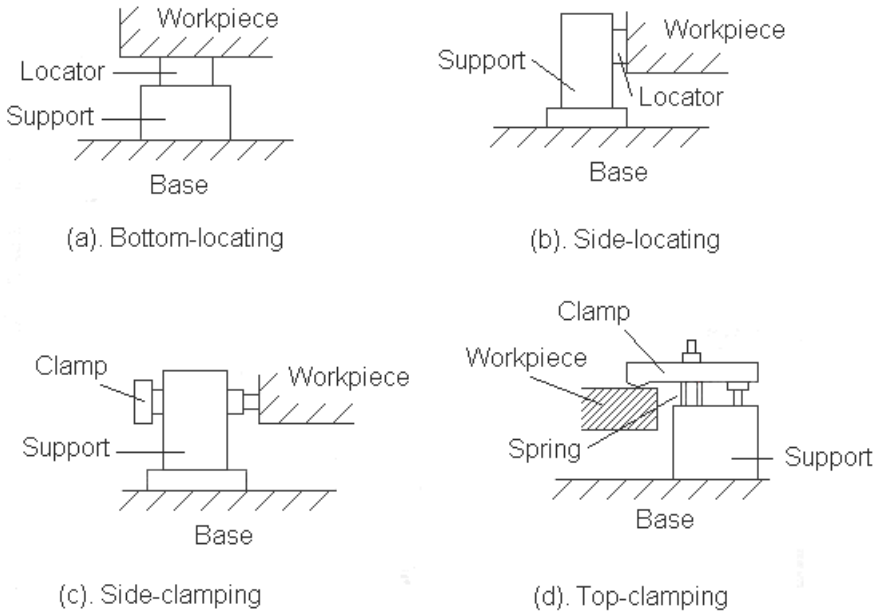

Figure 1.1 Typical Functional Units

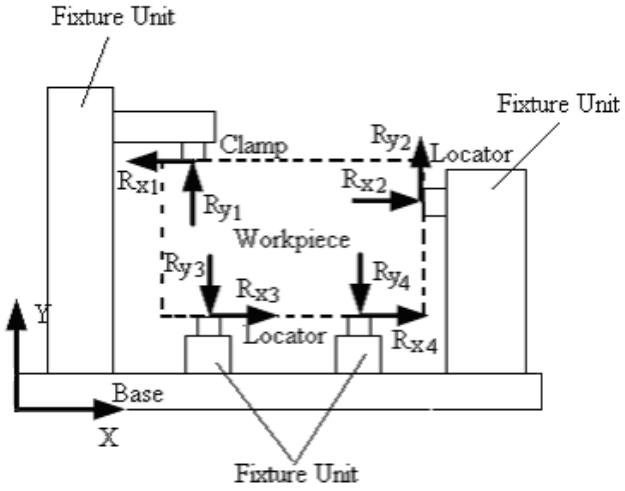

Figure 1.2 Sketch of Fixture Units

Fixture unit stiffness is defined as the force required for a unit deformation of the fixture unit in normal and tangential directions at the contact position with the workpiece. For example, Figure 1.3 shows the definition of the fixture unit stiffness K_{Un} in the normal

direction: $K_{U_n} = \frac{F}{\delta}$. The fixture unit stiffness can be static if the external load is static (such as clamping force), and dynamic if the external load is dynamic (such as machining force). Fixture unit stiffness is the key parameter used in analyzing the relative performance of different fixture designs and optimizing fixture configuration. When fixture unit stiffness is obtained, the fixture stiffness can be estimated (Kang, 2003). Fixture stiffness is defined as the force required for a unit deformation of the fixture in the tolerance sensitive direction.

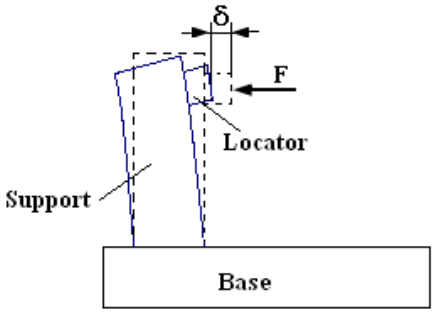

Figure 1.3 Fixture Unit Stiffness

The development of a CAFD tool with predictable fixture stiffness has been recognized as more and more important. The significance of fixture stiffness was demonstrated in a preliminary experimental study by Zhu (1993), which showed the nature of fixture deformation in T-slot based modular fixtures. Figure 1.4 shows the experiment configuration: a basic assembly unit, where structural supports are bolted to a baseplate. When an external force (F) is exerted on the upper portion of the supports in the horizontal direction, the fixture component deformation is measured as y_s in the horizontal direction. The experiment showed that the total fixture deformation (y_s), as shown in Figure 1.5, can be decomposed into four individual deformations: the elastic deformations of the baseplate (y_b) and support (y_e), the contact deformation between the baseplate and the support (y_j), and the shift displacement (y_t). As the exerted external

force increases, the four individual deformations make different contributions to the nonlinear deformation curve. Figure 1.6 shows the typical fixturing deformation curves of fixture units. In most machining and assembly applications, fixtures of both flexible and dedicated types are composed of a number of fixture units with elastic components such as locators /clamps, supports. Given that large forces and moments can be generated in machining and assembly, high fixture stiffness is a critical design goal that needs to be achieved. Unfortunately, a systematic and scientific design approach for representing the experimental results and realizing this goal is not available (Hurtado, 2001). In all previous work, fixture stiffness was either not considered or is assumed to be known, or only the elasticity of the workpiece and fixture components in the contact region were taken into account because of the expense of computation.

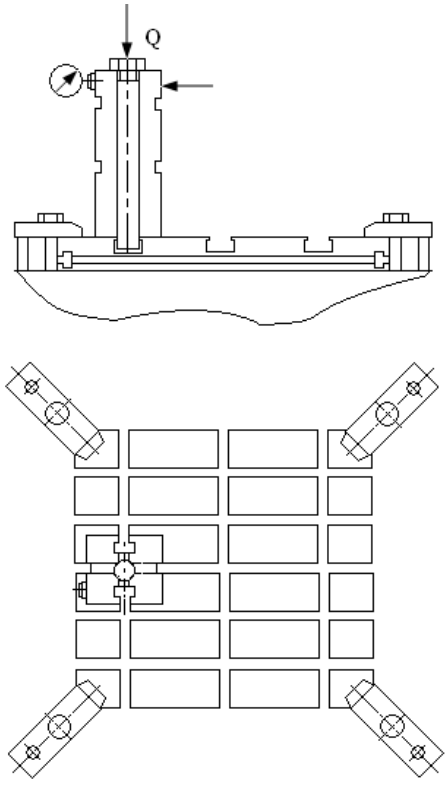

Figure 1.4 A Basic Assembly Unit of T-Slot-Based Modular Fixture

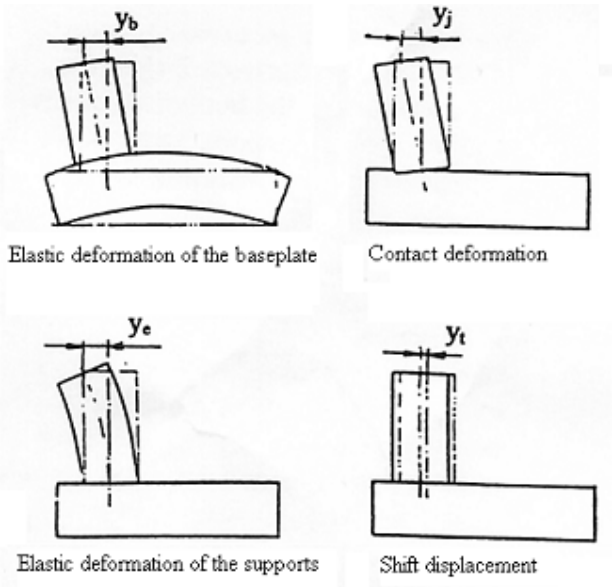

Figure 1.5 Sketch of Fixture Deformations

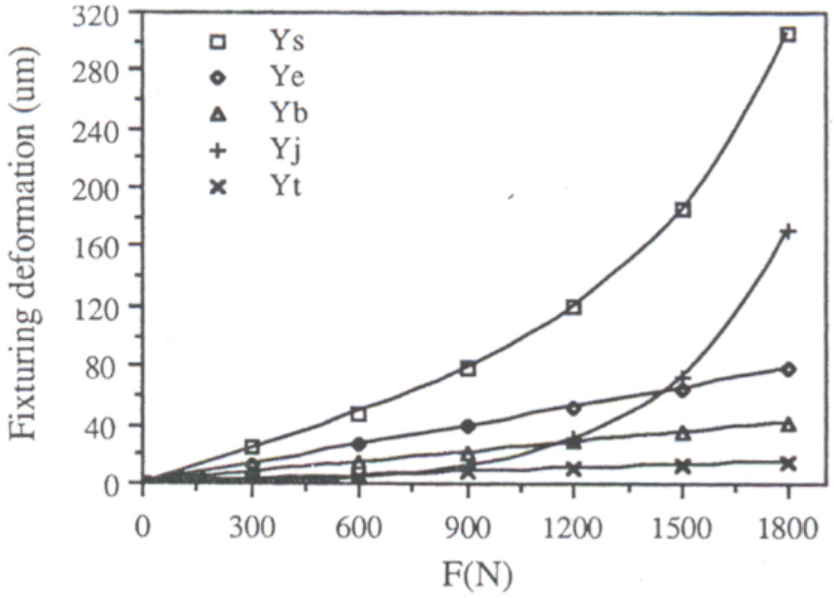

Figure 1.6 Typical Fixturing Deformation Curves of Fixture Units

Current computer-aided fixture design methods rely extensively on heuristics and lack a formal engineering approach to determine the necessary fixture stiffness. This requires a

fundamental understanding of fixture stiffness in order to develop an accurate model of the fixture–workpiece system.

1.2 Research Goal and Objectives

The final goal of this research is to develop a CAFD system with predictable fixture stiffness. First of all, the stiffness of typical fixture units is studied with consideration of contact and friction conditions. The results of the fixture unit stiffness analysis are integrated into CAFD as a database, with variation capability driven by parametric representations of fixture units. When a fixture is designed with CAFD, the fixture stiffness at the contact locations (locating and clamping positions) to the workpiece can be estimated and/or designed, based on the machining operation constraints (e.g., fixture deformation and dynamic constraints). Figure 1.7 shows a diagram of the integrated fixture design system.

The goal of dissertation research is to provide a model of the fixture unit stiffness analysis and to develop a method for identifying the contact stiffness parameters. The model and the method offer potentials for a more realistic analysis of the stiffness properties of a fixture–workpiece system, based on a fixture unit description. In order to study fixture stiffness, the following objectives are to be addressed:

- To develop a finite element analysis (FEA) model of fixture stiffness. The effect of friction between the fixture components should be considered together with the constraints of the physical phenomena in the fixturing process.

- To demonstrate the validity of the finite element model through a series of case studies.
- To experimentally investigate the contact stiffness between fixture components so as to gain insight into the nature of the interaction between fixture components.

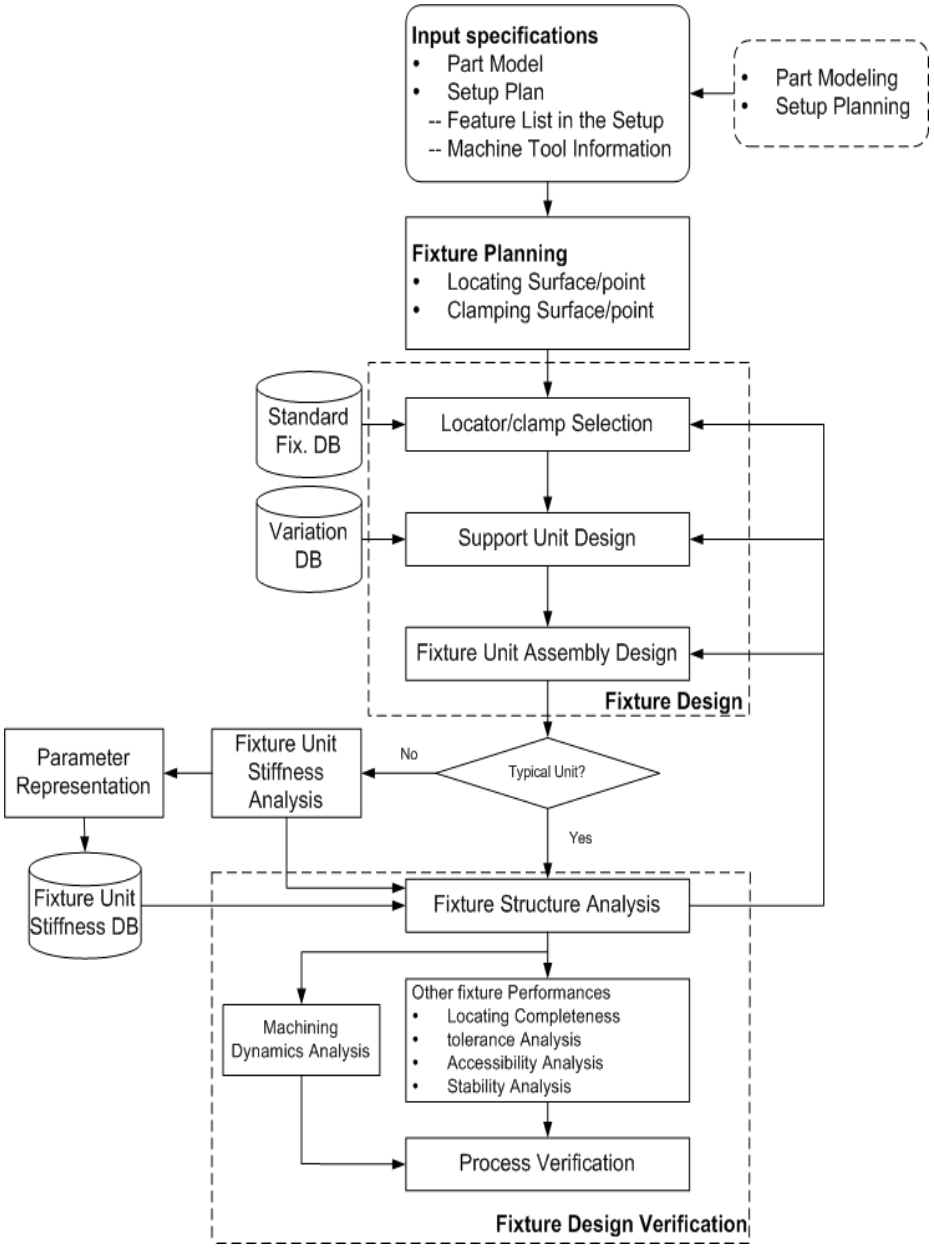

Figure 1.7 Integrated Fixture Design System

1.3 Research Tasks

1.3.1 Finite Element Analysis (FEA) Modeling of Fixture Unit Stiffness

In a fixture unit, all components are connected one to another, while only one is in contact with the fixture base directly, and one or more are in contact with the workpiece, serving as the locator, clamp, or support. When a workpiece is located and clamped in a fixture, the fixture units are subjected to the external loads that transmitted from the workpiece. If the external load is known and acting on a fixture unit, and the displacement of the fixture unit at the contact position is measured or calculated, based on an FEA model, the fixture unit stiffness can be determined according to the definition. In the development of FEA model, the challenge is how to describe the nonlinear contact conditions as identified in the previous experiments.

1.3.2 Contact Stiffness Identification

A typical fixture unit usually consists of several fixture components, which are in contact each other. One of the key issues in the analysis of fixture unit stiffness is how to handle the contact problems. During development of the contact model, the most troublesome problem encountered is the lack of accurate system parameters, such as contact stiffness, to form the finite element formulation. Contact stiffness is very difficult to find through theoretical methods. Therefore, experimental identification methods become more and more important. That experimental approach, which should avoid the use of complicated equipment with the aim of easy application, needs to be developed. Experimental work is required to gain insight into the nature of the interaction between the fixture elements.

1.4 Dissertation Organization

This dissertation is organized into five parts, as shown in Figure 1.8.

Part I: (Chapters1-2) Introduction and literature review

- Chapter 1 introduces the motivation, objectives, and goal of the research, and the overall tasks of finite element analysis of fixture stiffness.
- Chapter 2 gives a review of earlier studies on the computer-aided fixture design system with predictable fixture stiffness. The focus is put on four aspects: (i) CAFD (ii) Workpiece model (iii) Fixture stiffness (iv) Contact parameters. The existing state-of-the-art systems are compared and summarized according to their applied technologies.

Part II: (Chapter 3) Development of FEA model for fixture unit stiffness analysis

- Chapter 3 develops a finite element model of fixture unit stiffness. The contact element is utilized for solving the contact problems encountered in the study of fixture unit stiffness. The finite element model and the analysis procedure are validated by a case study.

Part III: (Chapter 4) Contact stiffness identification

- Chapter 4 addresses the problems of contact stiffness identification. In this chapter, theoretical models of contact stiffness are discussed, followed by the development of the experimental methods that deal with the identification of normal contact stiffness and tangential contact stiffness, respectively. The corresponding experimental methods are developed, the test structures are described, and the experimental setup is presented, the measurements are then explained and the contact stiffness is estimated.

Part IV: (Chapter 5) Summary and future work

- Chapter 5 gives a summary of the research.

Part V: References and Appendices

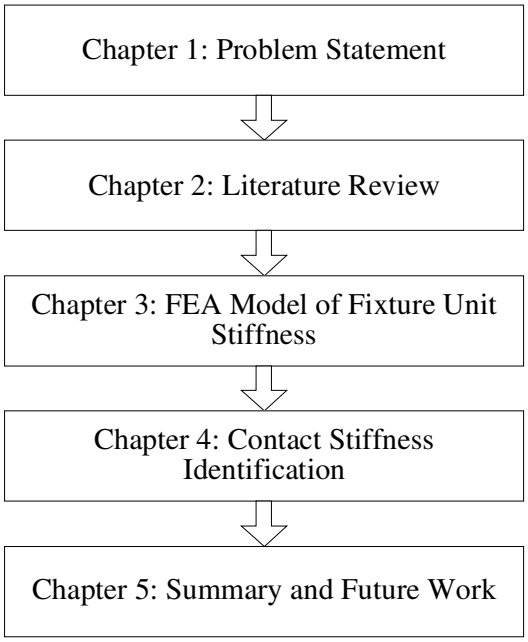

Figure 1.8 Dissertation Structure

Chapter 2: Literature Review

This chapter gives a review of the literature related to this dissertation. First, the research on CAFD is discussed, including the basic methodologies of CAFD, different viewpoints in CAFD, and the key technologies applied in CAFD. Secondly, the literatures on workpiece models, fixture stiffness, and contact parameters are discussed in depth. Finally, a summary is presented about the current status of FEA of fixture stiffness, including the problems remaining, and the principal focus in this research on the FEA of fixture stiffness.

2.1 Overview of Computer-Aided Fixture Design

Fixture design is a complex task, and represents a critical design–manufacturing link, especially in a modern computer integrated manufacturing (CIM) environment. In the past fifteen years, CAFD has been recognized as an important focus for reducing manufacturing lead-time and costs. CAFD activities include three steps:

- Fixture planning, to determine the locating datum surfaces and locating/clamping positions on the workpiece surfaces, for totally constrained locating and reliable clamping.
- Fixture configuration design, to generate a design of fixture structure seen as an assembly, according to different production requirements such as volume and machining conditions.
- Fixture design verification, to evaluate whether fixture design performances satisfy production requirements such as completeness of locating, tolerance stack-up, accessibility, fixturing stability, and ease of operation.

For many years, fixture planning has been the focus of academic research with significant progress in both theoretical (Chou, 1989; Xiong, 1998; Wu, 1998; Brost, 1996; Asada, 1985; Marin, 2002; DeMeter, 1998; Wang, 1999; Whitney, 1999; Roy, 2002) and practical studies (Ma, 1999; Fuh, 1994). In theoretical studies of fixture planning, some previous efforts include: a method for automating fixture location and clamping (Chou, 1989); an algorithm for the selection of locating/ clamping positions that provide maximum mechanical leverage (De Meter, 1993); fixture planning based on kinematic analysis (Menassa, 1990; Mani, 1988); and rule-based systems to design modular fixtures for prismatic workpieces (Markus, 1984; Pham, 1990). Given the lack of study on automating the configuration of workpiece on the fixtures, a geometric analysis for automated fixture planning has been presented by Wu (1998). The initial conditions for modular fixture assembly have been established, together with geometric relationships between fixture components and the workpiece to be analyzed. In addition, several authors have addressed the development of clamp actuation intensity analysis (CAIA) models to optimize the clamp actuation preloads. These optimization models treat a fixture–workpiece as a system of contacting rigid bodies subject to Coulomb friction at the joints. Predicted external forces from the machining process are supplied from the execution of static chip load in machining process models. Examples of various formulations of these models can be found in Wang (1999), Meyer (1998), and Sayeed (1994). Because of the assumption of a rigid body, the fixture–workpiece joint load distributions predicted by these models are strictly influenced by the position and direction of the external loads, relative to the fixture components. A paper has described an experimental study that was used to characterize the accuracy of the LCPL model with regard to the application of a ramping external load to a fixture–workpiece system. This

experimental study also revealed the sensitivity of the computed preloads to the relative compliance of the fixture components (De Meter, 2001). Considering several technical issues relative to modular fixture design, such as fixturing stability, access analysis, and selection of locating and clamping points, a comprehensive fixture planning system that can be used to generate fixture plans for industrial applications has been developed by Ma (1998). Although the study of fixture planning has made extensive progress, most of these analyses of fixture planning are based on rigid assumptions, e.g., frictionless smooth surfaces in contact, rigid fixture body, and a single objective function for optimization.

Fixture design is a complex problem with many operational requirements to consider. Four generations of CAFD techniques and systems have been developed: group technology (GT)-based part classification for fixture design and on-screen editing (Grippo, 1987, Rong, 1992); automated modular fixture design (Rong, 1997; Kow, 1998); permanent fixture design with predefined fixture components types (Wu, 1997; An, 2000; Chou, 1993); and variation fixture design for part families (Han, 2003). The study of a new generation of CAFD recently started to consider operational requirements (Rong, 2003). Geometric reasoning (Ma, 1998; An, 2000), knowledge-based resoning (Markus, 1988; Nee, 1991; Nnaji, 1990; Pham, 1990) and case-based reasoning (CBR) (Kumar, 1995; Sun, 1995) techniques have been intensively studied for CAFD. How to make use of the best practice knowledge in fixture design and how to verify the quality of fixture design under different conditions has become a challenge in CAFD study.

In fixture design verification, the most important criteria for fixturing are workpiece position accuracy and workpiece deformation. During clamping and machining, there are

frictional contacts between workpiece and fixture components, to hold the workpiece and prevent detachment from the locator. A good fixture design minimizes geometric and machining accuracy errors on a workpiece. Previous researchers (Asada and By,1985; Rong, 1994; 1995b; 1996; Chou, 1989; Wu, 1995; Kang, 2003) have studied several areas of fixture verification: geometric analysis, kinematic analysis, force analysis and deformation analysis. In the literature, fixturing is generally considered using the rigid workpiece and fixture components concept; however, workpiece and fixture components are elastic and deformable. Generally, the stiffest fixture elements absorb the majority of the external load applied to a workpiece. High fixture stiffness is needed to minimize displacement of the workpiece from its nominal position during clamping and machining, thereby keeping the machined-feature error within tolerance (De Meter, 2001). It was also proved that when the fixture stiffness and machining force are known and are used as input information, the fixturing stability problem could be completely solved (Kang, 2003).

2.2 State-of–the–art in the Analysis of the Fixture-Workpiece System

Although numerous CAFD techniques have been proposed and implemented, fixture design still continues to be a major bottleneck in the product design and manufacturing process. One reason for this is that the fixture design approaches being developed do not fully consider the integration of the fixture-workpiece system. Although researchers have analyzed and studied the ways to analyze workpiece deformation with fixturing boundary conditions, there has been less attention paid to the development of strategies, models, and formulations that would specifically enhance or optimize the performance of the

fixture system. Since, as noted above, the stiffest fixture elements absorb the majority of the external load applied to a workpiece, it is consequently important to model the compliance of fixture components as accurately as possible. All sources of elasticity should be considered, including the deformation of the fastening systems (De Meter, 2001). In the entire fixture-workpiece system, the external loads, contact interaction between workpiece and fixture components, fixture stiffness, and contact parameters have considerable impact on the accuracy of the finished part. Therefore, research in these areas is discussed in depth.

2.2.1 Workpiece Deformation with Fixturing Boundary Condition

In studying the fixture–workpiece systems, most researchers focus on analyzing workpiece deformation with a fixturing boundary condition. One of the key issues in the analysis of workpiece deformation is the handling of the contact problems between workpiece and fixture components. Contact problems are traditionally classified in terms of surface friction (frictionless, stick, and slip), initial undeformed geometry (conforming and nonconforming), initial conditions (interference fit, tied, and gaps), relative rigidity (deformable-rigid or deformable-deformable) and behavior under loading (stationary, advancing, receding, and self contact) (Fischer-Cripps, 2000). The fixture relies on static friction at the fixture–workpiece interface to restrain the workpiece during machining. Clamping harder than necessary may damage the part or produce deformations that reduce the final part accuracy. On the other hand, clamping too gently may permit the part to slip during machining and be ruined. In view of the importance of static friction for machining fixture design, a better understanding of frictional contact for a given fixture-workpiece pair is desirable. The formulations of frictional contact between

workpiece and fixture components have been studied in the literature, both from a rigorous mathematical viewpoint and, more recently, in the context of finite element analysis (Mijar, 2000). Several kinds of fixture–workpiece models have been developed in the past decades, which aim to demonstrate the interaction between the fixture and the workpiece during the machining operation. Previous researches have used the analytical approach or the finite element modeling approach to build the fixture–workpiece models for fixture analysis and synthesis.

Several researchers have developed methods to analyze fixture-workpiece interaction. An initial model was developed by Lee (1991) to construct a limited surface in force/moment space for determining when and how a clamped workpiece may slip, and to help in specifying clamping forces. The central idea is that once a workpiece starts to slip, the instantaneous velocity and the resulting frictional force are uniquely related. By establishing a mapping between velocities and corresponding forces and moments, one can solve the inverse problem of determining how a part will slip in response to applied forces. The process of mapping between motions and forces results in a limited surface in force/moment space.

In the machining process, holding the workpiece relies mainly on friction, so it cannot be neglected in the modeling. Considering the effect of the friction, Tao (1999) introduced a geometrical-reasoning verification approach for fixturing schemes, in the presence of friction, during machining. In this approach, the workpiece and fixture conpoments are treated as rigid bodies. Coulomb friction is assumed to act between the part and the fixturing components, and the locators and clamps are spherically tipped so that only point contacts exist between the workpiece and the fixture.

Some researchers presented an elastic contact model of workpiece and fixture components for predicting the fixture–workpiece contact force due to clamping (Li, 1999). The model predicts the normal force, magnitude, and direction of the friction force at each fixture–workpiece contact. Fixture locators and the workpiece are taken as elastic bodies and a small contact area is assumed. An improved elastic contact model for analyzing fixture–workpiece contact forces and moments in machining fixtures with large contact areas has been devised (Li, 2001). A minimum-energy principle is used to solve the multiple contact problems, yielding unique predictions of the fixture-workpiece contact forces and moments due to clamping and machining forces. The Coulomb friction law applies to each fixture–workpiece contact. These previous works assume either a rigid workpiece or take into account only local workpiece compliance. In addition, these fixture-workpiece models were usually developed with the assumption of rigid or linear elastic fixture stiffness as boundary conditions.

FEA has been widely used to analyze the workpiece deformation under machining forces. FEA treats the workpiece as an isotropic deformable body, based on linear elasticity, and takes into account the friction that develops at the fixturing component/workpiece interfaces. Lee (1987) was among the first to use the finite element method for fixture design and analysis. Computer software was created to find the optimal design of the fixturing system by minimizing the total work done on the workpiece. An intelligent fixturing system was developed to adjust the clamping forces, to achieve minimum deformation of the workpiece according to cutting forces. Linear static finite element analysis was used to find the workpiece deformation (Wang, 1999). Roy introduced a system that first generates a preliminary fixturing configuration, based on the workpiece representation and other required information, and then analyzes the preliminary fixturing

configuration (1997). A finite element method was used to determine the deformations. Dynamic machining conditions and frictional effects are not taken into account. Liao presented an FEA model of fixture configuration analysis, based on a dynamic model, which analyzes the fixture–workpiece system subject to time varying machining loads (2000). The frictional effect was taken into account, but the chip removal effect was not considered. Previous work has focused on the use of the finite element model in optimizing fixture layout (Menassa, 1991; Rearick ,1993; Trappey,1995; Cai,1996). These studies used finite element models of the fixture-workpiece system as input for layout optimization. Other researchers have presented a model for analyzing the accuracy of workpiece location, using the elastic contact model to represent the contact problem (Li and Melkote, 1999). Location errors due to localized elastic deformation of the workpiece at the fixturing points were handled by optimally placing the locators and clamps around the workpiece. The FEA model of the fixture-workpiece system was used as output to determine the workpiece deformations. The frictional effect was considered, but the chip removal effect was not taken into account. Wardak (2001) used a finite element method and optimization algorithms to design optimal fixturing layouts for the drilling processes. Figure 2.1 shows the fixture-workpiece model that was used in FEA.

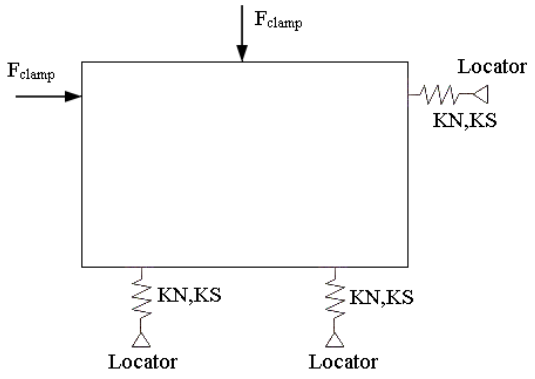

Figure 2.1 Fixture–Workpiece Model

Despite extensive work in the fields of mathematics and engineering, frictional contact remains one of the most challenging problems, due to the difficulties involved in the highly nonlinear formulation and solution procedures. In the analysis of workpiece deformation with the fixturing boundary condition, the shortcoming of most previous work is that either the fixture components are treated as rigid bodies or else only the locators are considered as elastic bodies. The analytic and computational results cannot represent the nonlinear deformation in fixture connections that was identified in previous experiments (Zhu, 1993). Table 2.1 summarizes the study of the fixture-workpiece model developed in the analysis of workpiece deformation. For realistic case studies, both the workpiece and fixture components must be treated as flexible models. Therefore, significant consideration must be given to improving the existing analytic and numerical solution algorithms or to developing new contact algorithms for numerical solution approaches. These algorithms would converge without problems in considering complex geometrical shapes and the nonlinear nature of contact forces with a wide variety of boundary conditions, since numerical solution algorithms have often had convergence problems in the analysis of three-dimensional contact problems.

Table 2.1 Literature Survey of Fixture-workpiece Model

Reference	Fixture-workpiece model				
	Method	Workpiece	Fixture		
			Locators	Clamps	Fixture unit stiffness
Tao (1999)	Analytic approach	Rigid	Rigid, Coulomb friction	Rigid	U/A
Li (2001)		Elastic	Linear elastic in local contact area, Coulomb friction	Linear elastic in local contact area	U/A
Lee (1987)	FEA	Elastic	Rigid area constraint, Coulomb friction	U/A	U/A
Trappey (1995)		Elastic	3-D solid deformable constraints	Rigid	U/A
DeMeter (1998)		Elastic	Rigid area constraint, Coulomb friction	Rigid	U/A
Wardak (2001)		Elastic	Elastic, Coulomb friction	Elastic	U/A

Key: U/A Unavailable

2.2.2 Fixture Stiffness

In most machining and assembly applications, high fixture stiffness is a critical design goal that needs to be achieved. Unfortunately, a systematic and scientific design approach for realizing this goal is unavailable. Analysis of fixture stiffness may be divided into three categories: analytical, experimental, and FEA. Conventional structural analysis methods may not work well in estimating the fixture stiffness due to nonlinearity caused by the interaction between fixture components. An analytical model, which allows systematic determination of the optimum fixture stiffness needed to maintain the contribution of fixture deflection to the machined feature tolerance within a designer

specified level, is introduced based on the stiffness optimization model (Hurtado, 2001). The model relies on the assumption that the workpiece is considered to be structurally rigid, and elasticity is taken into account only at workpiece-fixture component contacts. This model ignores the overall fixture stiffness, and considers only the stiffness of locators and clamps. Preliminary experimental study has shown the nature of fixture deformation in T-slot-based modular fixtures (Zhu, 1993). Experimental results show that the total deformation of the basic assembly unit of T–slot-based modular fixtures can be decomposed into individual deformations: elastic deformation of fixture components, contact deformation between fixture components, and shift displacement. At different stages of the exerted external force, the contributions of the individual deformations of the total deformation play different roles. The deformation of fixture components under the clamping force and machining force may significantly affect machining accuracy and stability (Zhu, 1993). An integrated model of a fixture-workpiece system was established for predicting surface quality (Liao, 2001), based on experimental results in Zhu's work (1993), but with the assumption that the contact stiffness was known. In analyzing a fixture-workpiece system, most of the numerical solutions are carried out for flexible workpiece and rigid fixture elements. There is no additional work on fixture stiffness analysis due to the complexity of the contact condition and the large computation effort for the many fixture components involved.

Compared with the other two approaches, the FEA has advantages for the analysis of fixture stiffness when nonlinearities caused by the interaction between fixture components must be considered to compute internal stresses and displacements. The numerical analysis of contact interaction problems can be formulated based on variation inequalities. The penalty function method, as well as the Lagrange multiplier method, is

one of the most powerful approaches to solve such constraint problems. In the Lagrange multiplier method, both displacement and contact pressure are regarded as independent variables; then the constraints conditions, which are the contact conditions, can be strictly satisfied, and contact pressure can be obtained accurately. But the method has disadvantages: the number of unknowns varies with the change of the number of active contact nodes, where contact actually takes place, and the stiffness matrix contains zero components in its diagonal (Yagawa, 1993). While the penalty function method provides approximate solutions, it has the advantages of a fixed number of unknowns and ease of implementation (P. Wriggers, 1996). Table 2.2 summarizes the study of fixture stiffness. In this research, the FEA model of fixture unit stiffness based on the penalty function method will be developed.

Table 2.2 Literature Survey of Fixture Stiffness

Method	Reference	Fixture stiffness
Analytic approach	Hurtado (2001)	Clamp/locator elastic; Fixture stiffness U/A
Experimental approach	Zhu (1993) Liao (2001)	Module Fixture unit stiffness was studied
FEA approach	U/A	U/A

Key: U/A Unavailable

2.2.3 Contact Parameters Identification

In a fixture-workpiece system, an actual fixture unit usually consists of many fixture components that are in contact with each other. The analysis of fixture stiffness is generally complicated by the fact that the contact surface can experience slipping, sliding,

or tension release, depending on the magnitude of the normal and tangential forces at the contact interface. The nonlinearity of the problem arises both from the variation of contact stiffness and also from the effects of friction. So the most troublesome problem encountered is the lack of accurate system parameters, such as contact stiffness and the coefficient of friction, to form the finite element formulation.

The determination of contact stiffness between fixture components is the key barrier in FEA modeling. Up to 60% of the deformation and 90% of the damping in a fabricated structure can arise from various connections (Beards, 1986). In the study of joints, a more general joint model, which is expressed by stiffness and damping coefficient matrices, was proposed (Wang, 1990). The essential algorithm for identifying the joint parameters is to transform the assembled system into several single DOF systems using selected eigenvectors. These eigenvectors should be sensitive to the identified parameters. It is obvious that this method relies on the availability and accuracy of the mode shapes of the assembled structure. It is not very promising for practical applications. To extract joint parameters without interference from complicated dynamic characteristics of substructures, a method based on rigid-body dynamics and frequency-response function measurement was developed by Becker (1999). Connecting rigid bodies, instead of elastic substructures, isolates the joints. It is easy to obtain the stiffness matrix of the joint by means of this method, but the application of this technique is quite limited, and these studies are based on a linear joint model. Nonlinear joint modeling has not been studied as thoroughly because of the difficulty in understanding the mechanisms for practical applications. A systematic study of the micro-slip condition was reported by Menq (1986), and a micro-slip model was proposed, based on physical model of a continuous

friction contact. Tangential contact stiffness normally exhibits friction-related nonlinearities, it also has not been studied as thoroughly as normal contact stiffness.

Although, the literature is full of research on contact stiffness and its application, it lacks research that relates to the contact found in the fixture-workpiece system. Contact conditions for machining fixturing was considered by Yeh (1999), and this paper summarizes the analytical model established and the application to the analysis of the modular fixturing system. Experimental analysis was conducted to verify the analytical model. The analytic model for the identification of contact stiffness is based on the modified Hertz contact model. Some researchers (Melkote, 2001) presented a new algorithm, based on the contact elasticity method for determining the optimum clamping forces for a multiclamp workpiece/fixture system. The algorithm uses a closed-form Hertzian model to determine a set of contact forces and displacements, which are then used for optimizing clamping force. The frictional condition existing between any pair of contacting surfaces is determined by the relative magnitude of the normal and tangential tractions at the contacting surface. The problem is formulated as a multi-objective, constrained optimization problem; one of the constraints is for the forces to satisfy Coulomb's law of friction. These previous works on the fixture-workpiece system are very preliminary; they either simply apply the Hertzian contact model or consider the effective contact area.

Many researchers made an effort to investigate the coefficient of friction in the fixture-workpiece system. A model was presented by Moslehy (1991) for the prediction of the steady-state coefficient of friction. In his model, the relative contribution of asperity, adhesion, asperity plowing, and debris were considered. In an initial effort (Xie, 1999),

experiments were carried out to characterize friction for commercially available fixture components in dry contact with A356 aluminum. This study revealed that the coefficient of friction was very sensitive to fixture-component geometry and workpiece surface topography, but it was relatively insensitive to clamping force and fixture-component size. It also revealed that even under controlled conditions, the value of the coefficient of friction varies significantly from test to test. While it was a good start, this work did not present evidence of the phenomena that may have resulted in variations of the friction values, nor did it address important issues such as the effects of residual cutting fluid and normal joint rigidity on friction (Deiab, 2004). Xie (2000) presented a method for the experimental evaluation of the coefficient of friction for a workpiece/fixture system. The method is based on previous work (Nivatvongs,1991; Xie, 1999), where studied the effect of workpiece surface topography, fixture element type, fixture element size, clamping force, the presence of cutting fluid at the joint, and normal joint rigidity on the coefficient of friction. They assumed that friction is due to asperity interlocking and shearing at the joint interface, which is typically assumed in fixture research. Deiab (2004) carried out an experimental investigation to characterize the relation between normal force and the friction coefficient for fixture applications. He studied effect of workpiece roughness, fixture tip roughness, and the clamping force on the friction coefficient.

Table 2.3 summarizes the study of contact parameters. In this research work, t contact stiffness needs to be identified and friction coefficient is obtained from previous study. The design of experiments for the investigation of the contact stiffness is pursued, and the experiments are repeated as many times as needed for the average to converge.

Table 2.3 Literature Surveys of Contact Parameters

Reference	Method	Contact Parameters		
		Friction	Contact stiffness	
Deiab (2004)	Experimental approach	Consider effect of workpiece roughness, fixture tip roughness, and clamping force.	Normal	Tangential
			N/A	
Yeh (1999)	Analytical approach	N/A	Adjusted Hertz contact	U/A
Melkote (2001)	Analytical approach	N/A	Adjusted Hertz contact	Adjusted Hertz contact

Key: U/A Unavailable; N/A Not Applicable

2.3 Summary of Current Research

As a result, the current state-of-the art technologies suffer some major limitations that can be described as follows:

1. In previous works, fixture stiffness is not considered or is assumed to be known, or only the contact stiffness is taken into account, while friction is not considered. Most of the previous studies are focused on the "fixtured workpiece" model, i.e, how to configure positions of locators and clamps for an accurate and secured fixturing, with an assumption of rigid or linear elastic fixture stiffness as boundary conditions. Only preliminary experimental work exists.

2. The determination of contact stiffness between fixture components is the key barrier in FEA modeling. The existing work is very preliminary, either simply applying the

Hertzian contact model or considering the effective contact area. Such work is not very promising for practical applications.

This dissertation offers a comprehensive study on the finite element analysis of fixture stiffness. Initially, a finite element model of the fixture unit stiffness study will be developed. A contact element needs to be utilized for solving the contact problems encountered in the study of fixture unit stiffness. The finite element model and the analysis procedure will be validated by case study. Also, an experimental methodology, which should avoid the use of complicated equipment with the aim of easy application, needs to be derived to estimate contact stiffness. Both the normal contact stiffness and the tangential contact stiffness must be taken into account. Experimental work is required to gain insight into the nature of the interaction between the fixture elements. Table 2.4 shows a summary of existing research work and the focus of the research work in this dissertation.

Table 2.4 Overview of the Dissertation Research

Tasks	Previous work	Challenge in previous work	Dissertation research
Developing the FEA model of fixture unit stiffness with contact and friction Conditions.	Fixtured workpiece model. Experimental work of nonlinear deformation in fixture connections Hertzian contact model	Represent contact condition in fixture model Identify contact stiffness parameters	A penalty function method is used to model nonlinear contact conditions with contact elements. FEA Model is validated and results are compared previous experimental results. Dynamic experimental method is developed to identify the contact stiffness in normal and tangential directions. The method is validated by the results from the static experiment method and analytical calculation.

Chapter 3: Finite Element Model of Fixture Unit Stiffness

In fixture design, a thoughtful economic fixture-workpiece system maintains uniform maximum fixture stiffness throughout machining, while also providing the fewest fixture components, open workpiece cutting access, and shortest setup and unloading cycles. The computer-aided fixture design with predictable fixture stiffness provides the appropriate design solution for improving fixture performance. In order to study fixture stiffness, a general fixture structure is decomposed into functional units with fixture components and functional surfaces (Rong, 1999). In a fixture unit, all components are connected to each other; only one is in contact directly with the fixture base, and one or more are in contact with the workpiece, serving as the locator, clamp, or support. When a workpiece is located and clamped in the fixture, the fixture units are subjected to external loads, which transmitted from the workpiece. If the external load is known and acting on a fixture unit, and the displacement of the fixture unit at the contact position is measured or calculated based on a FEA model, the fixture unit stiffness can be estimated. Once the stiffness of fixture units are known, the overall fixture stiffness can be obtained regarding the tolerance sensitivity.

In finite element analysis of fixture stiffness, the main task is to describe the fixture unit stiffness by using a numerical method. In this chapter, a finite element model of fixture unit stiffness is developed. A contact element is utilized to solve the contact problems encountered in the study of fixture unit stiffness analysis. Due to the contact conditions, the status of contact elements may change, and contact stiffness is not constant in the analysis of process. In the FEA model, the contact and friction conditions will be

represented mathematically and discussed in detail. The finite element model and the analysis procedure are validated by case study.

3.1 FEA Formulation

Consider a general fixture unit with two components I and J, as shown in Figure 3.1. For multi-component fixture units, the model can be expanded. The fixture unit is discretized into finite element models using a standard procedure, except for the contact surfaces, where each nodes on the finite element mesh for the contact surface is modeled by a pair of nodes at the same location belonging to components I and J, respectively, which are connected by a set of contact elements. The basic assumptions include that material is homogenous and linearly elastic, displacements and strains are small in both components I and J, and the frictional force acting on the contact surface follows the Coulomb law of friction.

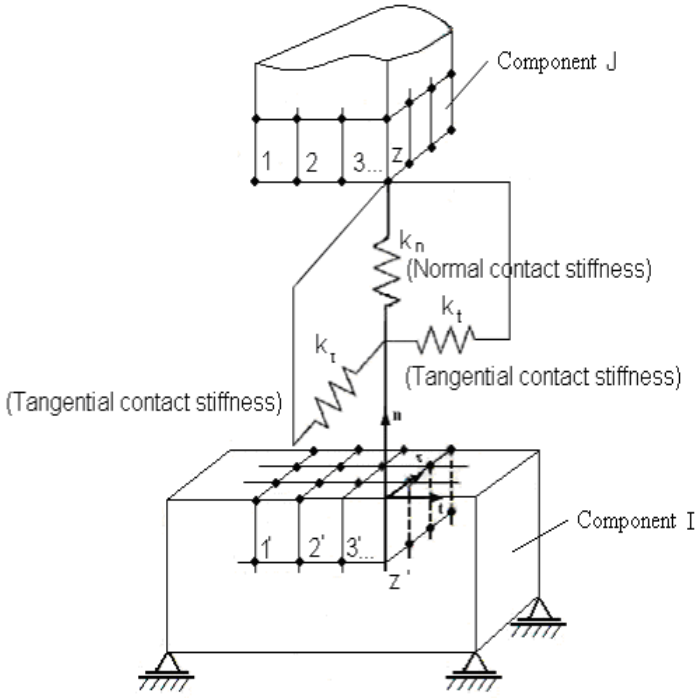

Figure 3.1 Contact Model of Two Fixture Components

The total potential energy Π_p of a structural element is expressed as the sum of the internal strain energy U and the potential energy Ω of the nodal force; that is,

$$\Pi_p = U + \Omega \tag{3.1}$$

It is well known that the element strain energy can be expressed as,

$$U = \frac{1}{2}\{q\}^T [K]\{q\} \tag{3.2}$$

where $[K]$ is the element stiffness matrix; and

$\{q\}$ is the element nodal displacement vector.

The potential energy of the nodal force is,

$$\Omega = -\{q\}^T \{R\} \tag{3.3}$$

where $\{R\}$ is the vector of the nodal force. It includes internal force and external force.

When the two components I and J are in contact, a number of three-dimensional contact elements are in effect on the contact surfaces. It should note that the problem is strongly nonlinear, partially due to the fact that the number of contact elements may vary with the change of contact condition. The original contacting nodes might separate or recontact after separation, based on the deformation condition on the contact surface; also contact stiffness may not constant either. The contact elements are capable of supporting a compressive load in the normal direction and tangential forces in the tangential directions. When the two components are in contact, and the displacements in the tangential directions and normal direction are assumed as independent, the element itself can be

treated as three independent contact springs: two having stiffness k_t and k_τ in the tangential directions of the contact surface at the contact point and one having stiffness k_n in the normal direction.

Usually, there are two methods used to include the contact condition in the energy equation: the Lagrange multiplier and the penalty function methods (Cook, 1989). In order to understand these methods, a physical model of the contact conditions is presented, shown in Figure 3.2. When two contact surfaces of fixture components, i.e., body J and I, are loaded together, they will contact at a few asperities, such as shown in Figure 3.2(c).

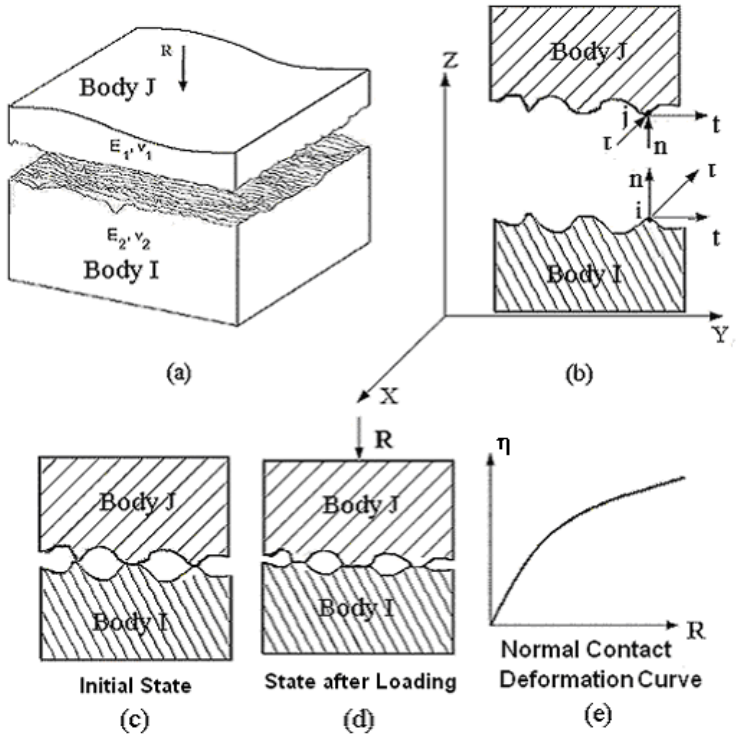

Figure3.2 Physical Model of the Contact Conditions

The contact criteria can be written as:

$$\eta \geq 0; \quad f_{ni} \leq 0; \quad \eta f_{ni} = 0$$

where

η is distance from a contact point i in body I to a contact point j on the body J in the normal direction of contact;

f_{ni} is the contact force acting on point i of body I in the normal direction.

It shows the kinematic condition of no penetration and the static condition of compressive normal force. To prevent interpenetration, the separation distance η for each contact pair must be greater or equal to zero. If $\eta>0$, the contact force $f_{ni}=0$. When $\eta=0$, the points are in contact and $f_{ni}<0$. If $\eta<0$, penetration occurs. In real physics, the actual contact area increases, and contact stiffness is enhanced when the load increases. Therefore, the contact deformation is nonlinear as a function of the preload as shown Fig 3.2(e). In the Lagrange multiplier method, the function w (η, f_{ni}) represents the constraint, which prevents the penetration between contact pairs. In the penalty function method, an artificial penalty parameter is used to prevent the penetration between contact pairs.

In the penalty function method, the contact condition is represented by the constraint equation,

$$\{t\} = [K_C]\{q\} - \{Q\} \tag{3.4}$$

where $\{t\}$ is the constraint equation

$[K_C]$ is the contact element stiffness matrix,

$\{Q\}$ is the contact force vector of the active contact node pairs. When $\{t\}=\{0\}$, it means that the constraints are satisfied. So the constraint equation Eq. 3.4 becomes

$$[K_C]\{q\}=\{Q\} \tag{3.5}$$

The total potential energy Π_p in Eq. 3.1 can be augmented by a penalty function $\frac{1}{2}\{t\}^T[\alpha]\{t\}$ where $[\alpha]$ is a diagonal matrix of penalty value α_i. The total potential energy in the penalty function method becomes

$$\Pi_{pP}=\frac{1}{2}\{q\}^T[K]\{q\}-\{q\}^T\{R\}+\frac{1}{2}\{t\}^T[\alpha]\{t\} \tag{3.6}$$

The minimization of Π_{pP} with respect to $\{q\}$ requires that $\left\{\partial\Pi_{pP}/\partial q\right\}=\{0\}$, which leads to

$$\left([K]+[K_C]^T[\alpha][K_C]\right)\{q\}=\{R\}+[K_C]^T[\alpha]\{Q\} \tag{3.7}$$

where $[K_C]^T[\alpha][K_C]$ is the penalty matrix.

On the other hand, in the Lagrange multiplier method, the contact constraint equation can be written as:

$$w=\{\eta\}^T\left([K_C]\{q\}-\{Q\}\right) \tag{3.8}$$

where the components of the row vector η_i (i=1, 2, …, N), are often defined as Lagrange multipliers η_i.

Adding Eq. 3.8 to the potential energy in Eq. 3.1, we have the total energy in the Lagrange multiplier method,

$$\Pi_{pL} = \frac{1}{2}\{q\}^T [K]\{q\} - \{q\}^T \{R\} + \{\eta\}^T ([K_C]\{q\} - \{Q\}) \tag{3.9}$$

The minimization of Π_{pL} with respect to $\{q\}$ and $\{\eta\}$ requires that $\left\{\partial \Pi_{pL} / \partial q\right\} = \{0\}$ and $\left\{\partial \Pi_{pL} / \partial \eta\right\} = \{0\}$, which leads to,

$$\left\{\partial \Pi_{pL} / \partial q\right\} = [K]\{q\} + [K_C]^T \{\eta\} - \{R\} = \{0\} \tag{3.10}$$

$$\left\{\partial \Pi_{pL} / \partial \eta\right\} = [K_C]\{q\} - \{Q\} = \{0\} \tag{3.11}$$

In a matrix form, Eq. 3.10 and 3.11 can be expressed as,

$$\begin{bmatrix} [K] & [K_C]^T \\ [K_C] & [0] \end{bmatrix} \begin{Bmatrix} \{q\} \\ \{\eta\} \end{Bmatrix} = \begin{Bmatrix} \{R\} \\ \{Q\} \end{Bmatrix} \tag{3.12}$$

While the constraints in Eq. 3.8 can be satisfied, the Lagrange multiplier method has disadvantages. Because the stiffness matrix in Eq. 3.12 may contain a zero component in its diagonal, there is no guarantee of the absence of the saddle point. In this situation, the computational stability problem may occur. In order to overcome that difficulty, a perturbed Lagrange multiplier method was introduced (Aliabadi, 1993).

$$\begin{aligned} \Pi^p{}_{pL} &= \Pi_{pL} - \frac{1}{2\alpha'}\{\eta\}^T \{\eta\} \\ &= \frac{1}{2}\{q\}^T [K]\{q\} - \{q\}^T \{R\} + \{\eta\}^T ([K_C]\{q\} - \{Q\}) - \frac{1}{2\alpha'}\{\eta\}^T \{\eta\} \end{aligned} \tag{3.13}$$

where α' is an arbitrary positive number. At the limit α' goes to ∞, the perturbed solutions converge to the original solutions. The introduction of α' will maintain a small force across and along the interface. This will not only maintain stability but also avoid the stiffness matrix being singular, due to rigid body motion. Similarly, the minimization of $\Pi^{p}{}_{pL}$ with respect to $\{q\}$ and $\{\eta\}$ results in the following matrix,

$$\begin{bmatrix} [K] & [K_C]^T \\ [K_C] & -\frac{1}{\alpha'}[I] \end{bmatrix} \begin{Bmatrix} \{q\} \\ \{\eta\} \end{Bmatrix} = \begin{Bmatrix} \{R\} \\ \{Q\} \end{Bmatrix} \tag{3.14}$$

Eq. 3.14 can be expressed as:

$$[K]\{q\} = \{R\} - [K_C]^T \{\eta\} \tag{3.15}$$

$$\{\eta\} = \alpha'([K_C]\{q\} - \{Q\}) \tag{3.16}$$

Substitute Eq. 3.16 into Eq. 3.15,

$$\left([K] + [K_C]^T \alpha' [K_C]\right)\{q\} = \{R\} + [K_C]^T \alpha' \{Q\}$$

For simplicity, let all α_i in $[\alpha]$ of penalty function equal to α', i.e. $\alpha_i = \alpha'$. Thus, the perturbed Lagrange multiplier is equivalent to the penalty function method.

In the Lagrange multiplier method, both displacement and contact force are regarded as independent variables; thus, the constraint (contact) conditions can be satisfied and the contact force can be calculated. It has disadvantages. The stiffness matrix contains zero components in its diagonal, and the Lagrange multiplier terms must be treated as additional variables. This leads to the construction of an augmented stiffness matrix, the order of which may significantly exceed the size of the original problem in the absence of

constraint equations (Aliabadi, 1993). In comparison with the Lagrange multipliers method, the implementation of the penalty function method is relatively simple and does not require additional independent variables. It is often adopted in the practical analysis because of its simple implementation.

3.2 Contact Conditions

Based on an iterative scheme (Mazurkiewicz, 1983), the contact conditions in FEA model are classified into the following three cases:

1. Open condition: gap remains open;
2. Stick condition: gap remains closed, and no sliding motion occurs in the tangential directions; and
3. Sliding condition: gap remains closed, and the sliding occurs in the tangential directions.

Let f_{ji} and u_{ji} be the contact nodal load vector and the nodal displacement, respectively, which are defined in the local coordinate system, where the subscript j indicates the component number (j = I or J), and i indicates the coordinate (i = n, t, τ), as shown in Figure 3.3. By equilibrium of the contact element, $\vec{f}_{In} + \vec{f}_{It} + \vec{f}_{I\tau} + \vec{f}_{Jn} + \vec{f}_{Jt} + \vec{f}_{J\tau} = 0$. F_i (i = n, t, τ) is the external nodal load in i direction $\{R\} = \sum_{x=1}^{n} \begin{pmatrix} F_n \\ F_t \\ F_\tau \end{pmatrix}_x$ where x is the node number of body I or body J. The displacement and force must satisfy the equilibrium

equations in the three contact conditions (note that {n, t, τ} is the local coordinate system).

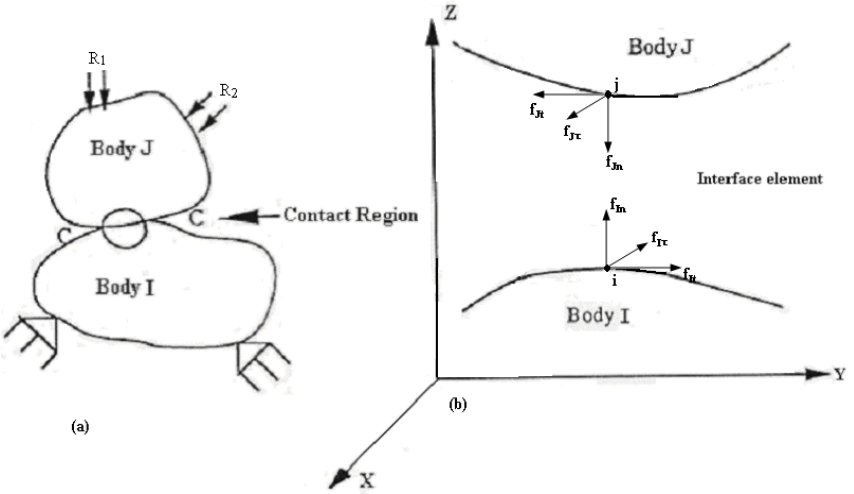

Figure 3.3 Sketch of Contact Force on the Contact Surface

3.2.1 Open Condition

When the normal nodal force F_n is positive (tension), the contact is broken, and no force is transmitted. The displacement change in the normal and tangential directions, denoted respectively by $\Delta u_i \quad (i = n,t,\tau)$, then is

$$\Delta u_n = u_{Jn} - u_{In} + \delta_n, \quad f_{Ji} = f_{Ii} = 0 \qquad (i = n,t,\tau) \tag{3.17}$$

where u_{Jn} and u_{In} are the current displacements of node J and node I in a normal direction, respectively. For each structural contact element, stiffness and forces are updated, based upon current displacement values, in order to predict new displacements and contact forces. δ_n is the gap between a pair of the potential contact points. In each increment of load, the gap status and the stiffness values are iteratively changed until convergence. As

the load is increased, δ_n will change and hence should be adjusted as $\delta_n = \delta^0{}_n - \delta^T{}_n$, where $\delta^0{}_n$ is the initial gap before any deformation and $\delta^T{}_n$ is the gap change caused by the total combined normal movement at the pair of points.

3.2.2 Stick Condition

The force in the tangential direction (F_S), which is the composition of the nodal force in t and τ directions (F_t and F_τ), is defined only when $F_n < 0$ (compression). When the absolute value of F_S is less than $\mu \mid F_n \mid$, where μ is the Coulomb friction coefficient, there is no slide-motion in the interface, and the contact element responds like a spring. The stick condition exists if $\mu \mid F_n \mid > \left\| \left(u_{Jt} k_t + u_{J\tau} k_\tau\right) - \left(u_{It} k_t + u_{I\tau} k_\tau\right) \right\|$. That is,

$$f_{Ii} = -f_{Ji}, \quad u_{Jn} - u_{In} + \delta_n = 0, \quad u_{Ji} - u_{Ii} = 0, \quad (i = t, \ \tau), \tag{3.18}$$

where k_t and k_τ are the tangential contact stiffness in t and τ directions, respectively. In the analysis of fixture unite stiffness, set $k_t = k_\tau$.

3.2.3 Sliding Condition

Slide-motion will occur when the absolute value of F_S is more than $\mu \mid F_n \mid$. The slide-motion may occur in both the element t and τ directions. That is, if $\mu \mid F_n \mid < \left\| \left(u_{Jt} k_t + u_{J\tau} k_\tau\right) - \left(u_{It} k_t + u_{I\tau} k_\tau\right) \right\|$, then,

$$f_{It} = -f_{Jt} = \left(\pm \mu F_n\right)_t, \quad f_{I\tau} = -f_{J\tau} = \left(\pm \mu F_n\right)_\tau, \quad f_{In} = -f_{Jn}, \quad u_{In} - u_{Jn} + \delta_n = 0 \tag{3.19}$$

where $\left(\pm \mu F_n\right)_t$ and $\left(\pm \mu F_n\right)_\tau$ mean the maximum friction force in t and τ directions.

3.3 Solution Procedure

The model presented in the previous section can be implemented to determine the fixture unit stiffness in clamping and machining. Because the model involves high nonlinearity, the Newton-Raphson (N-R) approach is used to solve the problem. Considering the full Newton-Raphson iteration it is recognized that in general the major computational cost per iteration lies in the calculation and factorization of the stiffness matrix. Since these calculations can be quite expensive when large-order systems are considered, the modified Newton-Raphson algorithm is used in this research (Bathe, 1996). Given the applied load R and the corresponding displacement u, the applied load is divided into a series of load increments. At each load step, the contact stiffness and contact conditions remain constant. And several iterations may be necessary to find a solution with acceptable accuracy. The modified Newton-Raphson method is used first to evaluate the initial out-of-balance load vector at the beginning of the iteration at each load step. The out-of-balance load vector is defined as the difference between the applied load vector R and the vector of restoring loads R_i^r. When the out-of-balance load is non-zero, the program performs a linear solution, using the initial out-of-balance loads, and then checks for convergence. If the convergence criteria are not satisfied, the out-of-balance load vector is reevaluated, the new contact conditions and the stiffness matrix are updated, and a new solution is obtained. This iterative procedure continues until the solution converges. A flowchart of the analysis procedure is outlined in Figure 3.4(a). Figure 3.4(b) shows the modified Newton-Raphson method.

Figure 3.4 (a) Flow Chart of the Analysis Procedure

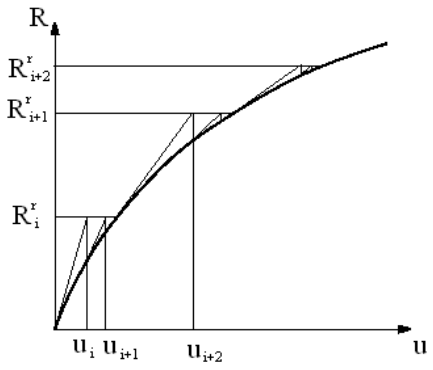

Figure 3.4 (b) Modified Newton-Raphson Method

3.4. Modeling Validation

To determine its effectiveness, the FEA model of the fixture unit stiffness was used to analyze two cases. The first case is the static contact problem of two, three-dimension identical beams, each having a dimension of 10×10×50 in. as shown in Figure 3.5. The left side of the first beam is fixed, and its right side is connected the second beam by nine contact elements. A distributed compressive load, Q, is horizontally applied to the nodes on the right side of the second beam, and a concentrated load, F, is vertically applied to the lowest node at the right side of the second beam. The contact conditions of the two beams are specified by the friction coefficient, μ=0.2, the normal contact stiffness, k_n = 1.75×10^7 lb/in, and the tangential contact stiffness, k_t = 1.75×10^7 lb/in.

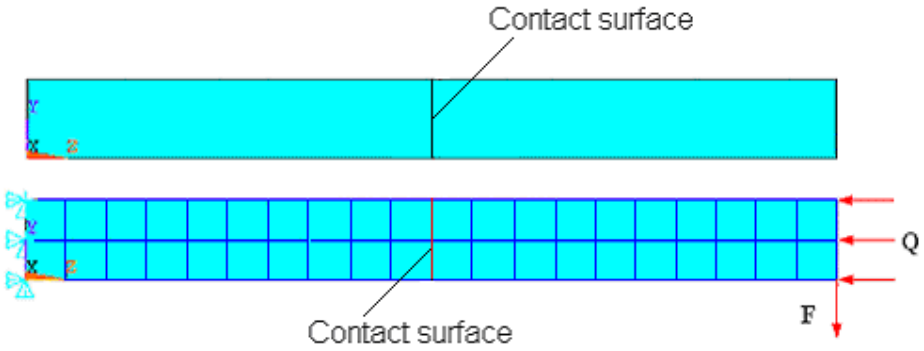

Figure 3.5 Contact Problem between Two Beams Subjected to End Loads

In the contact problem of the two beams, the contact elements are used to model the interface between two beams. When two beams are in contact, the contact element itself can be treated as three independent linear springs, having stiffnesses k_t, k_τ, and k_n, oriented in tangential and normal directions, respectively. The contact stiffnesses k_t and k_n may vary with respect to different contact conditions. When the contact stiffness

becomes infinitely large, the structure should become a single continuous beam, as shown in Figure 3.6, whose analytic solution can be easily obtained.

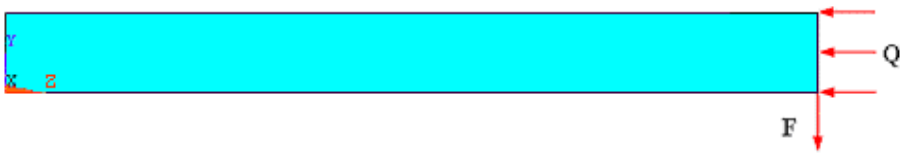

Figure 3.6 An Equivalent Single Continuous Beam

Figure 3.7 shows a comparison of the deflection curves of the contacted beam with different contact stiffness, as well as the analytical solution of the corresponding single continuous beam. In Figure 3.7, when the contact stiffness is sufficiently large, the deflection curve is very close to the analytical solution, and the difference between the two solutions becomes invisible. When the contact stiffness is smaller, the deflection of the right beam becomes larger. The results from the FEA validate the contact model and show the significant effects of contact stiffness on the deformation of the contact beams.

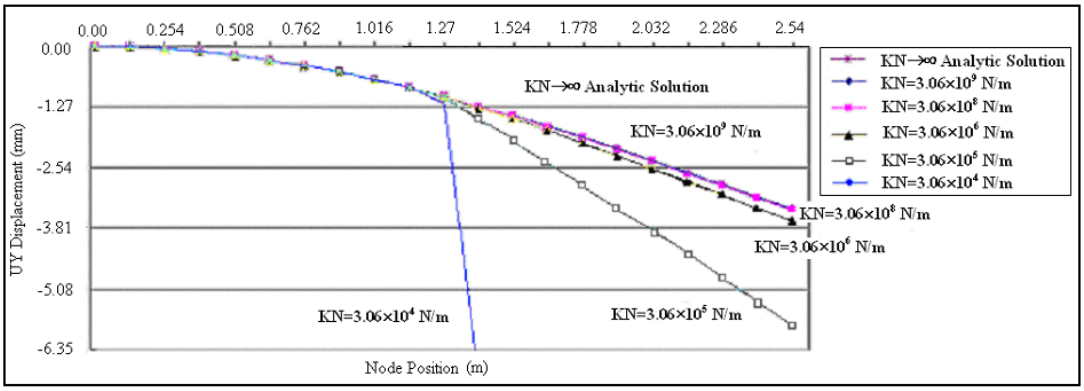

Figure 3.7 Comparison of the Deflection of a Contact Beam (at the Position Y=0 in. and Z=10 in.) Having Variable Contact Stiffness with the Corresponding Single Continuous Beam

The other case is to analyze the typical fixture unit, which includes two deformable components (a 500×500×100 mm fixture base and a 100×100×300 mm support), as shown in Figure 3.8.

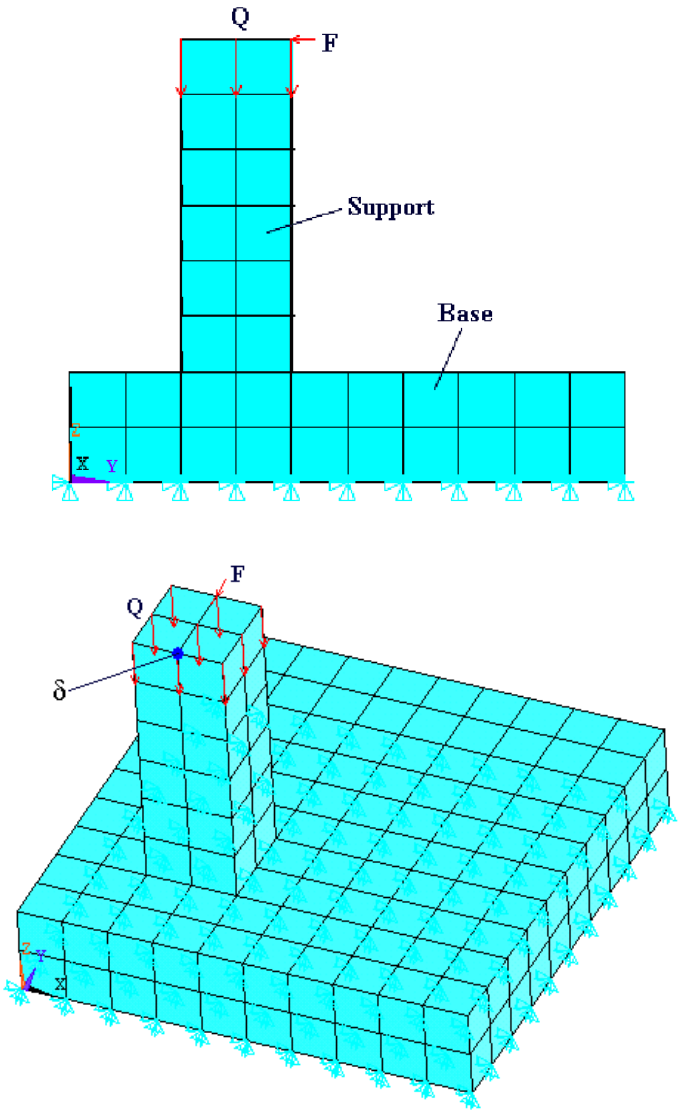

Figure 3.8 The FEA Model of a Typical Fixture Unit

The bottom of the fixture base is fixed. The evenly distributed load, Q, is applied to the nodes on the top of support, simulating the fastening force in the fixture. A concentrated

load F, parallel with the fixture base, is applied to the node on the top of the support, in simulating the external (clamping and/or machining) force passed through the workpiece fixtured. The fixture-unit deflection is measured as δ (at the position of x=150mm, y=100mm, and z=400mm) in y direction at the top of the support, as shown in Figure 3.8. Similar contact conditions to those in Figure 3.5 are considered in this case. Contact stiffness and the friction condition between the fixture base and support are considered. Table 3.1 shows the numerical results of a FEA simulation on the fixture-unit deflection under different combinations of the fastening force Q and the external force F.

Table 3.1 Deflection of the Fixture Unit for Different Load Combinations

Case1 Q=3555N (800lb)		**Case2** Q=5337N (1200lb)		**Case3** Q=7110N (1600lb)	
F (N)	δ (mm)	F (N)	δ (mm)	F (N)	δ (mm)
300	0.00958	300	9.62E-03	300	9.66E-03
400	0.01442	400	1.28E-02	500	1.60E-02
500	2.47E-02	600	2.16E-02	700	2.25E-02
550	3.01E-02	700	3.18E-02	900	3.90E-02
580	3.33E-02	800	4.24E-02	1000	4.94E-02
590	3.44E-02	850	4.77E-02	1100	6.00E-02
593.5	3.49E-02	891.5	5.25E-02	1189	7.00E-02

Case4 Q=8892N (2000lb)		**Case5** Q=10674N (2400lb)		**Case6** Q=12456N (2800lb)	
F (N)	δ (mm)	F (N)	δ (mm)	F (N)	δ (mm)
300	9.70E-03	300	9.73E-03	300	9.77E-03
500	1.60E-02	500	1.61E-02	500	1.61E-02
700	2.24E-02	700	2.24E-02	700	2.24E-02
900	2.90E-02	900	2.87E-02	900	2.88E-02
1100	4.62E-02	1100	3.55E-02	1100	3.52E-02
1300	6.71E-02	1300	5.34E-02	1300	4.20E-02
1485	8.74E-02	1500	7.41E-02	1500	6.05E-02
		1700	9.54E-02	1700	8.11E-02
		1782	0.10479	1900	0.10242

Note that different ranges of force F are selected for a given Q in Table 3.1. Physically, a given fastening force Q can only hold a working external force to a fixed limit. Numerically, an extremely large value of F for a given Q may cause a solution not to converge.

A typical curve of fixture deflection against the external force of FEA results is shown in Figure 3.9. The curve can be divided into three stages: the linear first stage (I), the second nonlinear stage (II), and the third linear stage (III), which is consistent with previous experimental results (Zhu, 1993). In the first stage, for a small external force F, the deflection of the fixture components contributes to elastic deformation. The nonlinearity of the deflection curve in the second stage is mainly caused by the interface between the fixture base and the support, which dominates the overall deflection. In this stage, the support begins to separate from the fixture base, which causes a decrease of actual contact area and a rapid increase in the deflection. When the external force continuously increases, the separation becomes stabilized, and the deflection tends to be linear again in the third section.

Under variable fastening forces, the division of the three stages may be different. When the fastening force Q is small, the contact stiffness between fixture components is also small, is the overall fixture unit stiffness. Figure 3.10 summarizes the deflection curves of the typical fixture unit, where the fastening force is fixed in each case and external force increases. Figure 3.11 shows the experimental results of the deflection curves under different fastening forces (Zhu, 1993). It is obvious that the FEA results match the

experimental results in trend. The difference between experimental results and FEA results is caused by the simplification of the FEA model.

It can be seen that increasing the fastening force will enhance the fixture unit stiffness and decrease total deformation. However, large fastening forces may cause other problems, such as the wear of fixture components, particularly when using modular fixtures.

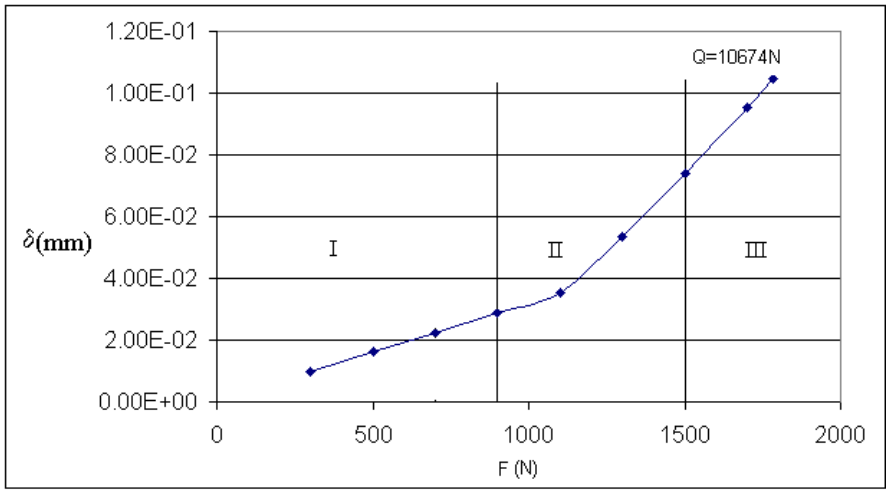

Figure 3.9 Typical Deflection Curve of Fixture Units from FEA

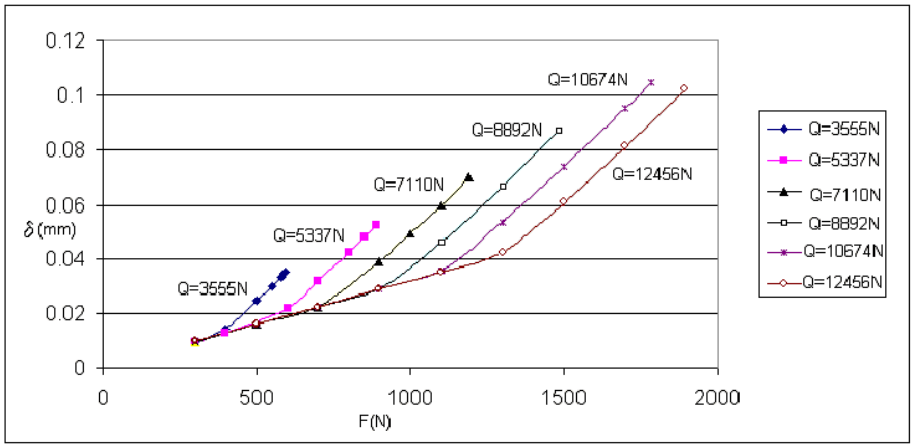

Figure 3.10 Deflection Curves under Different Fastening Forces from FEA

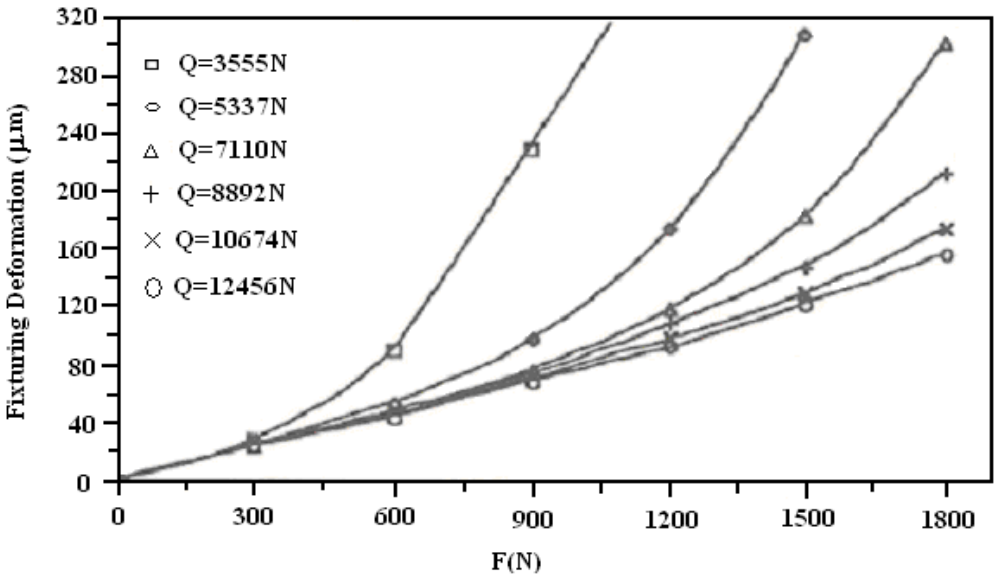

Figure 3.11 Deflection Curves from Previous Experiments (Zhu, 1993)

3.5. Conclusions

In this chapter, an FEA model of fixture unit stiffness was developed. A contact element is utilized for solving the contact problem encountered in the study of fixture unit stiffness. The FEA model and the analysis procedure were validated by two examples: a simple beam analysis and a typical fixture unit. The results are compared with the corresponding analytical solution and experimental results in the literature. The agreements between those results demonstrate the great potential of the proposed model for the future study of stiffness of fixture units in general configurations, such as a fixture with multiple units and components. The analysis of the beam shows that contact stiffness has a significant effect on the accuracy of the results. The contact stiffness of fixture components is one of the key parameters in the analysis of fixture stiffness, which is assumed known in this chapter.

Chapter 4: Contact Stiffness Identification

4.1 Introduction

In the study of fixture unit stiffness, an FEA model has been applied to fixture unit stiffness analysis, where contact elements are used to model the contact and friction conditions. It is assumed that contact stiffness is known. This study shows that contact stiffness has a significant contribution on fixture unit stiffness and that it is one of the critical parameters used to form the FEA formulation. Consequently, in order for the FEA model to be used with confidence, the contact stiffness for the fixture-workpiece system must be known along with their expected ranges of variation.

Contact stiffness includes normal contact stiffness and tangential contact stiffness illustrated in Figure 4.1, and may vary with respect to its contact condition, such as external load, geometry, material property, etc. Previous works on the fixture-workpiece system are very preliminary; they either simply apply the Hertzian contact model or consider the effective contact area. Contact stiffness data that correlate directly to contact conditions typically found in machining fixture applications are difficult to find. Consequently, a need exists for the experimental estimation of contact stiffness in normal and tangential directions, and the investigation of the parameters that the contact stiffness is most sensitive to.

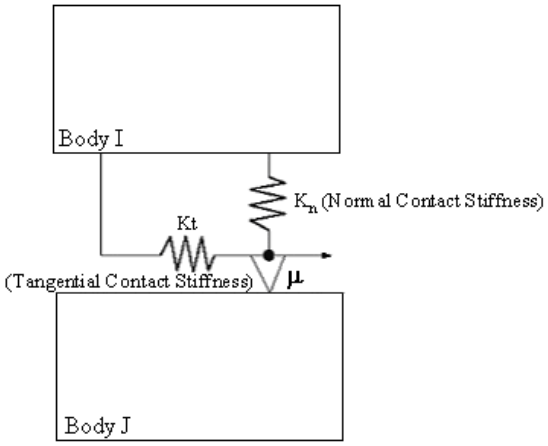

Figure 4.1 Sketch of Contact Stiffness

The purpose of this chapter is to present the methods and results of a more comprehensive experimental study that is conducted to determine contact stiffness. In this chapter, two identification methods are proposed to extract contact stiffness. First, the static test for normal contact stiffness estimation is discussed, and the effects are studied. Then the dynamic test method is developed, since it is difficult to use a static test to estimate tangential contact stiffness. The validity and feasibility of the proposed dynamic methods are verified by the results based on the static tests of normal contact stiffness.

4.2 Normal Contact Stiffness Estimation Using Static Experiments

4.2.1 Experimental system

When two fixture components are in contact, they will contact at a few asperities. If the normal loads increase, the contact deformation in the interface may increase nonlinearly. Additionally, the contact stiffness may change. The conceptual model for the identification of normal contact stiffness is shown in Figure 4.2. First of all, the proximity was selected for contactless measurement of the total displacement of the specimens. The

proximity is connected to a multimeter. The system outputs a voltage proportional to the total displacement at the measuring position. When normal loads change, there is a corresponding change in the output voltage. Therefore, the total displacements are measured under different normal loads at the measuring point, relative to the base. The total displacement of the specimen includes contact displacement and structure displacement. The structure displacements between the measuring point and the contact surface of the specimen can be calculated theoretically. The contact displacements can be obtained from the difference between total displacement and structure displacement. The contact stiffness, K_n, would be estimated according to the definition of contact stiffness. Contact stiffness is equal to surface pressure divided by contact displacement. Therefore contact stiffness can be estimated. This static experimental approach is principally useful for the estimation of normal contact stiffness, since it is difficult to measure displacement in a tangential direction. The assumptions involved are: 1) The material is homogenous and linearly elastic; 2) When normal load changes, contact stiffness will also change; 3) The frictional force acting on the contact surface follows the Coulomb law of friction.

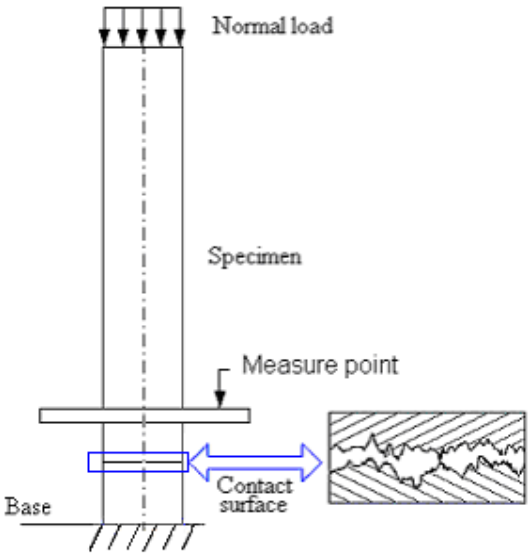

Figure 4.2 Experimental Model

The environmental conditions and fixture component parameters investigated in this research are those chosen as being pertinent to the fixture-workpiece system. Since the magnitude of contact stiffness depends on the normal load and the contact surfaces, the effects of the normal load, contact area, and surface roughness are investigated. Figure 4.3 shows the factors used in this work and their levels. Each experiment is executed under different normal loads. The test is repeated thirty-two times. There are three additional factors investigated: 1) testing environment: measurements over two days are compared; 2) contact area: two samples that have different contact areas are used to compare the effect of the contact area; 3) surface roughness: three samples that have the same size but different surface roughness are used to compare the effect of surface roughness. The effect of each factor can be estimated by finding the average value for the response variable at all levels, then comparing the arithmetic difference between these average values. Since the factors are independent, the other factors do not distort the estimate of the effect of any particular factor.

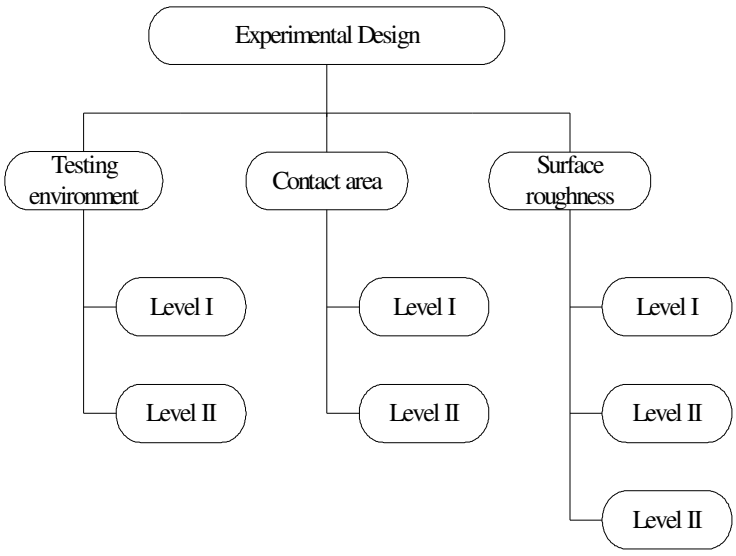

Figure 4.3 Levels of Independent Variables

An experimental setup is designed to study the relationship of normal contact stiffness and normal loads according to the experimental model. Figure 4.4 shows the experimental sketch. The study was conducted employing cylindrical specimens with different contact areas made of steel AISI 4150. The material prosperity is shown in Table 4.1. The contact surface was generated in a turning operation.

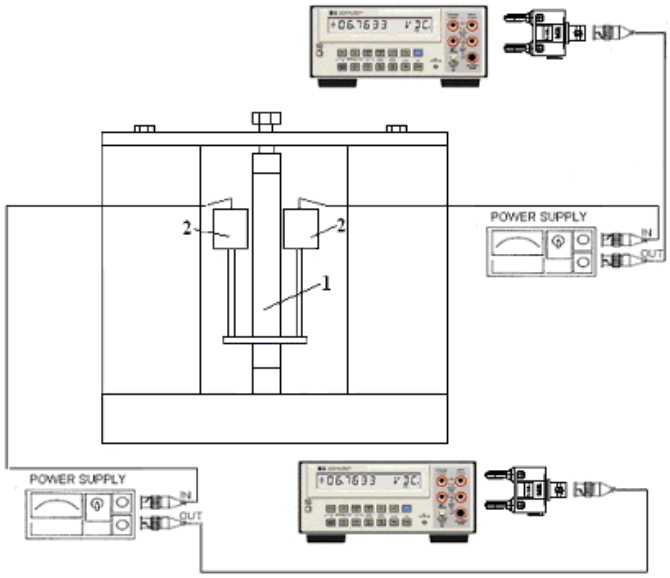

1. Specimen 2. Proximity

Figure 4.4 Experimental Sketch

Table 4.1 Material Prosperity of Specimens

Material	AISI 4150
Elastic Module	$E=29.7\times10^{6}$ lbf/in^2
Density	0.008827 slug/in^3
Poisson's ratio	0.33

The experimental setup is comprised of multimeters (HP3478A), the power supply (482A04), the fixture, and the proximity (PX032-1), as shown in Figure 4.5. The

specimens are fixed into the fixture. In order to apply preloads, the upper plate, two blocks, two riser plates, and the base plate were chosen as a fixed reference frame. The preload bolt and the indenter are used to apply uniform distribution of normal loads in a normal direction. A torque wrench with a capacity of 250 in-lb is used to measure normal loads. The proximities are calibrated.

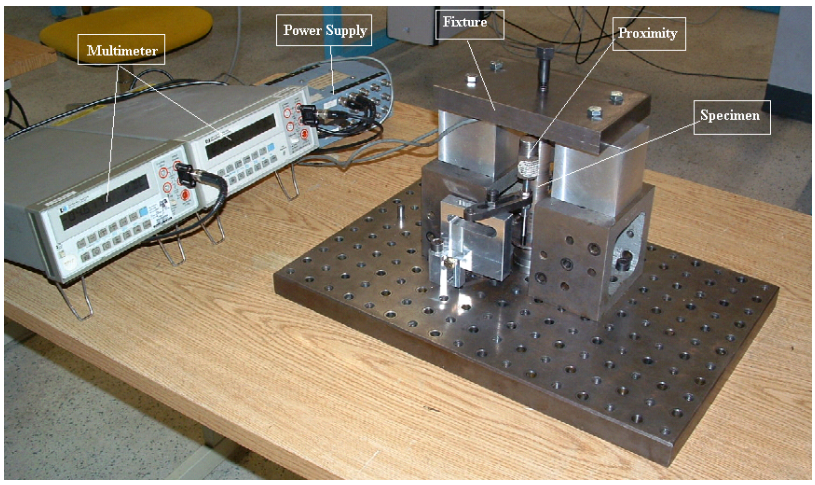

(a) Experimental Setup

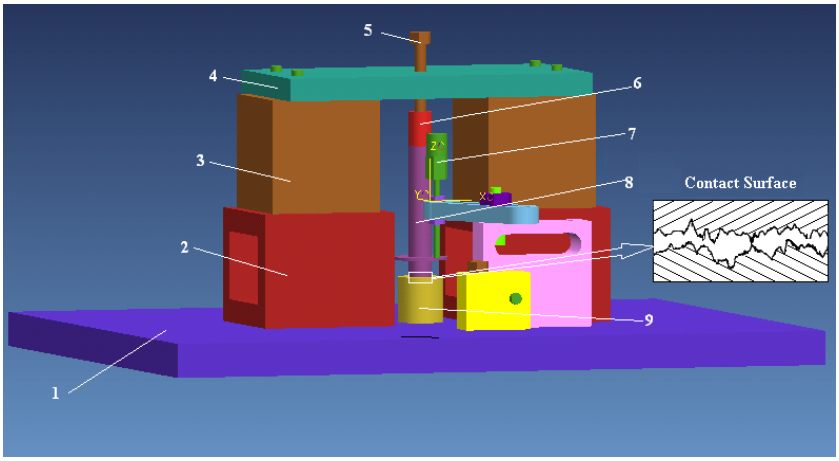

(b) Fixture Setup Sketch

1. Base plate, 2. Riser plate, 3. Block, 4. Upper plate, 5. Preload bolt, 6. Indenter, 7. Proximity, 8. Sample, 9. Base plate

Figure 4.5 Experimental Setup

4.2.2 Experimental Procedure and Results

The experiments are performed by displacing the indenter against the specimens by a specified force magnitude, using a torque wrench. The normal load caused by bolt preload can be computed as follows (Shigley, 2001):

$$N = \frac{T}{(K \times D)} \tag{4.1}$$

where N is normal load, T is bolt installation torque, K is torque coefficient K=0.2, and D is bolt nominal diameter D=0.5in.

The experiment of each specimen involves different magnitudes of normal loads. The purpose for the linearly increase of the normal load is to identify the nonlinearity that may occur in the contact deformation process. The designated measure of normal load adopted is surfaces pressure. Surface pressure, P, is calculated by

$$P = N / A_s \tag{4.2}$$

where A_s is the area of the cross-section of the specimen. Table 4.2 shows applied torques, the resulted normal loads and surface pressure.

Table 4.2 Applied torque, the resulted normal loads and surface pressure

Torque (in-lbf)	Normal loads (lbf)	Surface Pressure (lbf/in^2)
25	250	318.47
40	400	509.55
55	550	700.64
70	700	891.72
85	850	1082.8
100	1000	1273.88
115	1150	1464.97
130	1300	1656.05
145	1450	1847.13
160	1600	2038.22

The proximity sensor measures the relative displacement between the sensor probe and the measured point of the specimen by recording the output voltage change. A negative or positive value of measurement indicates that the measuring point of the specimen is getting close to or far away from the sensor. Therefore, the displacement at the measured point is calculated with the aid of the proximity. In the test, the output voltage is recorded and then converts to the displacement corresponding to the different normal loads. The total displacement can be calculated from the relative output voltage as Eq. 4.3, since the output voltage is proportional to the displacement

$$D_t = V \times \hbar \tag{4.3}$$

where D_t is total displacement; V is relative output voltage; $\hbar$ is the calibration coefficient.

The total displacement can be decomposed into two individual components: the structure displacements and the contact displacement. The structure displacement D_s can be achieved using Eq. 4.4

$$D_s = \frac{Nl_s}{EA_s} \tag{4.4}$$

where D_s is the structure displacement; l_s is the measurement length; E is Young's module; and A_s is the cross-section area. Since the structure displacements can be theoretically calculated, the contact displacement (D_c) can be obtained by Eq. 4.5.

$$D_c = D_t - D_s \tag{4.5}$$

A measure of the contact load adopted is surface pressure, P. According to the definition of the stiffness, normal contact stiffness can be computed from the contact deformation and contact surface pressure, as shown in Eq. 4.6. Figure 4.6 shows the procedure for contact stiffness identification.

$$k_n = \frac{P}{D_c} \tag{4.6}$$

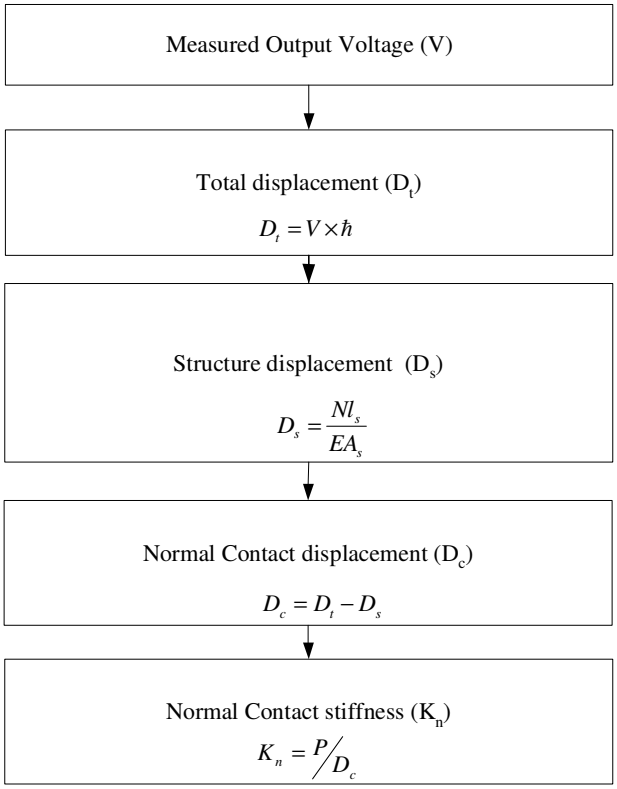

Figure 4.6 Procedure of Normal Contact Stiffness Identification

Since the total displacement of the specimen is obtained by measuring output voltage in the various normal loads, Figure 4.7(a) shows the relative measured output voltage. The experiments are repeated thirty-two times. Figure 4.7 (b) shows the arithmetic mean of the relative measured output voltage. It shows that the trend is nonlinear. Because the voltage output is proportional to displacement, the total displacement of the specimen can be obtained according to Eq. 4.3. The total displacement is also nonlinear. Eqs. 4.4 and 4.5 are adopted to obtain the structure displacement and contact displacement as shown in Figure 4.8. Figure 4.9 shows the contact stiffness and structure stiffness according to Eq.

4.6. It is clear that the nonlinearity occurs in the contact deformation process. The contact displacement is nonlinear, and the contact stiffness is linear to the normal load. Compared to the contact displacement, the structure displacement is small because it is only a portion of the structure displacement, i.e., the portion from measuring point to contact surface. Therefore, the corresponding structure stiffness is large.

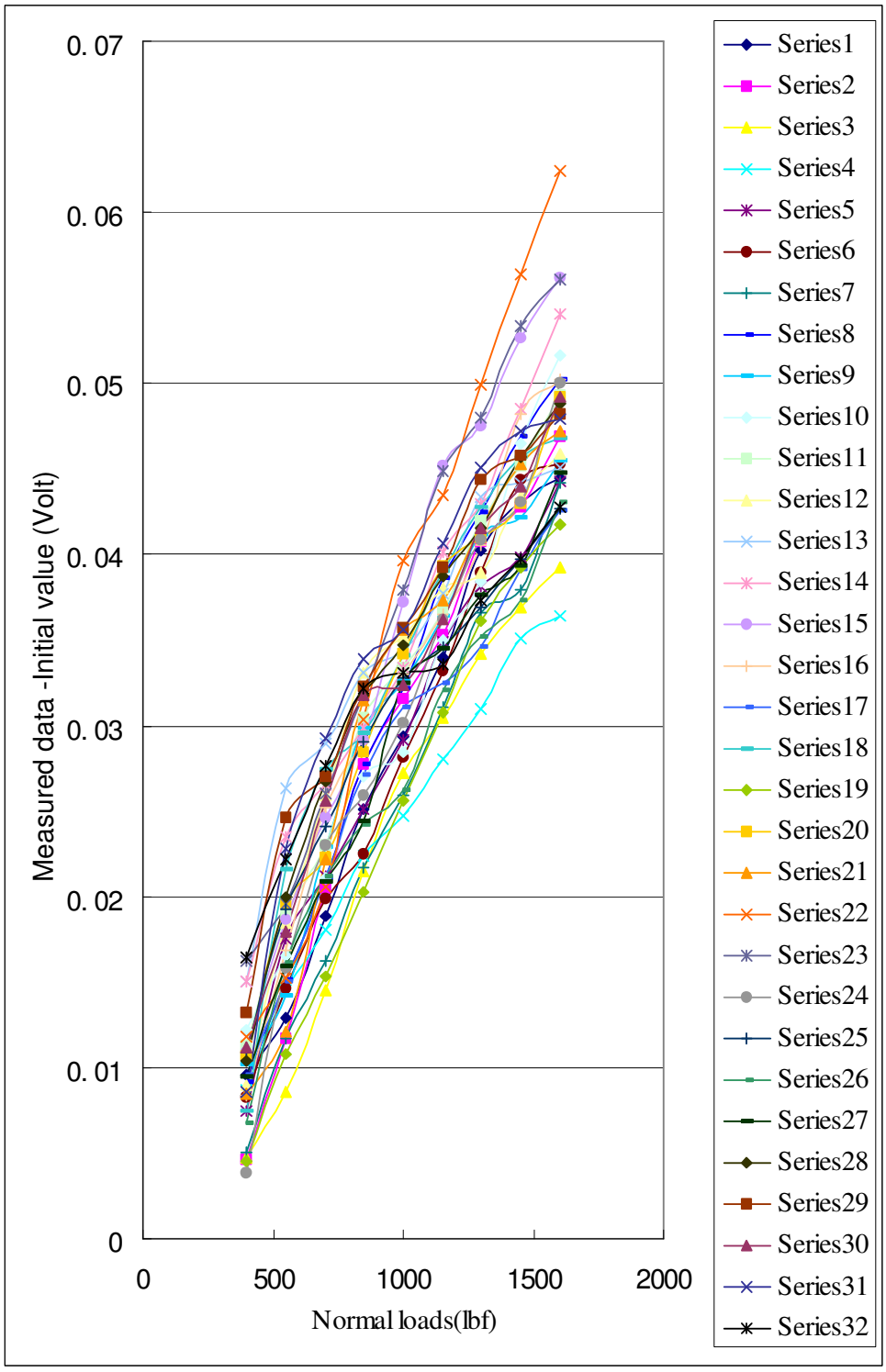

(a) All Relative Data Versus Normal Loads

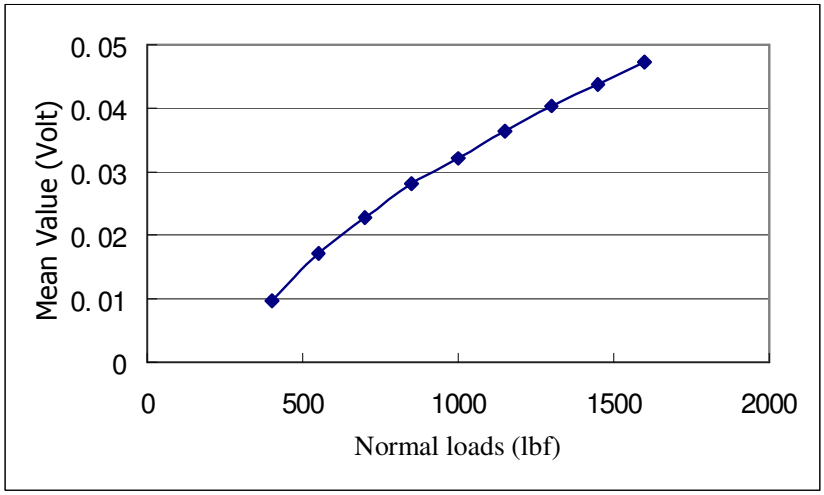

(b) Mean Value of the Relative Measured Data

Figure 4.7 Measured Results of Output Signal versus the Normal Loads
(Surface finish Ra = 3.08; Radius =0.5in)

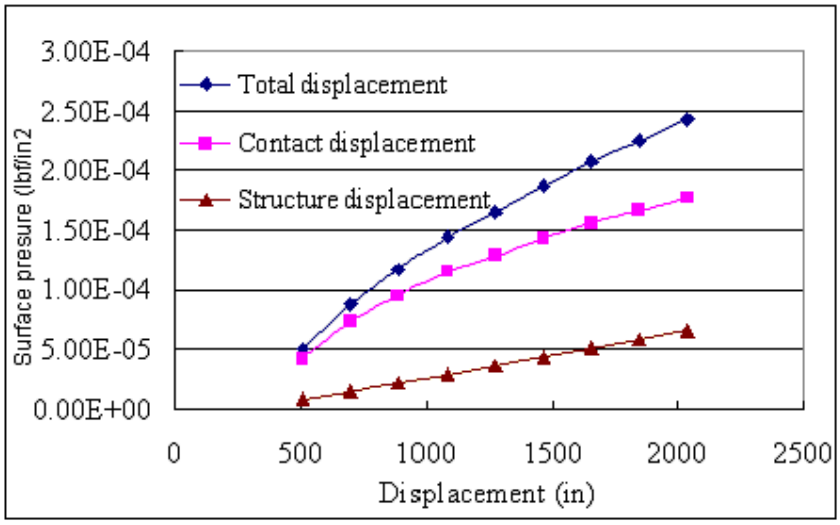

Figure 4.8 Structure and Contact Displacements versus Surface Pressure
(Surface Finish Ra = 3.08; Radius =0.5in)

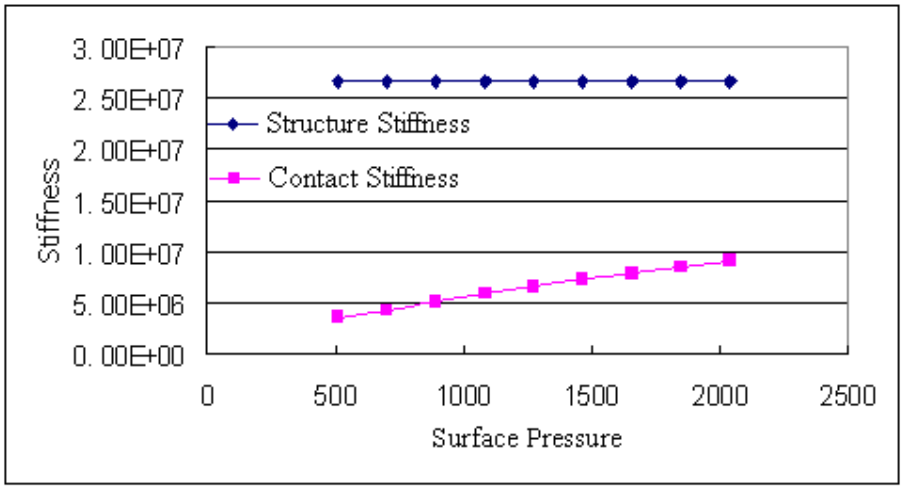

Figure 4.9 Structure Stiffness and Contact Stiffness versus Normal Loads
(Surface Finish Ra = 3.08; Radius =0.5in)

4.2.3 Experimental Result Analysis

Three additional sets of factorial experiments were performed to characterize contact stiffness for various fixture component joints and to identify factors that have a significant effect on contact stiffness. As mentioned before, the factors investigated are: (1) test environmental effect, (2) contact area effect, (3) surface finish effect.

4.2.3.1 Test Environmental Effect

In order to investigate the effects of the testing environment on the experimental results, two sets of experiments were conducted at different dates, as shown in Appendix A.1 (a) and (b). Figure 4.10 shows the variation through the comparison of the mean value of the relative measured data. The confidence that the mean output voltages in day 1 and day 2, and the total mean value are located within 95% confidence interval. The mean output voltages in day 1 and day 2 are also shown in Figure 4.10, which shows no significant difference in the results.

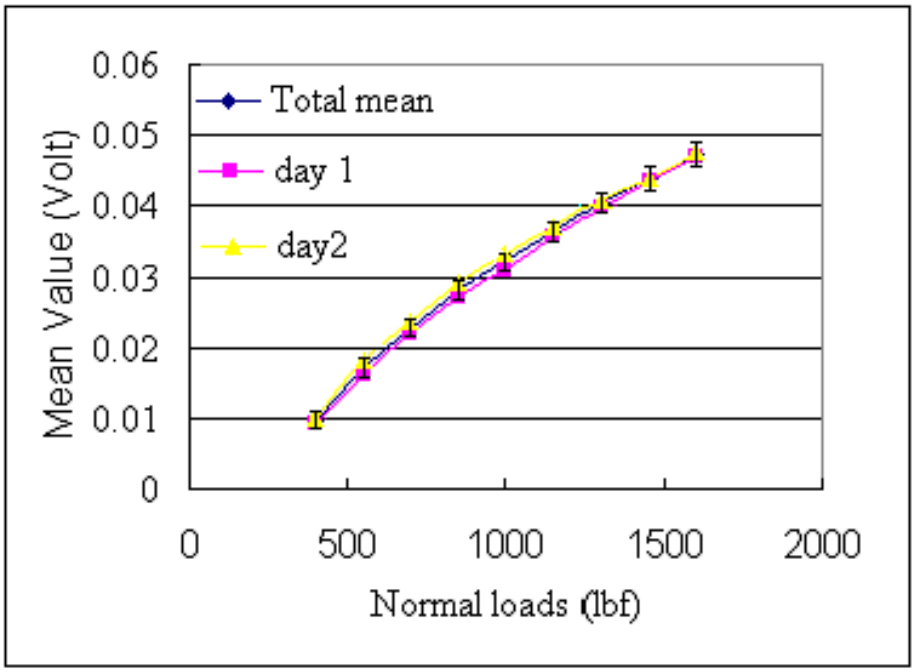

Figure 4.10 Measured Results of Output Signal vs. the Normal Loads
(Surface Finish Ra = 3.08; Radius =0.5in)

4.2.3.2 Contact Area Effect

In order to study the effects of the contact area, two different diameters of the specimens are used in the experimental study. The diameters of the specimens are 1.0 in and 0.75 in, respectively. The measurement data is shown in Appendices B, and C. Figure 4.11 shows the comparison of the related contact stiffness. When contact stiffness is defined as the ratio of the normal load in a unit area over contact displacement, contact stiffness is independent of the contact area.

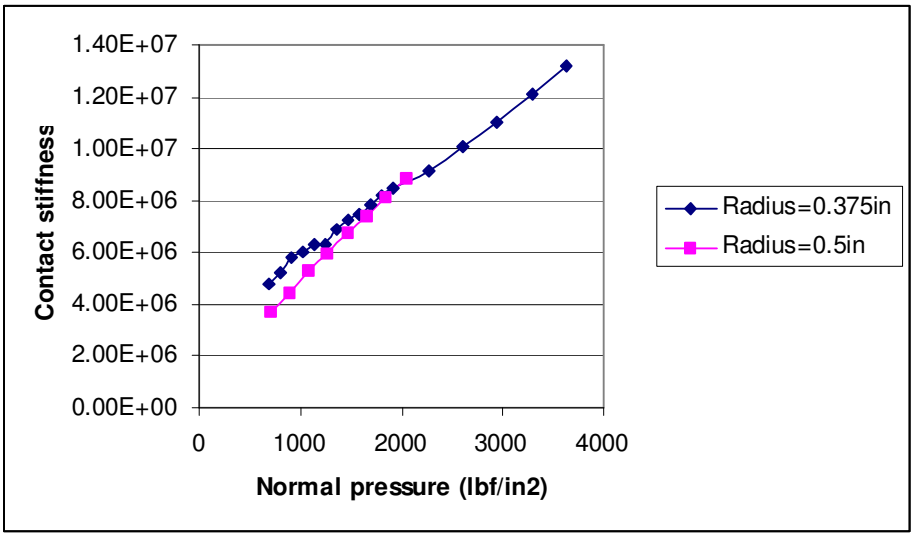

Figure 4.11 Effects of the Contact Area on the Contact Stiffness

Once the contact stiffness data are obtained from the measurements and the analytical solution, a mathematical expression can be derived through statistical regression. It is proved by an adequate test that the relationship of normal contact pressure and contact stiffness is linear. The relationship between global contact stiffness and local contact stiffness was established as shown in Appendix E. The model is obtained for the case of steel-steel that is studied in this research, with residual square summation (RSS),

$$K_n = 2.63\times10^6 + 2.94\times10^3 \times P$$

and RSS=0.97. The RSS value is the estimates of the "goodness of fit" of the line. It represents the variation of the data explained by the fitted line; the closer the points to the line, the better the fit. (Cobb, 1998) Therefore, this mathematical model presents relationships between the contact stiffness and normal contact pressure. This information can be used in fixture stiffness analysis for CAFD.

4.2.3.3 Effect of Surface Finish

When two surfaces are brought together, in most practical situations the real area of contact is only a tiny fraction of the nominal contact area due to the existence of surface irregularities. Therefore contact stiffness may be different for different surface finishes. It is important to know the effect of surface finish, and understanding about these effects needs to be studied. Three samples with different surface finish are measured. First of all, the roughness profiles, R_a, are measured by contact profilometer (Mahr Perthometer PRK), as shown in Figure 4.12. R_a is the arithmetic mean of the magnitude of the deviation of the profile from the mean line. The formula usually adopted for the R_a is given below as shown in Eq.4.7.

$$R_a = \frac{1}{l}\int_0^l |z(x)|dx \tag{4.7}$$

where | | indicates that the sign is ignored and z(x) is the profile measured from the mean line at position x; l is the sample length. The roughness profiles R_a of three samples are listed in Table 4.3 and shown in Figure 4.13.

(a) Roughness Profile Measurement

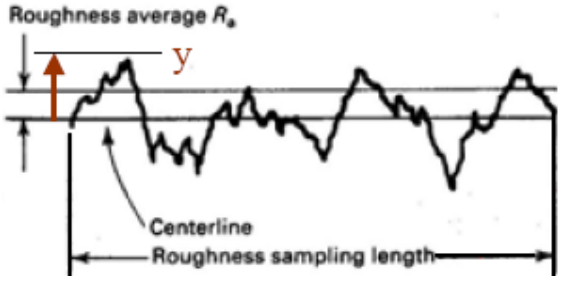

(b) R_a parameter

Figure 4.12 Roughness Profile Measurement

Table 4.3 Roughness Profiles R_a (μm)

Test	Sample 1	Sample 2	Sample 3
1	5.710	3.160	1.270
2	5.500	3.660	1.410
3	5.530	3.490	1.170
4	5.410	2.870	1.290
5	5.450	3.368	1.450
6	5.540	2.853	1.480
7	5.430	2.752	1.450
8	5.840	3.097	1.490
9	5.390	3.432	1.420
10	5.780	3.013	1.310
11	6.240	3.273	1.360
12	5.530	2.785	1.490
13	5.670	3.033	1.530
14	5.320	3.314	1.530
15	5.420	2.761	1.470
16	5.680	2.989	1.570
17	5.430	3.212	1.560
18	5.140	2.810	1.540
19	5.240	2.830	1.500
20	5.720	3.050	1.540
Mean value	5.55	3.08	1.44
Standard deviation	0.24	0.27	0.30
95% Confidence interval	0.11	0.12	0.05

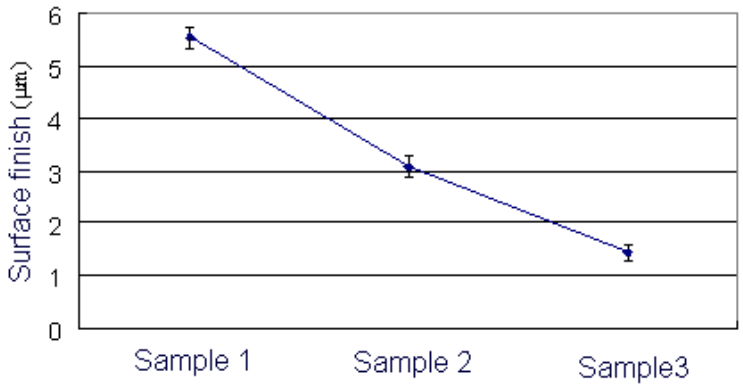

Figure 4.13 Mean Value of Surface Finish Measurement

Normal contact stiffness experiments are conducted for each of the three samples. The measurement results are shown in appendices A, B, and D. The contact stiffness data are obtained from the measurement and analytical solution. Figure 4.14 shows the contact stiffness comparison of three samples with different roughness profiles and the surface finish has a significant effect on contact stiffness. Contact stiffness is sensitive to changes in the surface finish; for different surface finishes, contact stiffness will vary. A smoother surface finish leads to higher contact stiffness.

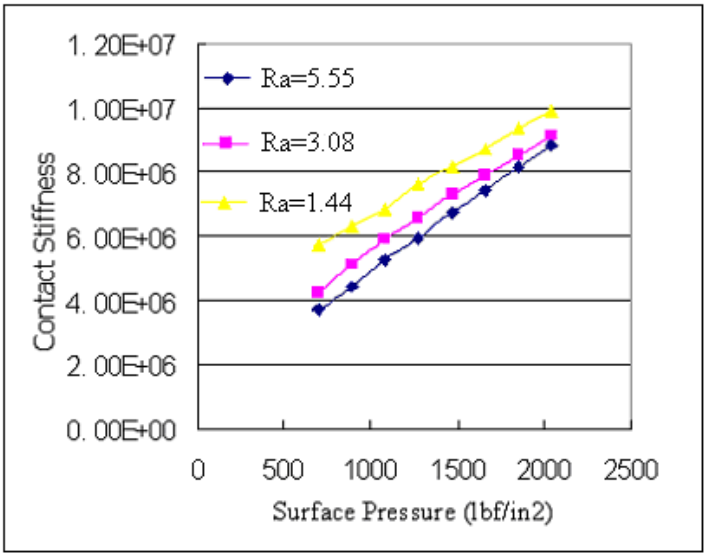

Figure 4.14 Effects of the Surface Finish on the Contact Stiffness

4.2.4 Summary

This dissertation has involved the experimental and theoretical study of normal contact stiffness. In this research, experiments are run for steel samples. Results show that nonlinearity is caused by contact displacement and contact stiffness is linear to the normal loads. Variation in the experimental data is without significant bias to the experimental conditions. Therefore, normal contact stiffness can be estimated during different normal loads by the static direct method. The experiments with three additional factors were conducted to determine the effects on normal contact stiffness. With regard to tests of environmental effects, there is no significant difference between the results of the experiment in the first day and the experiments in second day. This is evidenced by the standard deviations and confidence level of the measured values. Regarding contact surface, when contact stiffness is defined as the ratio of the normal load in a unit area over contact displacement, contact stiffness is independent of the contact area. The mathematical expression derived through statistical regression to present the relationships between contact stiffness and normal contact pressure. This information can be used in fixture stiffness analysis for CAFD. Considering the effect of surface finish, contact stiffness is sensitive to changes of surface finish. For different surface finishes, contact stiffness will vary. A smoother surface finish leads to greater contact stiffness. Although normal contact stiffness can be obtained and easily implemented by the static method, the study on tangential contact stiffness is difficult to estimate by this method. Therefore the dynamic experimental approach is discussed to identify contact stiffness in both normal and tangential directions.

4.3. Contact Stiffness Identification Using a Dynamic Approach

When two surfaces come into contact at certain number of asperity due to the inherent roughness of all the surfaces, contact stiffness results from both the elasticity of these asperities on the contacting surfaces and the total resulting stiffness or compliance of the contacting surfaces. It is difficult to use a static test to estimate tangential contact stiffness, and therefore a dynamic test method is developed. First, the dynamic method is studied for use in the estimation of normal contact stiffness. The results of the dynamic methods are compared with the results based on the static test of normal contact stiffness; then the dynamic test method is used in estimation of tangential contact stiffness.

4.3.1 Theoretical Formulation of 1-D Normal Contact Stiffness

The idea behind the identification of normal contact stiffness is that we can use an impact test to obtain natural frequencies, along with a theoretical model, to infer normal contact stiffness. When body I is in contact with the ground, the dynamic model of the entire structure can be shown as in Figure 4.15. In this theoretical model, the contact interface is modeled by a discrete linear spring. When the preload is changed, contact stiffness will change.

In the one-dimensional model of body I, m is the mass of body I, k_n is the contact stiffness, p is the preload, f(t) is impulse excitation, u(x,t) is the longitudinal displacement of the bar at distance x from a fixed reference.

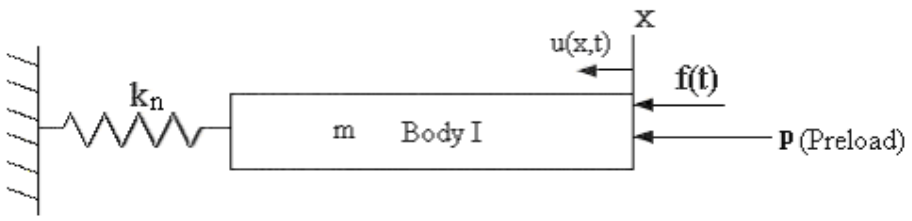

Figure 4.15 One-Dimensional Model for Normal contact Stiffness

With use of a bar in Figure 4.15, a small element of length dx (the limiting case of δx) at position x is shown in Figure 4.16. The longitudinal strain at x is given by

$$\varepsilon = \frac{\partial u(x,t)}{\partial x} \tag{4.8}$$

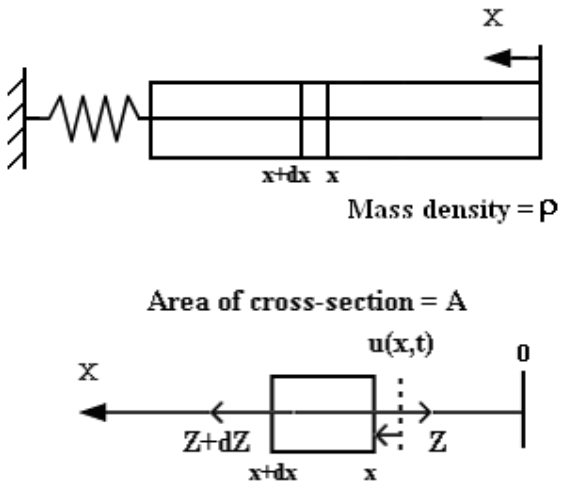

Figure 4.16 A Small Element of the Bar

The longitudinal stress at the cross-section at x is σ=Eε and, hence, the longitudinal force is

$$Z = EA\frac{\partial u}{\partial x} \tag{4.9}$$

where E is Young's modulus of the bar; A is the area of cross section.

The equation of motion for the small element shown in Figure 4.16 is

$$\rho A dx \frac{\partial^2 u(x,t)}{\partial t^2} = Z + dZ - Z \tag{4.10}$$

where ρ is mass density per unit length. From Eq. 4.9, the differentiation of the force becomes

$$dZ = \frac{\partial}{\partial x}\left(EA \frac{\partial u}{\partial x} \right) dx \tag{4.11}$$

When substituted into Eq. 4.10, it gives the governing equation of the longitudinal vibration of the bar

$$\rho A \frac{\partial^2 u(x,t)}{\partial t^2} = \frac{\partial}{\partial x}\left(EA \frac{\partial u(x,t)}{\partial x} \right) \tag{4.12}$$

The boundary conditions of the bar are:

At x=0:

$$EA \frac{\partial u(0,t)}{\partial x} = 0 \tag{4.13}$$

and at x=l:

$$EA \frac{\partial u(l,t)}{\partial x} = -k_n u \tag{4.14}$$

Initially, the system starts from rest, from the static equilibrium position of the bar, such that the initial displacement condition is:

At t=0;

$$u(x,0) = 0 \tag{4.15}$$

The response of a system to an impulsive force can also be obtained by considering that the impulse produces an instantaneous change in the momentum of the system before any

appreciable displacement occurs. The second initial condition is $\frac{\partial u(x,0)}{\partial t} = \frac{1}{m}$

(4.16)

Assume

$$u(x,t) = X(x)q(t) \tag{4.17}$$

The orthogonality of natural modes was proved in the Appendix F.

Substitute Eq. 4.17 into Eq. 4.12 to obtain

$$\begin{aligned} X(x)\frac{d^2q(t)}{dt^2} &= c^2\frac{d^2X(x)}{dx^2}q(t) \\ \frac{1}{X(x)}\frac{d^2X(x)}{dx^2} &= \frac{1}{c^2q(t)}\frac{d^2q(t)}{dt^2} = -\lambda^2 \end{aligned} \tag{4.18}$$

$-\lambda^2$ is called the separation constant and is designated to be negative (De Silva, 1999).

Therefore, the mode shapes X (x) satisfies

$$\frac{d^2X(x)}{dx^2} + \lambda^2 X(x) = 0 \tag{4.19}$$

whose general solution is

$$X(x) = C_1 \sin\lambda x + C_2 \cos\lambda x \tag{4.20}$$

According to the general solution and the modal boundary conditions, one can get

$$\tan\lambda l = \frac{k_n}{EA\lambda} \tag{4.21}$$

Set the structure stiffness as $k^* = \frac{EA}{l}$ and the ratio of the stiffness as $\beta = \frac{k_n}{k^*}$. Since the structure stiffness k* is constant and known, the ratio of the stiffness β is proportional to the contact stiffness k_n. Therefore Eq. 4.21 can be expressed as

$$\tan\lambda l = \frac{\frac{k_n}{k^*}}{\lambda l} = \frac{\beta}{\lambda l} \tag{4.22}$$

This transcendental equation has an infinite number of solutions λ_i (i= 1,2,…)that correspond to the modes of vibration. When β is changed, the solution of λ_i will change. When β is changed from 0.1 to 10, one can get the corresponding $\lambda_i l$. The natural frequencies can also be obtained using

$$\varpi_i = \lambda_i c = \lambda_i \sqrt{\frac{E}{\rho}} \tag{4.23}$$

Table 4.4 Relationship between β and λ_i When β is Changed from 0.1 to 10

β	$\lambda_1 l$	$\lambda_2 l$	$\lambda_3 l$	$\lambda_4 l$
0.1	0.3111	3.1731	6.2991	9.4354
0.2	0.4328	3.2039	6.3148	9.4459
0.4	0.5932	3.2636	6.3461	9.4670
0.6	0.7051	3.3204	6.3770	9.4879
0.8	0.7910	3.3744	6.4074	9.5087
1	0.8603	3.4256	6.4373	9.5293
2	1.0769	3.6436	6.5783	9.6296
4	1.2646	3.9352	6.8140	9.8119
6	1.3496	4.1116	6.9924	10.0000
8	1.3978	4.2264	7.1268	10.0949
10	1.4289	4.3058	7.2281	10.2003

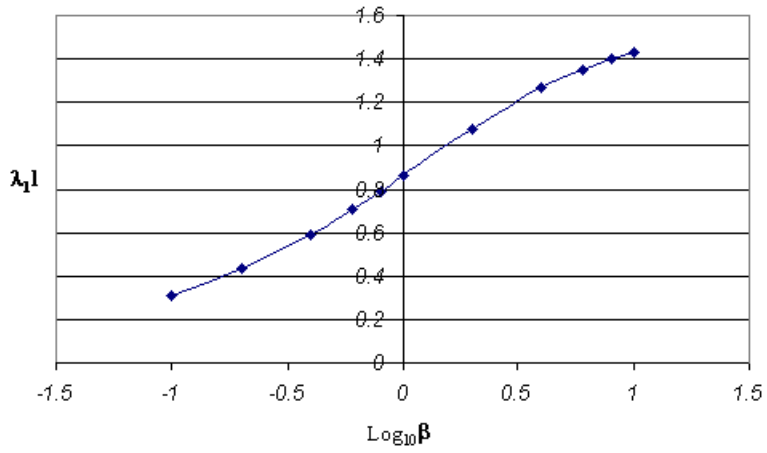

(a) First Mode

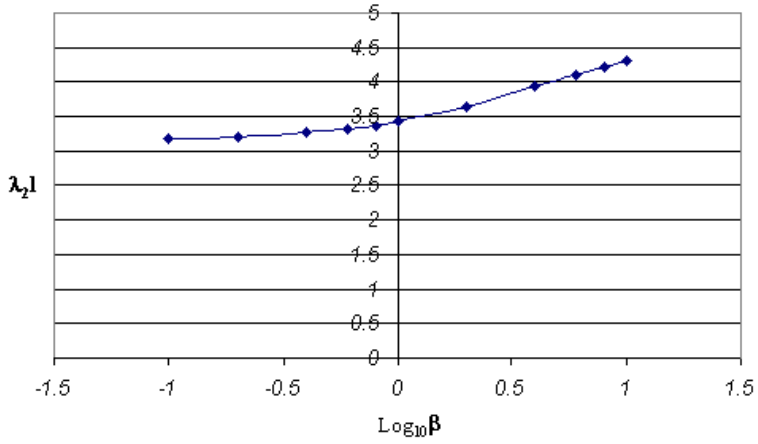

(b) Second Mode

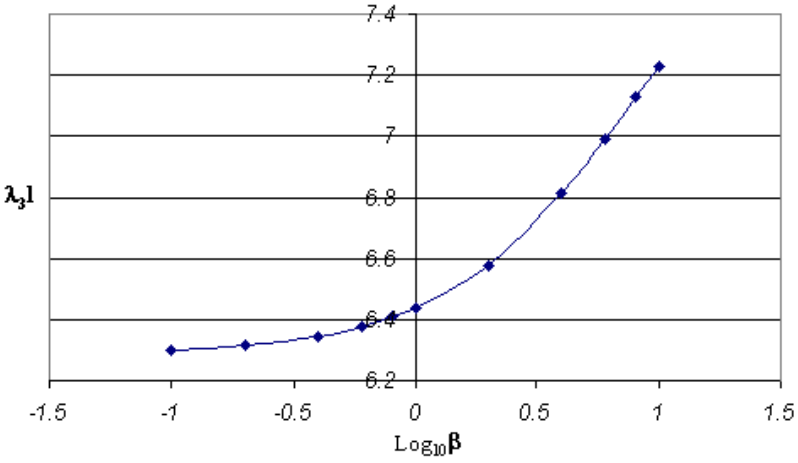

(c) Third Mode

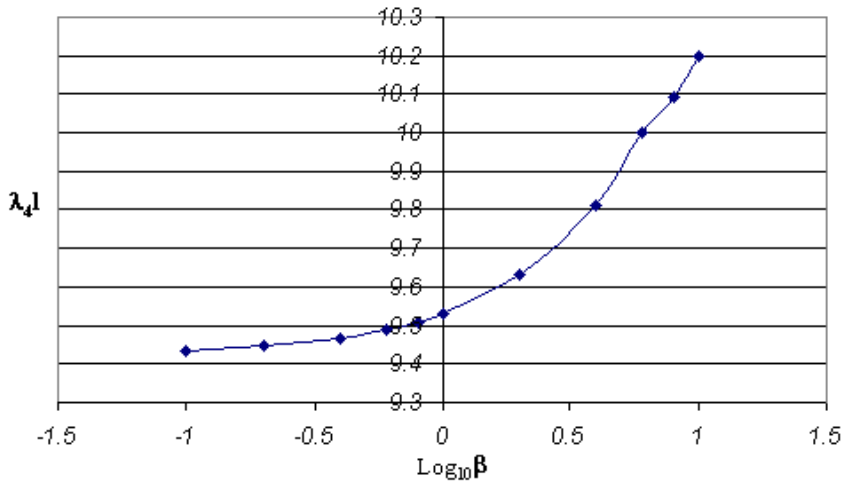

(d) Fourth Mode

Figure 4.17 Relationships between the Nondimensional Natural Frequencies and the Stiffness Ratio β in the First Four Modes

In an experimental study, the natural frequencies can be obtained by an impact test. λ_i can calculated from Eq. 4.23 since the natural frequencies are related to the system characteristics. Then β can be determined from Eq. 4.22. Finally, the contact stiffness, k_n, can be estimated based on the definition of β. According to the assumption that contact stiffness is a function of the preload, the natural frequencies can be determined in experiments under different preloads. The change of contact stiffness can then be identified based on the change of the preloads, through measurement of the natural frequency variation. It should be noted that although any mode of the natural frequency can be used to estimate the contact stiffness, some modes might be more sensitive than others to the change of the preloads.

4.3.2 Experimental Procedure and Results

The experiments were conducted in order to verify the method of identifying contact stiffness in the normal direction. The experiment model is shown in Figure 4.18.

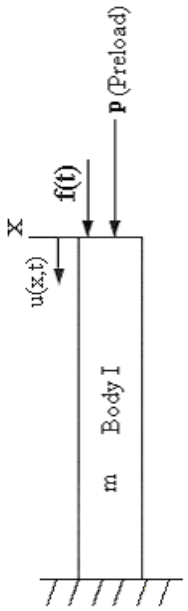

Figure 4.18 Experimental Model for the Normal Contact Stiffness Identification

The measurement instrumentation is relatively simple. It includes the proximity (PX032-1), the impact hammer with a load cell (Dytran 5850A), power supply (482A04), and a Fast Fourier transformation (FFT) analyzer (HP35665A), as shown in Figure 4.19. The experimental procedure can be expressed as follows:

1. Frequency response function (FRF) of the bar is measured by using the hammer to excite the system. Thus, the natural frequencies of the bar can be obtained.
2. According to the natural frequency equation $\varpi_i = \lambda_i \sqrt{\frac{E}{\rho}}$, λ_i is calculated.

3. Based on the relationship between $\lambda_i l$ and β in Figure 4.15, the β can be inferred from the comparison of experimental results and theoretical results. Then the normal contact stiffness can be obtained from the equation $\beta = \frac{k_n}{k^*}$.

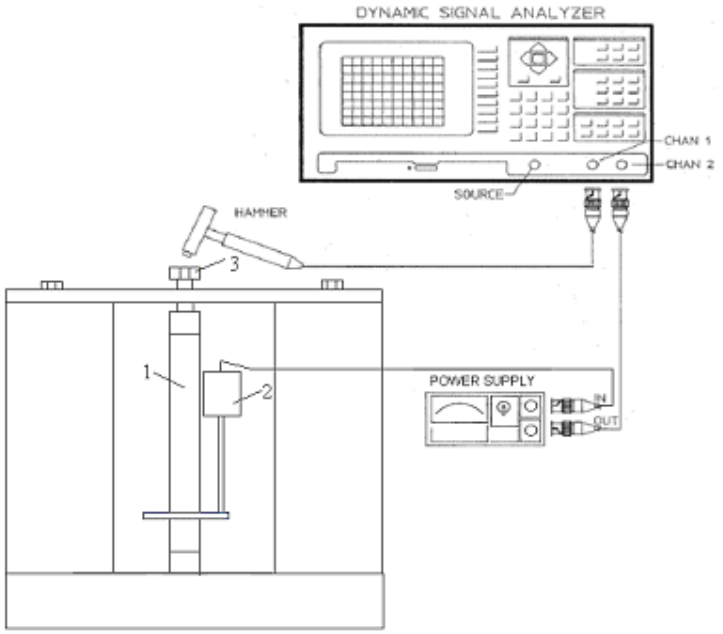

Figure 4.19 Measurement Setup

When the natural frequencies are obtained from the experiment, along with the curves of the relationships between $\lambda_i l$ and β, contact stiffness can be determined from each mode of vibration. However, when the preload changes, the natural frequencies may not necessarily change significantly with the change of normal load for certain modes. Contact stiffness should be identified from the mode most sensitive to changes of a preload. Figure 4.20 shows the FRF of the test system under different preload. Figure 4.21 shows the relationships between the natural frequencies and preload. The natural frequency of the third mode f_3 is the most sensitive to changes in a preload.

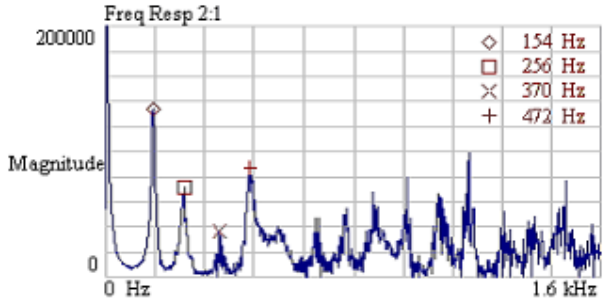

(a) FRF When Preload P=1600lbf

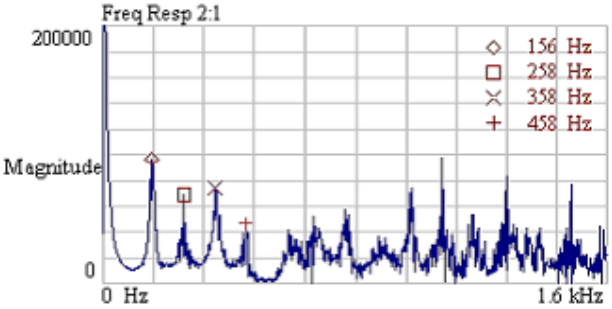

(b) FRF When Preload P=1300lbf

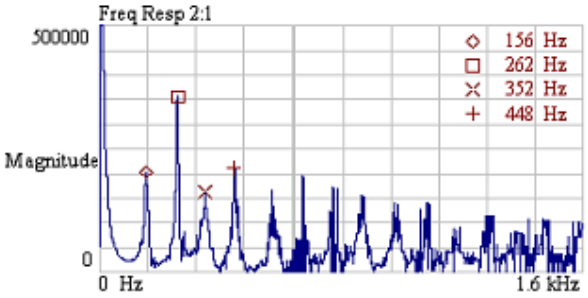

(c) FRF When Preload P=1000lbf

Figure 4.20 Frequency Response Functions (FRF) of the Test System

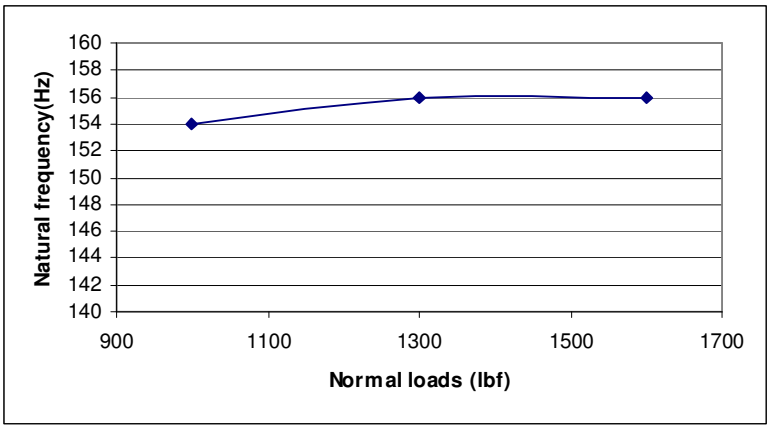

(a) Preloads versus f_1

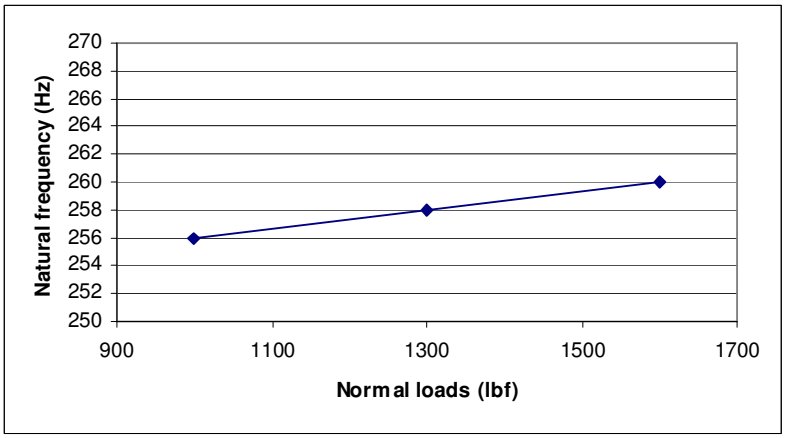

(b) Preloads versus f_2

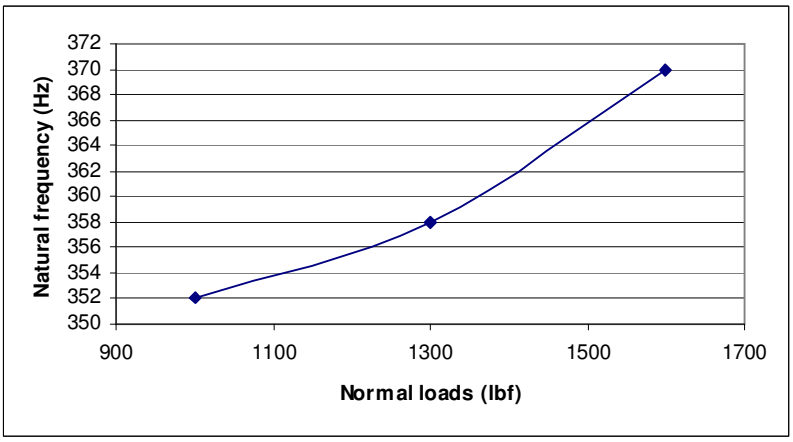

(c) Preloads versus f_3

Figure 4.21 Natural frequencies of the first four modes versus normal loads

Once the natural frequency is obtained from the test, contact stiffness can be estimated by calculating $\lambda_i l$, β, and k_n. In order to verify the results, these calculations were compared with the previous static measurement results of contact stiffness. Under the same experimental condition, i.e., the same experimental device and preloads, contact stiffness is obtained and used in the calculation of natural frequencies, and then compared with the results of dynamic tests, as shown in Figure 4.22.

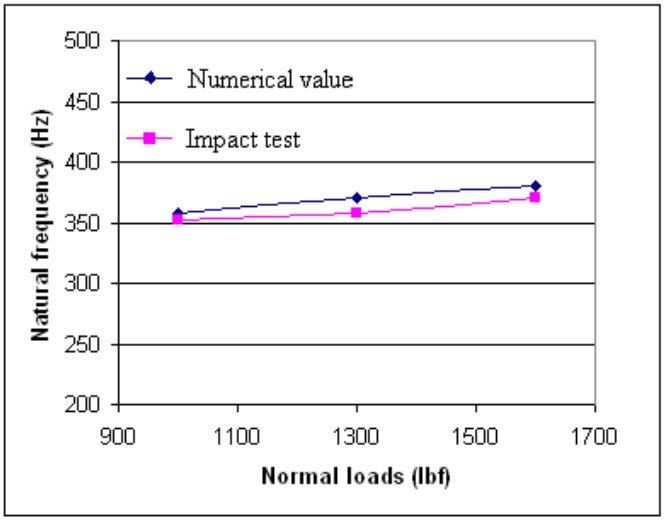

(a) Natural Frequency vs. Preloads

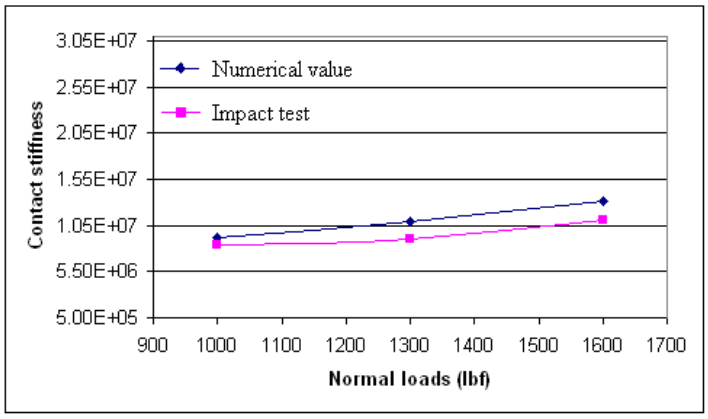

(b) Normal Contact Stiffness vs. Preloads

Figure 4.22 Comparison between Experimental Results of Dynamic Test and Numerical Values Based on Static Test

It can be seen that the results from the dynamic tests are consistent with the numerical calculation results based on the static test results. When the results of the dynamic test are consistent with the static test results, the dynamic test method can be used in identifying tangential contact stiffness, for which the static tests are too difficult to conduct.

4.3.3 Theoretical Formulation of Tangential Contact Stiffness

Two fixture components are in contact at a certain number of asperities due to the inherent roughness of the surface. When they are subjected to tangential forces, the components are mutually constrained through frictional contacts. A friction model based on the Coulomb friction theory is shown in Figure 4.23. The tangential contact stiffness results from the elasticity of asperities of the contact surfaces, and the total resulting stiffness of these contact surfaces depends on their statistical topographical parameters.

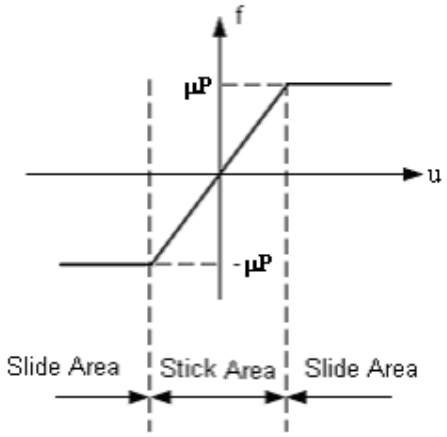

Figure 4.23 A Friction Model

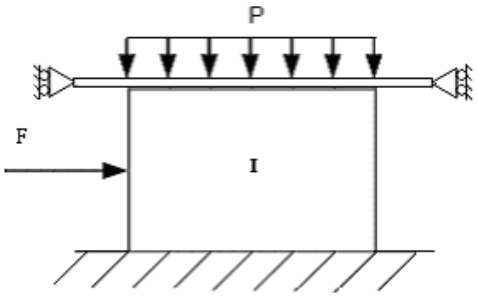

Figure 4.24 Load Model of Elastic Body I

Consider that body I is brought into contact with the flat surface of the support under a uniform preload, P, and is subjected to an small excitation, F, as shown in Figure 4.24. It is assumed that the tangential contact stiffness will change as the preload increases. The friction at each contact point is governed by Coulomb's law. When force is applied in the tangential direction, the asperities in body I will also deform until the shear stress between the asperities exceeds the limit, then the contact surface will slide each other. The friction model of body I in contact is shown in the Figure 4.25. The friction force is given by Eq. 4.24.

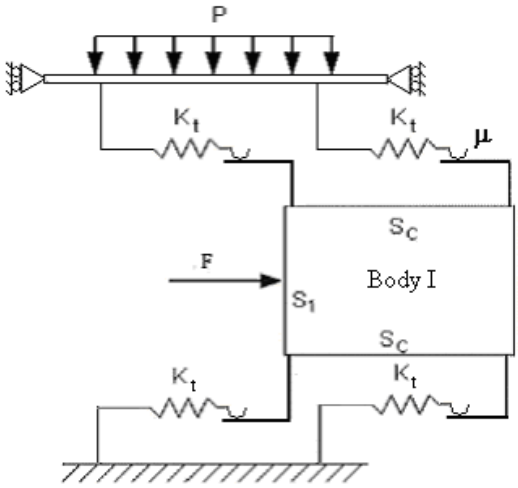

Figure 4.25 Model of the Fixture Components in Contact

$$f = \begin{cases} = K_t u & |u| \le \mu P / K_t \\ \mu P & otherwise \end{cases} \tag{4.24}$$

The idea of the identification of the tangential contact stiffness is to compare the two sets of system natural frequencies: one set is identified from the measured impulse response in tangential direction under different preloads, and the other set is calculated from the FEA model of the system. Based on the numerical simulation, a relationship between tangential contact stiffness and the natural frequencies can be established. If the natural frequencies are measured in the experiments under different preloads, the contact stiffness can be calculated from the relationship obtained by the numerical simulation.

In order to do the numerical simulation, the effect of the contact force needs to be included into FEA model of the system. The additional contact stiffness matrix will be introduced in the general FEA model. The derivation of contact stiffness matrix is briefly given as follows.

Consider an elastic body I in Figure 4.25, the kinetic, strain, and potential energies of the system can be expressed respectively as:

$$K = \int_V \frac{\rho}{2} \left(\frac{\partial \{u\}}{\partial t} \right)^T \left(\frac{\partial \{u\}}{\partial t} \right) dV \tag{4.25}$$

$$U = \int_V \frac{1}{2} \{\sigma\}^T \{\varepsilon\} dV \tag{4.26}$$

$$W = -\left(\int_{S_1} \left\{ \hat{F} \right\}^T \{u\} dS + \int_{S_C} \left\{ \hat{R}_c \right\}^T \{u\} dS \right) \tag{4.27}$$

where K is the kinetic energy; {u} is the displacement vector; V is the volume of the elastic body I; ρ is the mass density of the material; U is the strain energy; $\{\varepsilon\}$and {σ};

are the strain and stress components, respectively. W is the potential energy of external forces; $\{\hat{F}\}$ is the external surface force vector specified on the boundary S_1; $\{\hat{R}_c\}$ is the contact force vector on the contact surface S_c. Note that $S_c \cap S_1 = \{\Phi\}$; The body force is ignored. Using the above energy expressions the total potential energy of the system is

$$\Pi = K - (W + U) \tag{4.28}$$

Based on the well-known Hamilton's principle, a discretized FEA formulation for a typical element can be expressed as

$$[M^e]\{\ddot{d}(t)\} + \{[K^e] + [\tilde{K}_C]\}\{d(t)\} - \{F^e\} = 0 \tag{4.29}$$

To obtain the matrix form, the displacement field of a typical element {u}, which is a function of both space and time, can be written as:

$$\{u\} = [N(x)]\{d(t)\} \qquad \{\dot{u}\} = [N(x)]\{\dot{d}(t)\} \qquad \{\ddot{u}\} = [N(x)]\{\ddot{d}(t)\} \tag{4.30}$$

where [N(x)] is a vector of the space function; and {d(t)} is the nodal response vector. Using the interpolation relationship the element,

Mass matrix is given by

$$[M^e] = \int_{V_e} \rho [N(x)]^T [N(x)] dV \tag{4.31}$$

And the element stiffness matrix is

$$[K^e] = \int_{V_e} [B]^T [D][B] dV_e \tag{4.32}$$

where [B] is the geometry matrix.

Comparing to the standard FEA formulation an additional term of $\tilde{K}_C$, referred as the contact stiffness matrix in included in Eq. 4.29. The term stems from the work done by the contact force on the contact surface. A brief derivation is presented as follows.

The work done by the contact force on the contact surface can be written as

$$E_{ce} = \int_{S_{Ce}} \{u\}^T \{\hat{R}_{ce}\} dS \tag{4.33}$$

Using the contact element, the contact force can be expressed as

$$\{\hat{R}_{ce}\} = [D_c]\{u\} \tag{4.34}$$

Substituting Eqs. 4.30 and 4.34 into Eq.4.33 yields

$$E_{ce} = \{d(t)\}^T \int_{S_{Ce}} [N(x)]^T [D_c][N(x)] dS \{d(t)\} \tag{4.35}$$

Therefore, the contact stiffness matrix can thus be defined as

$$[\tilde{K}_C] = \int_{S_{Ce}} [N(x)]^T [D_c][N(x)] dS \tag{4.36}$$

where $[D_c]$ is the contact property matrix. In the section, the displacements of contact element in the normal direction are assumed to keep stick.

The derived contact stiffness matrix should be added to the general FEA model for the fixture stiffness analysis to take into account the effects of the contact force. Followed the standard procedure of the eigenvalue problem, the system natural frequencies can be obtained using the FEA method to establish the relationship between the tangential contact stiffness and natural frequencies. For example, a specimen that has the dimensions 5×3×0.75in was used to measure dynamic characteristics. Figure 4.26 shows the FEA model of the specimen. Contact elements were modeled as separate springs on

the top and bottom surfaces of the specimen. There are two nodes for each contact element. One node is on the contact surface of the specimen. The other node is constrained at all degrees of freedom. The impulse force was applied at the side of the specimen. The response was obtained at point M, at the other side of the specimen.

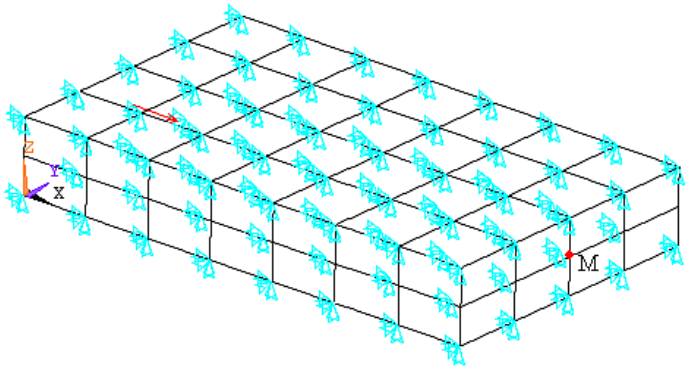

Figure 4.26 Finite Element Model of Specimen

Figure 4.27 shows the relationships between tangential contact stiffness and natural frequencies of the first two vibration modes. The results are obtained through numerical simulation. From experiments, the frequency response is measured under the different preloads. The contact stiffness can be determined based on the relationships shown in Figure 4.27.

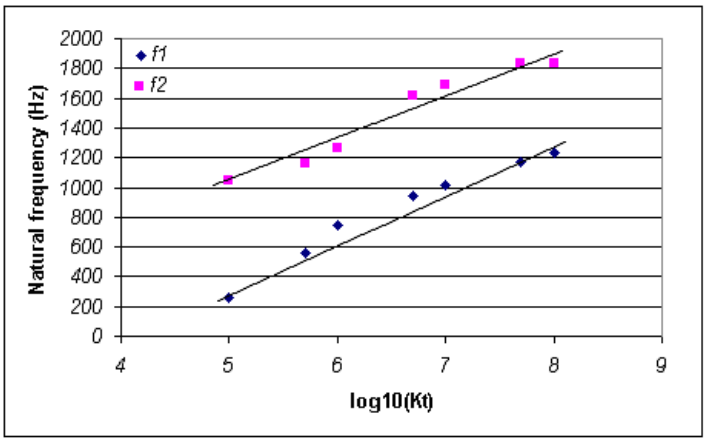

Figure 4.27 Tangential Stiffness vs. the First Two Natural Frequencies

4.3.4 Experimental Procedure and Results

The experimental setup of tangential contact stiffness identification is shown in Figure 4.28. It includes the proximity (PX032-1), impact hammer (Dytran 5850A), power supply (482A04) and an FFT analyzer (HP35665A). The load cell mounted in the impact hammer is connected to Channel 1 of the dynamic signal analyzer. The proximity is connected to Channel 2. The frequency response of the system can be measured by using the hammer to excite the system. The experimental setup is similar to the dynamitic test of normal contact stiffness estimation. Thus the experiment procedure can be expressed as:

1. FRF of the specimen can be measured using experimental setup in Figure 4.28. The natural frequency f_i can be obtained from the test.

2. Based on the relationship between f_i and tangential stiffness in Figure 4.27, tangential contact stiffness can be inferred from the comparison of experimental results and numerical results.

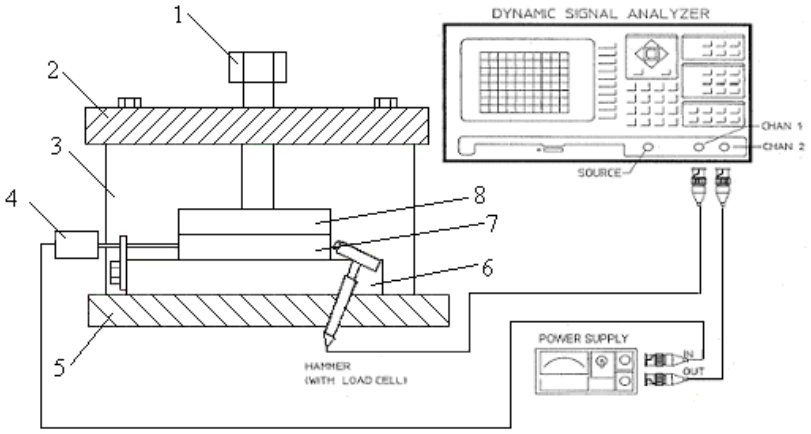

1. Preload bolt 2. Upper plate 3. Riser Plate 4. Proximity 5. Base plate 6. Support 7. Specimen 8 Indenter

Figure 4.28 Experimental Setup for Tangential Contact Stiffness Identification

Figure 4.29 shows the FRF under different preloads, and Figure 4.30 shows the natural frequencies under different preloads. According to the relationship of natural frequencies and tangential contact stiffness in Figure 4.27, the tangential contact stiffness can be estimated as shown in Figure 4.31, where an arithmetic mean was used to reduce the experimental errors. Comparison with experiment results shows that the prediction changes of tangential contact stiffness in different preloads are 0.2%, 3.6% and 5.2%. Therefore the estimations of tangential contact stiffness from different modes are in good agreement.

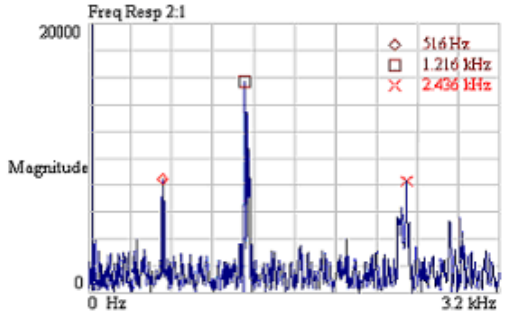

(a) Preload P=700lbf

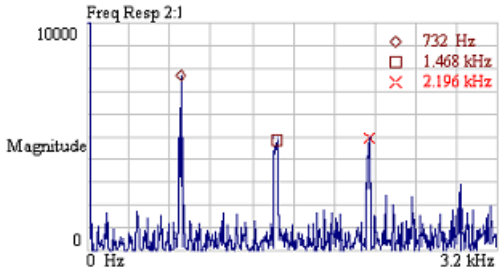

(b) Preload P=1000lbf

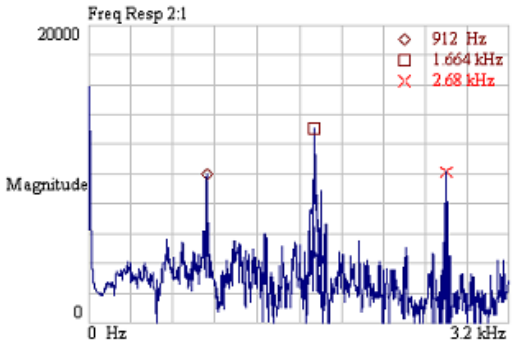

(c) Normal Force P=1300lbf

Figure 4.29 Frequency Response Function under Different Preloads

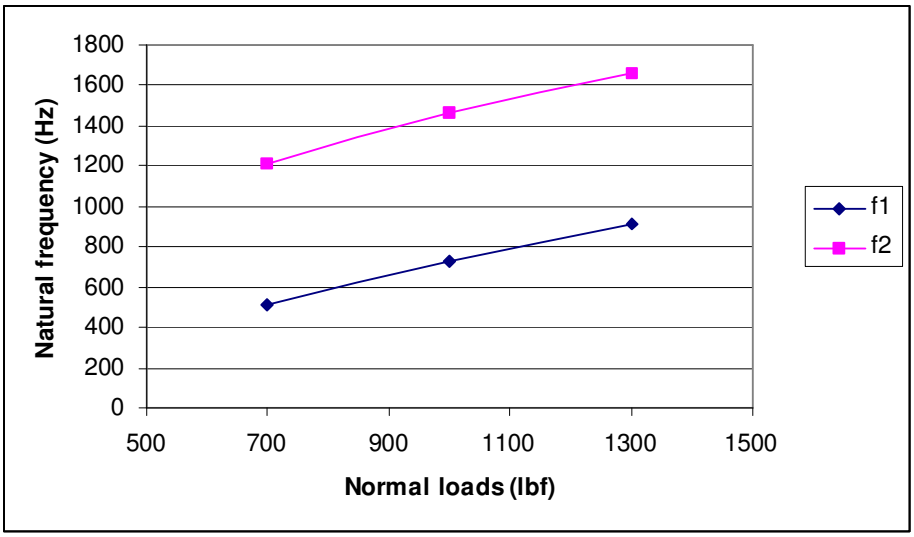

Figure 4.30 Natural Frequencies of First Two Modes versus Preloads

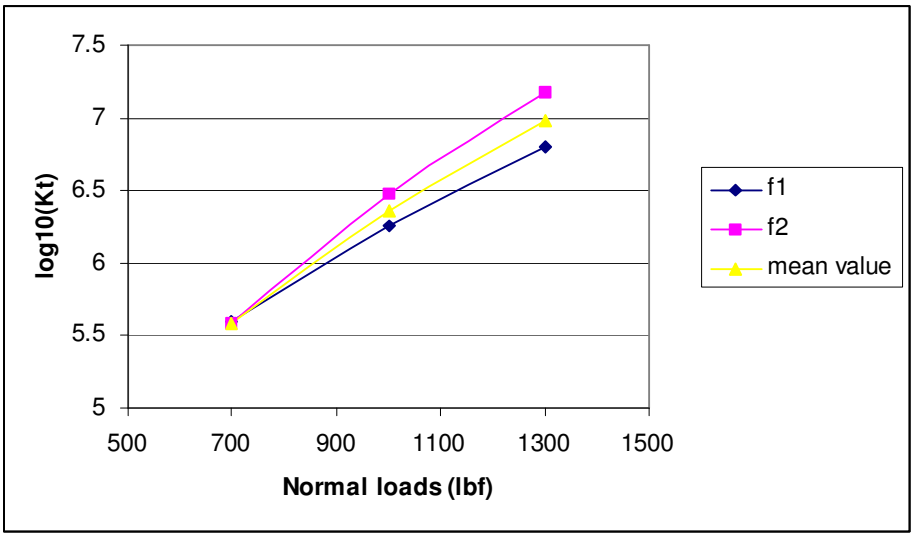

Figure 4.31 Tangential Contact Stiffness under Different Preloads

The dynamic experimental approach has been developed and implemented to identify the contact stiffness in both normal and tangential directions. The identification of normal

contact stiffness using the dynamic method has been discussed and the experimental results are compared with the results of the static test. It can be seen that the results from the dynamic tests are in good agreement with the numerical calculation results based on the static test results. This indicates that the developed methods are applicable to actual situations. The similar approach of the dynamic test is used to estimate tangential contact stiffness. Estimation of tangential contact stiffness cannot be fully validated. But comparison with experimental results shows that the estimations of tangential contact stiffness from different modes are in good agreement. It is inferred that the approach is feasible to apply to a real situation. Therefore, contact stiffness can be identified through experimental approaches. The results can be used in analyzing fixture stiffness, as studied in Chapter 3, and further used in CAFD.

4.4 Summary on Experiments for Contact Stiffness Identification

This chapter has described an experimental investigation to estimate the contact stiffness in normal and tangential directions. The static method has been used to estimate normal contact stiffness and to study the effecting factors. In order to study tangential contact stiffness, dynamic methods were developed to estimate contact stiffness in both normal and tangential directions. That study is validated by the results of the static method in the identification of normal contact stiffness.

Using the static experimental method, normal contact stiffness was estimated and the effects of the contact surface conditions were studied. In this research, experiments are run for steel samples. Statistical methods were used to reduce the experimental errors and assure creditability of the results. The experimental results show that contact displacement is nonlinear and that the contact stiffness is linear to the normal loads. The experiments are also conducted to determine the effects of test environmental, contact surface area, and surface roughness on the normal contact stiffness. With regard to test environment analysis, tests were conducted on different days. There is no significant difference in the results of the experiments of the first day and the experiments of the second day. This is evidenced by the standard deviations and confidence level of the measured values. Considering the effect of the contact surface area, when the contact stiffness is defined as the ratio of the normal load in a unit area over contact displacement, it is proved in the tests that the contact stiffness is independent of the contact area. Contact stiffness is sensitive to the change of the surface finish, and for different surface

finishes, contact stiffness will vary. A smoother surface finish leads to a higher contact stiffness.

Although normal contact stiffness can be obtained with the static method, tangential contact stiffness is difficult to estimate by this method. Therefore, the dynamic experimental approach was developed to identify contact stiffness in both normal and tangential directions. The identification of normal contact stiffness using the dynamic method has been discussed and the experimental results are compared with the results of static tests. It can be seen that normal contact stiffness estimated from the dynamic tests are in good agreement with the normal contact stiffness estimated from the static tests, which indicates that the developed method is applicable to actual situations. Therefore dynamic test is appropriate to estimate tangential contact stiffness. Although the estimation of tangential contact stiffness cannot be fully validated because there is no other directly efficient method to verify it, comparison with experimental results show the tangential contact stiffness estimated from different modes is in good agreement with each other. It is inferred that the approach is feasible to apply to the fixture application. Therefore, contact stiffness in normal and tangential directions can be identified through these experimental approaches, and the results can be used in the study of fixture stiffness presented in Chapter 3, and further can be used in the CAFD system.

Chapter 5: Conclusion and Future Work

This research involved a systematic and comprehensive study of fixture stiffness. The research includes an FEA modeling of fixture unit stiffness, model verifications, and static and dynamic experimental studies on the identification of contact stiffness parameter. This chapter summaries this research and proposes conclusions and future works.

5.1 Conclusion

Through theoretical analysis, simulation studies, and experimental identifications, this dissertation presents the theoretical foundation for CAFD with predictable fixture stiffness.

In order to analyze the nonlinear problem encountered in fixture stiffness analysis, an FEA model of fixture unit stiffness study has been developed, and a contact element is used to solve the contact problems involved in the study of fixture unit stiffness. The penalty function method, which is equivalent to the perturbed Lagrange multipliers method, is adopted in the practical analysis. In this method, the contact conditions are included in the energy equation of the general FEA model and the nonlinearity of connection, shown by previous experiment, is modeled. The contact conditions are classified into three cases: open condition, stick condition, and sliding condition, based on an iterative scheme. The effect of friction between the fixture components is also modeled. The FEA model and the analysis procedure were validated by two examples: a simple beam analysis and a typical fixture unit. The results are compared with the

corresponding analytical solution and experimental results in the literature. The agreements between those results demonstrate great potential for use of the proposed model in future studies of the fixture unit stiffness in general configurations, such as a fixture with multiple units and components. Analysis of the first case shows that contact stiffness has a great contribution on the deformation of the contact components. Thus, the contact stiffness of fixture components is one of key parameters in the analysis of fixture stiffness, which is assumed known in the study of the fixture unit stiffness.

An experimental study was carried out to identify the contact stiffness parameter, which includes estimating normal contact stiffness and tangential contact stiffness by static and dynamic methods. For normal contact stiffness, a static identification procedure was developed to estimate the parameters using experimental data. Four factors -- preloads, testing environmental, contact area, and surface finish of the specimen -- were examined to see how they affect the behavior of the contact interface. Results show that the contact deformation is nonlinear with an increase of normal loads and that the contact stiffness is linear to the normal loads. In order to investigate the effects of the testing environment on the experimental results, two sets of experiments were conducted over different days. The results show no marked difference. For the contact surface area, when contact stiffness is defined as the ratio of the normal load in a unit area over contact displacement, contact stiffness is independent of the contact area. The contact stiffness is sensitive to the change of the surface finish. Contact stiffness will vary for different surface finishes. A smoother surface finish leads to higher contact stiffness. Although normal contact stiffness can be obtained using the static method, tangential contact stiffness is difficult to estimate by this method. Therefore the dynamic experimental approach has been discussed to identify contact stiffness in both normal and tangential directions.

The identification of normal contact stiffness using dynamic method has been discussed. An eigenvalue analysis scheme is developed to estimate normal contact stiffness. The experimental results were compared with the results of static tests under the same experimental conditions. It can be seen that the results from the dynamic tests are consistent with the numerical results based on the static test results. Therefore, the dynamic test was used to estimate tangential contact stiffness because it is difficult to use static tests for this identification. Similar to that for identifying normal contact stiffness, a frequency–domain identification system was developed to identify tangential contact stiffness, using FEA and experimental results. A simulation study on the vibration data from tangential contact model has been presented in this study. The experimental study was carried out, and the parameters were estimated, along with numerical value and experimental data.

This research establishes the FEA model of fixture unit stiffness, and contact stiffness can be identified through the experimental approaches. Contact stiffness is relative to the material and preload, but it is independent of the contact area and test environment. Therefore, it is consistent in different fixture design. This study can be used in the fixture stiffness analysis, and further used in CAFD.

5.2 Future Work Discussion

Based on the scope of the present research on fixture stiffness, the following recommendations are made for future work:

(1) Theoretical models should be developed for studying multi-component fixture units. The present FEA modeling of fixture unit stiffness mainly concerns two-component contact. The model should be adjusted to fit the needs of multi-component fixture units.

(2) The theoretical model and experimental study of the identification of contact stiffness should be applied to actual fixture units. The investigation on contact stiffness in this dissertation provides a method to analyze and estimate contact stiffness. However, when it is used in a practical application, the efforts need to be drawn in building up a database of contact stiffness. Also special consideration should be given to the material used in the application of normal contact stiffness and tangential contact stiffness.

(3) In order to develop a comprehensive CAFD system, the relationship between fixture parameters and fixture unit stiffness needs to be built up. The present research in this dissertation provides a useful model to analyze fixture unit stiffness. However, for real applications of the CAFD system, the relationship with variation capability driven by parametric representations of fixture units needs to be built up.

Appendix A: Experimental Data (WP Radius =0.5in; Surface finish Ra = 3.08μm)

In this section, the static experiments were run for an AISI4150 sample under different normal loads. The sample radius is 0.5 in, and its surface finish is 3.08μm. In order to consider environmental effect, the experiment was intentionally repeated 16 times in day 1 and day 2, respectively. Table A.1 shows the original measured data. In order to reduce the measured error, Table A.2 lists the relative measured data. Figure A.1 (a) shows the relative measured results of day 1, and Figure A.1 (b) shows the relative measured results of day 2. Table A.3 lists the arithmetic mean of the relative measured results. The standard deviation and 95% confidence interval are calculated. Figure A.2 is a plot of the mean values of all relative data versus normal loads. From the relative measured data and Equation 4.3, the total displacement can be obtained, as shown in Table A.4. According to Equation 4.4, structure displacement can be computed theoretically. Therefore, contact displacement can be obtained by applying Equation 4.5, as shown in Table A.5. Table A.6 and Figure A.3 show the mean value of all kinds of displacements versus surface pressure. According to the definition of contact stiffness, Equation 4.6 can be used to obtain contact stiffness as shown in Table A.7.

Table A.1 Original Measured Output Voltage (Unit: volt)

Test	250	400	550	700	850	1000	1150	1300	1450	1600
1	5.1594	5.169	5.1723	5.1783	5.1845	5.1888	5.1934	5.1996	5.2025	5.2039
2	4.7288	4.7334	4.7405	4.7493	4.7565	4.7604	4.7641	4.7695	4.7716	4.7757
3	3.5936	3.5983	3.6022	3.6081	3.6151	3.6208	3.6241	3.6278	3.6305	3.6328
4	5.6844	5.6931	5.6989	5.7025	5.7068	5.7091	5.7124	5.7154	5.7195	5.7208
5	3.6743	3.6818	3.6919	3.6955	3.6994	3.7034	3.7092	3.7124	3.7141	3.7186
6	3.8092	3.8175	3.8238	3.8291	3.8317	3.8373	3.8424	3.8481	3.8536	3.8545
7	3.669	3.674	3.6807	3.6852	3.6907	3.6949	3.7001	3.7056	3.7069	3.7132
8	3.7812	3.7904	3.7963	3.8023	3.8089	3.8134	3.8198	3.8237	3.8281	3.8314
9	3.6663	3.6765	3.6805	3.6892	3.6962	3.6989	3.7027	3.7075	3.7085	3.7118
10	3.7776	3.7898	3.7941	3.7987	3.8046	3.806	3.8126	3.816	3.8241	3.8292
11	3.6975	3.7088	3.7165	3.7205	3.728	3.7309	3.7342	3.7395	3.7427	3.7468
12	3.8032	3.8122	3.8217	3.8291	3.8363	3.8384	3.8412	3.8421	3.8466	3.8491
13	3.6861	3.7011	3.7124	3.715	3.7192	3.7205	3.7238	3.7295	3.7303	3.7312
14	3.7774	3.7924	3.8009	3.8039	3.8073	3.8108	3.8175	3.8204	3.8259	3.8315
15	3.6219	3.6328	3.6406	3.6465	3.6511	3.6591	3.6671	3.6694	3.6746	3.6781
16	3.7299	3.7383	3.7467	3.7551	3.7589	3.7629	3.7664	3.7704	3.7781	3.7801
17	3.6257	3.6353	3.6407	3.6469	3.6528	3.6568	3.6582	3.6603	3.6648	3.6683
18	3.7241	3.7316	3.7457	3.7515	3.7537	3.7582	3.7631	3.7669	3.7698	3.7709
19	3.6581	3.6626	3.6689	3.6734	3.6784	3.6837	3.6889	3.6942	3.6973	3.6999
20	3.7073	3.718	3.7269	3.7296	3.7357	3.7415	3.7466	3.7483	3.7503	3.7565
21	3.2282	3.2367	3.2403	3.2504	3.2597	3.2638	3.2655	3.2698	3.2735	3.2754
22	4.0313	4.0431	4.0465	4.0519	4.0617	4.0709	4.0748	4.0812	4.0877	4.0937
23	3.6423	3.6585	3.6619	3.6683	3.6741	3.6802	3.6872	3.6903	3.6957	3.6984
24	3.7866	3.7904	3.8024	3.8096	3.8125	3.8168	3.8228	3.8274	3.8297	3.8366
25	3.7725	3.7834	3.7918	3.7966	3.8015	3.8053	3.8071	3.8094	3.8122	3.8152
26	4.1243	4.1311	4.1404	4.1455	4.1485	4.1505	4.1564	4.1595	4.1616	4.1674
27	4.1283	4.1378	4.1442	4.1492	4.1527	4.1608	4.1628	4.1659	4.1676	4.1731
28	3.8297	3.8401	3.8497	3.8564	3.8615	3.8644	3.8684	3.8713	3.8754	3.8785
29	4.169	4.1822	4.1936	4.196	4.2013	4.2047	4.2082	4.2134	4.2148	4.2172
30	3.8249	3.8361	3.8429	3.8505	3.8567	3.8573	3.8611	3.8665	3.8689	3.8741
31	4.1493	4.1579	4.1721	4.1786	4.1832	4.1849	4.1899	4.1944	4.1965	4.1972
32	3.8355	3.8519	3.8577	3.8631	3.8677	3.8686	3.8691	3.8728	3.8752	3.8783

Table A.2 Relative Measured Data (Unit: volt)

Group	400	550	700	850	1000	1150	1300	1450	1600
1	0.0096	0.0129	0.0189	0.0251	0.0294	0.034	0.0402	0.0431	0.0445
2	0.0046	0.0117	0.0205	0.0277	0.0316	0.0353	0.0407	0.0428	0.0469
3	0.0047	0.0086	0.0145	0.0215	0.0272	0.0305	0.0342	0.0369	0.0392
4	0.0087	0.0145	0.0181	0.0224	0.0247	0.028	0.031	0.0351	0.0364
5	0.0075	0.0176	0.0212	0.0251	0.0291	0.0349	0.0381	0.0398	0.0443
6	0.0083	0.0146	0.0199	0.0225	0.0281	0.0332	0.0389	0.0444	0.0453
7	0.005	0.0117	0.0162	0.0217	0.0259	0.0311	0.0366	0.0379	0.0442
8	0.0092	0.0151	0.0211	0.0277	0.0322	0.0386	0.0425	0.0469	0.0502
9	0.0102	0.0142	0.0229	0.0299	0.0326	0.0364	0.0412	0.0422	0.0455
10	0.0122	0.0165	0.0211	0.027	0.0284	0.035	0.0384	0.0465	0.0516
11	0.0113	0.019	0.023	0.0305	0.0334	0.0367	0.042	0.0452	0.0493
12	0.009	0.0185	0.0259	0.0331	0.0352	0.038	0.0389	0.0434	0.0459
13	0.015	0.0263	0.0289	0.0331	0.0344	0.0377	0.0434	0.0442	0.0451
14	0.015	0.0235	0.0265	0.0299	0.0334	0.0401	0.043	0.0485	0.0541
15	0.0109	0.0187	0.0246	0.0292	0.0372	0.0452	0.0475	0.0527	0.0562
16	0.0084	0.0168	0.0252	0.029	0.033	0.0365	0.0405	0.0482	0.0502
17	0.0096	0.015	0.0212	0.0271	0.0311	0.0325	0.0346	0.0391	0.0426
18	0.0075	0.0216	0.0274	0.0296	0.0341	0.039	0.0428	0.0457	0.0468
19	0.0045	0.0108	0.0153	0.0203	0.0256	0.0308	0.0361	0.0392	0.0418
20	0.0107	0.0196	0.0223	0.0284	0.0342	0.0393	0.041	0.043	0.0492
21	0.0085	0.0121	0.0222	0.0315	0.0356	0.0373	0.0416	0.0453	0.0472
22	0.0118	0.0152	0.0206	0.0304	0.0396	0.0435	0.0499	0.0564	0.0624
23	0.0162	0.0196	0.026	0.0318	0.0379	0.0449	0.048	0.0534	0.0561
24	0.0038	0.0158	0.023	0.0259	0.0302	0.0362	0.0408	0.0431	0.05
25	0.0109	0.0193	0.0241	0.029	0.0328	0.0346	0.0369	0.0397	0.0427
26	0.0068	0.0161	0.0212	0.0242	0.0262	0.0321	0.0352	0.0373	0.0431
27	0.0095	0.0159	0.0209	0.0244	0.0325	0.0345	0.0376	0.0393	0.0448
28	0.0104	0.02	0.0267	0.0318	0.0347	0.0387	0.0416	0.0457	0.0488
29	0.0132	0.0246	0.027	0.0323	0.0357	0.0392	0.0444	0.0458	0.0482
30	0.0112	0.018	0.0256	0.0318	0.0324	0.0362	0.0416	0.044	0.0492
31	0.0086	0.0228	0.0293	0.0339	0.0356	0.0406	0.0451	0.0472	0.0479
32	0.0164	0.0222	0.0276	0.0322	0.0331	0.0336	0.0373	0.0397	0.0428

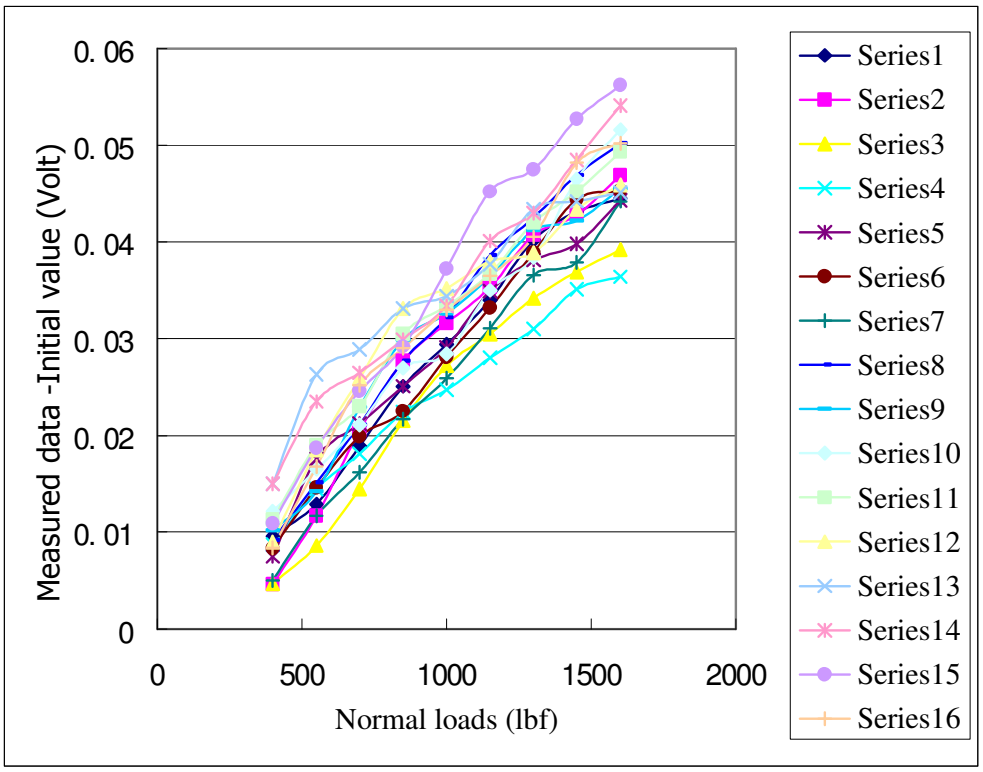

(a) All Relative Data in Day 1 vs. Normal Loads

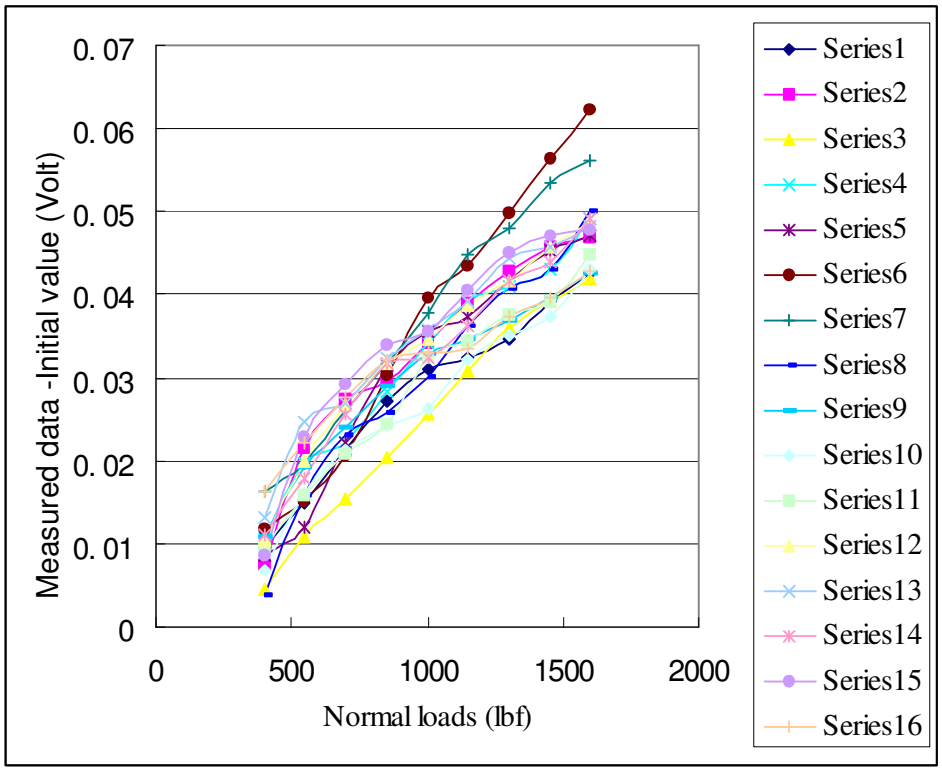

(b) All Relative Data in Day 2 vs. Normal Loads

Figure A.1 All Relative Data vs. Normal Loads

Table A.3 All Relative Data vs. Normal Loads

Normal loads (lbf)	400	550	700	850	1000	1150	1300	1450	1600
Mean value (Volt)	9.66E-03	1.72E-02	2.28E-02	2.81E-02	3.21E-02	3.64E-02	4.04E-02	4.38E-02	4.73E-02
Standard Deviation	3.30E-03	4.20E-03	3.81E-03	3.84E-03	3.74E-03	4.03E-03	4.15E-03	4.87E-03	5.18E-03
95% Confidence interval	1.14E-03	1.45E-03	1.32E-03	1.33E-03	1.30E-03	1.40E-03	1.44E-03	1.69E-03	1.79E-03

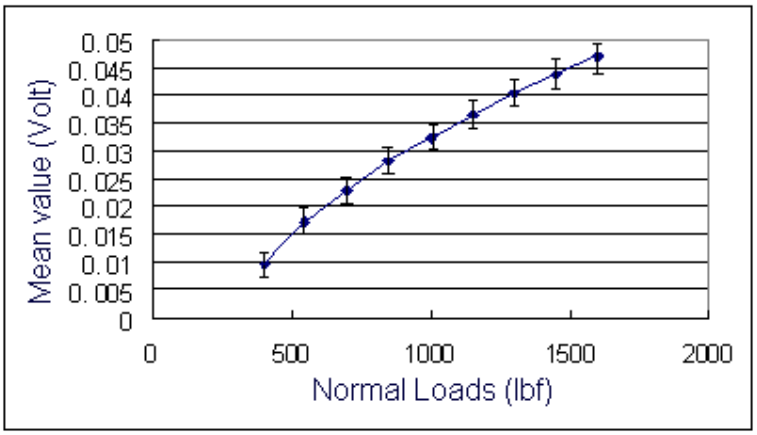

Figure A.2 Mean Values of All Relative Data vs. Normal Loads

Table A.4 Total Displacement (in)

Group	400	550	700	850	1000	1150	1300	1450	1600
1	4.933E-05	6.629E-05	9.712E-05	1.290E-04	1.511E-04	1.747E-04	2.066E-04	2.215E-04	2.287E-04
2	2.364E-05	6.012E-05	1.053E-04	1.423E-04	1.624E-04	1.814E-04	2.092E-04	2.199E-04	2.410E-04
3	2.415E-05	4.419E-05	7.451E-05	1.105E-04	1.398E-04	1.567E-04	1.758E-04	1.896E-04	2.014E-04
4	4.471E-05	7.451E-05	9.301E-05	1.151E-04	1.269E-04	1.439E-04	1.593E-04	1.804E-04	1.871E-04
5	3.854E-05	9.044E-05	1.089E-04	1.290E-04	1.495E-04	1.793E-04	1.958E-04	2.045E-04	2.277E-04
6	4.265E-05	7.503E-05	1.023E-04	1.156E-04	1.444E-04	1.706E-04	1.999E-04	2.282E-04	2.328E-04
7	2.569E-05	6.012E-05	8.325E-05	1.115E-04	1.331E-04	1.598E-04	1.881E-04	1.948E-04	2.271E-04
8	4.728E-05	7.760E-05	1.084E-04	1.423E-04	1.655E-04	1.984E-04	2.184E-04	2.410E-04	2.580E-04
9	5.242E-05	7.297E-05	1.177E-04	1.537E-04	1.675E-04	1.871E-04	2.117E-04	2.169E-04	2.338E-04
10	6.269E-05	8.479E-05	1.084E-04	1.388E-04	1.459E-04	1.799E-04	1.973E-04	2.390E-04	2.652E-04
11	5.807E-05	9.764E-05	1.182E-04	1.567E-04	1.716E-04	1.886E-04	2.158E-04	2.323E-04	2.533E-04
12	4.625E-05	9.507E-05	1.331E-04	1.701E-04	1.809E-04	1.953E-04	1.999E-04	2.230E-04	2.359E-04
13	7.708E-05	1.352E-04	1.485E-04	1.701E-04	1.768E-04	1.937E-04	2.230E-04	2.271E-04	2.318E-04
14	7.708E-05	1.208E-04	1.362E-04	1.537E-04	1.716E-04	2.061E-04	2.210E-04	2.492E-04	2.780E-04
15	5.601E-05	9.610E-05	1.264E-04	1.501E-04	1.912E-04	2.323E-04	2.441E-04	2.708E-04	2.888E-04
16	4.317E-05	8.633E-05	1.295E-04	1.490E-04	1.696E-04	1.876E-04	2.081E-04	2.477E-04	2.580E-04
17	4.933E-05	7.708E-05	1.089E-04	1.393E-04	1.598E-04	1.670E-04	1.778E-04	2.009E-04	2.189E-04
18	3.854E-05	1.110E-04	1.408E-04	1.521E-04	1.752E-04	2.004E-04	2.199E-04	2.348E-04	2.405E-04
19	2.312E-05	5.550E-05	7.862E-05	1.043E-04	1.316E-04	1.583E-04	1.855E-04	2.014E-04	2.148E-04
20	5.499E-05	1.007E-04	1.146E-04	1.459E-04	1.758E-04	2.020E-04	2.107E-04	2.210E-04	2.528E-04
21	4.368E-05	6.218E-05	1.141E-04	1.619E-04	1.829E-04	1.917E-04	2.138E-04	2.328E-04	2.426E-04
22	6.064E-05	7.811E-05	1.059E-04	1.562E-04	2.035E-04	2.235E-04	2.564E-04	2.898E-04	3.207E-04
23	8.325E-05	1.007E-04	1.336E-04	1.634E-04	1.948E-04	2.307E-04	2.467E-04	2.744E-04	2.883E-04
24	5.550E-05	8.119E-05	1.182E-04	1.331E-04	1.552E-04	1.860E-04	2.097E-04	2.215E-04	2.569E-04
25	5.601E-05	9.918E-05	1.238E-04	1.490E-04	1.686E-04	1.778E-04	1.896E-04	2.040E-04	2.194E-04
26	3.494E-05	8.273E-05	1.089E-04	1.244E-04	1.346E-04	1.650E-04	1.809E-04	1.917E-04	2.215E-04
27	4.882E-05	8.171E-05	1.074E-04	1.254E-04	1.670E-04	1.773E-04	1.932E-04	2.020E-04	2.302E-04
28	5.344E-05	1.028E-04	1.372E-04	1.634E-04	1.783E-04	1.989E-04	2.138E-04	2.348E-04	2.508E-04
29	6.783E-05	1.264E-04	1.388E-04	1.660E-04	1.835E-04	2.014E-04	2.282E-04	2.354E-04	2.477E-04
30	5.755E-05	9.250E-05	1.316E-04	1.634E-04	1.665E-04	1.860E-04	2.138E-04	2.261E-04	2.528E-04
31	4.419E-05	1.172E-04	1.506E-04	1.742E-04	1.829E-04	2.086E-04	2.318E-04	2.426E-04	2.462E-04
32	8.428E-05	1.141E-04	1.418E-04	1.655E-04	1.701E-04	1.727E-04	1.917E-04	2.040E-04	2.199E-04

Table A.5 Contact Displacement (in)

Group	400	550	700	850	1000	1150	1300	1450	1600
1	4.076E-05	5.169E-05	7.522E-05	9.978E-05	1.146E-04	1.309E-04	1.555E-04	1.630E-04	1.630E-04
2	1.507E-05	4.552E-05	8.345E-05	1.132E-04	1.259E-04	1.376E-04	1.580E-04	1.615E-04	1.753E-04
3	1.558E-05	2.959E-05	5.261E-05	8.129E-05	1.033E-04	1.130E-04	1.246E-04	1.312E-04	1.358E-04
4	3.614E-05	5.991E-05	7.111E-05	8.591E-05	9.043E-05	1.001E-04	1.082E-04	1.219E-04	1.214E-04
5	2.997E-05	7.584E-05	8.704E-05	9.978E-05	1.130E-04	1.356E-04	1.447E-04	1.461E-04	1.620E-04
6	3.408E-05	6.043E-05	8.036E-05	8.642E-05	1.079E-04	1.268E-04	1.488E-04	1.697E-04	1.671E-04
7	1.712E-05	4.552E-05	6.135E-05	8.231E-05	9.660E-05	1.160E-04	1.370E-04	1.363E-04	1.615E-04
8	3.871E-05	6.300E-05	8.653E-05	1.132E-04	1.290E-04	1.546E-04	1.673E-04	1.826E-04	1.923E-04
9	4.385E-05	5.837E-05	9.578E-05	1.245E-04	1.310E-04	1.433E-04	1.606E-04	1.584E-04	1.682E-04
10	5.412E-05	7.019E-05	8.653E-05	1.096E-04	1.094E-04	1.361E-04	1.462E-04	1.805E-04	1.995E-04
11	4.950E-05	8.304E-05	9.629E-05	1.275E-04	1.351E-04	1.448E-04	1.647E-04	1.738E-04	1.877E-04
12	3.768E-05	8.047E-05	1.112E-04	1.409E-04	1.444E-04	1.515E-04	1.488E-04	1.646E-04	1.702E-04
13	6.851E-05	1.206E-04	1.266E-04	1.409E-04	1.403E-04	1.500E-04	1.719E-04	1.687E-04	1.661E-04
14	6.851E-05	1.062E-04	1.143E-04	1.245E-04	1.351E-04	1.623E-04	1.699E-04	1.908E-04	2.123E-04
15	4.744E-05	8.150E-05	1.045E-04	1.209E-04	1.547E-04	1.885E-04	1.930E-04	2.124E-04	2.231E-04
16	3.460E-05	7.173E-05	1.076E-04	1.198E-04	1.331E-04	1.438E-04	1.570E-04	1.893E-04	1.923E-04
17	4.076E-05	6.248E-05	8.704E-05	1.101E-04	1.233E-04	1.232E-04	1.267E-04	1.425E-04	1.532E-04
18	2.997E-05	9.640E-05	1.189E-04	1.229E-04	1.387E-04	1.566E-04	1.688E-04	1.764E-04	1.748E-04
19	1.455E-05	4.090E-05	5.672E-05	7.512E-05	9.505E-05	1.145E-04	1.344E-04	1.430E-04	1.491E-04
20	4.642E-05	8.612E-05	9.270E-05	1.167E-04	1.393E-04	1.582E-04	1.596E-04	1.625E-04	1.872E-04
21	3.511E-05	4.758E-05	9.218E-05	1.327E-04	1.464E-04	1.479E-04	1.627E-04	1.744E-04	1.769E-04
22	5.207E-05	6.351E-05	8.396E-05	1.270E-04	1.670E-04	1.798E-04	2.053E-04	2.314E-04	2.550E-04
23	7.468E-05	8.612E-05	1.117E-04	1.342E-04	1.583E-04	1.870E-04	1.956E-04	2.160E-04	2.226E-04
24	4.693E-05	6.659E-05	9.629E-05	1.039E-04	1.187E-04	1.423E-04	1.586E-04	1.630E-04	1.913E-04
25	4.744E-05	8.458E-05	1.020E-04	1.198E-04	1.321E-04	1.340E-04	1.385E-04	1.456E-04	1.538E-04
26	2.637E-05	6.814E-05	8.704E-05	9.516E-05	9.814E-05	1.212E-04	1.298E-04	1.332E-04	1.558E-04
27	4.025E-05	6.711E-05	8.550E-05	9.619E-05	1.305E-04	1.335E-04	1.421E-04	1.435E-04	1.646E-04
28	4.487E-05	8.818E-05	1.153E-04	1.342E-04	1.418E-04	1.551E-04	1.627E-04	1.764E-04	1.851E-04
29	5.926E-05	1.118E-04	1.169E-04	1.368E-04	1.470E-04	1.577E-04	1.771E-04	1.769E-04	1.820E-04
30	4.898E-05	7.790E-05	1.097E-04	1.342E-04	1.300E-04	1.423E-04	1.627E-04	1.677E-04	1.872E-04
31	3.562E-05	1.026E-04	1.287E-04	1.450E-04	1.464E-04	1.649E-04	1.807E-04	1.841E-04	1.805E-04
32	7.571E-05	9.948E-05	1.199E-04	1.363E-04	1.336E-04	1.289E-04	1.406E-04	1.456E-04	1.543E-04

Table A.6 Displacements (Mean Value) vs. Surface Pressure

Surface Pressure (lbf/in^2)	509.55	700.63	891.72	1082.80	1273.88	1464.97	1656.05	1847.13	2038.22
Total displacement (mean value) in.	5.08E-05	8.81E-05	1.17E-04	1.45E-04	1.65E-04	1.87E-04	2.07E-04	2.25E-04	2.43E-04
Structure displacement of specimen (in)	5.63E-06	1.13E-05	1.69E-05	2.25E-05	2.81E-05	3.38E-05	3.94E-05	4.50E-05	5.07E-05
Structure displacement of fixture (in).	2.94E-06	3.34E-06	5.01E-06	6.68E-06	8.35E-06	1.00E-05	1.17E-05	1.34E-05	1.50E-05
Contact displacement (mean value) in.	4.22E-05	7.35E-05	9.52E-05	1.15E-04	1.28E-04	1.43E-04	1.56E-04	1.67E-04	1.77E-04

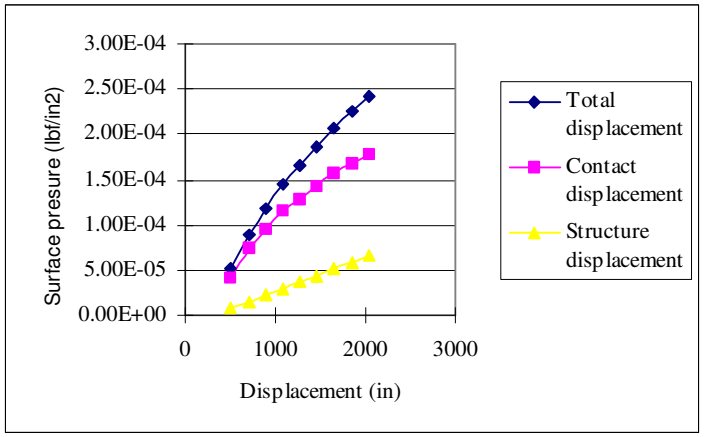

Figure A.3 Displacements (Mean Value) vs. Surface Pressure

Table A.7 Contact Stiffness

Group	509.55	700.63	891.72	1082.80	1273.88	1464.97	1656.05	1847.13	2038.22
1	4.69E+06	7.39E+06	7.62E+06	7.66E+06	8.34E+06	8.76E+06	8.60E+06	9.38E+06	1.06E+07
2	1.27E+07	8.39E+06	6.87E+06	6.76E+06	7.59E+06	8.33E+06	8.46E+06	9.47E+06	9.81E+06
3	1.23E+07	1.29E+07	1.09E+07	9.40E+06	9.25E+06	1.02E+07	1.07E+07	1.17E+07	1.27E+07
4	5.29E+06	6.38E+06	8.06E+06	8.90E+06	1.06E+07	1.15E+07	1.24E+07	1.25E+07	1.42E+07
5	6.38E+06	5.04E+06	6.59E+06	7.66E+06	8.45E+06	8.46E+06	9.25E+06	1.05E+07	1.06E+07
6	5.61E+06	6.32E+06	7.13E+06	8.84E+06	8.85E+06	9.04E+06	8.99E+06	9.01E+06	1.03E+07
7	1.12E+07	8.39E+06	9.34E+06	9.29E+06	9.89E+06	9.88E+06	9.77E+06	1.12E+07	1.07E+07
8	4.94E+06	6.07E+06	6.62E+06	6.76E+06	7.41E+06	7.42E+06	8.00E+06	8.37E+06	8.94E+06
9	4.36E+06	6.55E+06	5.99E+06	6.14E+06	7.29E+06	8.00E+06	8.33E+06	9.65E+06	1.02E+07
10	3.53E+06	5.44E+06	6.62E+06	6.98E+06	8.73E+06	8.43E+06	9.15E+06	8.47E+06	8.62E+06
11	3.86E+06	4.60E+06	5.95E+06	5.99E+06	7.07E+06	7.92E+06	8.12E+06	8.79E+06	9.16E+06
12	5.07E+06	4.75E+06	5.16E+06	5.42E+06	6.62E+06	7.57E+06	8.99E+06	9.29E+06	1.01E+07
13	2.79E+06	3.17E+06	4.53E+06	5.42E+06	6.81E+06	7.65E+06	7.78E+06	9.06E+06	1.04E+07
14	2.79E+06	3.60E+06	5.02E+06	6.14E+06	7.07E+06	7.06E+06	7.87E+06	8.01E+06	8.10E+06
15	4.03E+06	4.69E+06	5.48E+06	6.32E+06	6.18E+06	6.08E+06	6.93E+06	7.20E+06	7.71E+06
16	5.52E+06	5.33E+06	5.33E+06	6.38E+06	7.18E+06	7.97E+06	8.52E+06	8.08E+06	8.94E+06
17	4.69E+06	6.12E+06	6.59E+06	6.94E+06	7.75E+06	9.30E+06	1.06E+07	1.07E+07	1.12E+07
18	6.38E+06	3.96E+06	4.82E+06	6.22E+06	6.89E+06	7.32E+06	7.92E+06	8.67E+06	9.84E+06
19	1.31E+07	9.34E+06	1.01E+07	1.02E+07	1.01E+07	1.00E+07	9.95E+06	1.07E+07	1.15E+07
20	4.12E+06	4.44E+06	6.18E+06	6.55E+06	6.86E+06	7.25E+06	8.38E+06	9.41E+06	9.19E+06
21	5.44E+06	8.03E+06	6.22E+06	5.76E+06	6.52E+06	7.75E+06	8.22E+06	8.77E+06	9.72E+06
22	3.67E+06	6.02E+06	6.83E+06	6.02E+06	5.72E+06	6.38E+06	6.51E+06	6.61E+06	6.74E+06
23	2.56E+06	4.44E+06	5.13E+06	5.69E+06	6.04E+06	6.13E+06	6.84E+06	7.08E+06	7.73E+06
24	4.07E+06	5.74E+06	5.95E+06	7.36E+06	8.05E+06	8.06E+06	8.44E+06	9.38E+06	8.99E+06
25	4.03E+06	4.52E+06	5.62E+06	6.38E+06	7.24E+06	8.55E+06	9.66E+06	1.05E+07	1.12E+07
26	7.25E+06	5.61E+06	6.59E+06	8.03E+06	9.74E+06	9.46E+06	1.03E+07	1.15E+07	1.10E+07
27	4.75E+06	5.69E+06	6.70E+06	7.95E+06	7.32E+06	8.59E+06	9.41E+06	1.07E+07	1.05E+07
28	4.26E+06	4.33E+06	4.97E+06	5.69E+06	6.74E+06	7.39E+06	8.22E+06	8.67E+06	9.29E+06
29	3.22E+06	3.42E+06	4.91E+06	5.59E+06	6.50E+06	7.27E+06	7.55E+06	8.64E+06	9.45E+06
30	3.90E+06	4.91E+06	5.23E+06	5.69E+06	7.35E+06	8.06E+06	8.22E+06	9.12E+06	9.19E+06
31	5.36E+06	3.73E+06	4.46E+06	5.27E+06	6.52E+06	6.95E+06	7.40E+06	8.30E+06	9.53E+06
32	2.52E+06	3.84E+06	4.78E+06	5.61E+06	7.15E+06	8.90E+06	9.52E+06	1.05E+07	1.11E+07

Appendix B: Experimental Data (WP Radius =0.5in; Surface finish Ra = 5.55μm)

In this section, static experiments were conducted for an AISI4150 sample under different normal loads. The sample radius is 0.5 in, and its surface finish is 5.55μm. The experiment was repeated 32 times. Table B.1 shows the original measured data. In order to reduce the measured error, Table B.2 lists the relative measured data. Figure B.1 shows the relative measured results. Table B.3 lists the arithmetic mean of relative measured results. The standard deviation and 95% confidence interval are calculated. Figure B.2 is a plot of the mean values of all relative data versus normal loads. Table B.4 lists the surface pressure on the contact surface. From the relative measured data and Equation 4.3, the total displacement can be obtained as shown in the Table B.5. According to Equation 4.4, structure displacement can be computed theoretically. Therefore, contact displacement can be obtained by applying Equation 4.5, as shown in Table B.6. Table B.7 and Figure B.3 show the mean value of all kinds of displacements versus surface pressure. According to the definition of contact stiffness, Equation 4.6 can be used to obtain contact stiffness, as shown in Table B.8.

Table B.1 Original Measured Output Voltage (Unit: volt)

Group	250	400	550	700	850	1000	1150	1300	1450	1600
1	3.3644	3.3795	3.3896	3.3981	3.4047	3.4088	3.4109	3.4144	3.4188	3.4223
2	3.1122	3.1224	3.1434	3.1519	3.1567	3.1594	3.1607	3.1623	3.1632	3.1657
3	3.3454	3.3572	3.3704	3.3846	3.3935	3.3983	3.4053	3.4077	3.4092	3.4102
4	3.1579	3.1797	3.1953	3.2042	3.2089	3.2133	3.2154	3.2197	3.2216	3.2233
5	3.2772	3.293	3.3082	3.3189	3.3213	3.3257	3.3272	3.3278	3.3279	3.328
6	3.2284	3.2375	3.2481	3.2541	3.2594	3.2621	3.2634	3.2674	3.2694	3.2715
7	3.3256	3.3423	3.3494	3.3573	3.3602	3.3633	3.3655	3.3684	3.3711	3.3715
8	3.1906	3.1983	3.2098	3.2219	3.2252	3.2295	3.2316	3.2367	3.2398	3.2401
9	3.2522	3.2681	3.2749	3.2812	3.2853	3.288	3.2932	3.2964	3.2977	3.2983
10	3.2478	3.2588	3.2711	3.2752	3.2796	3.2841	3.2904	3.2932	3.2968	3.3004
11	3.463	3.4729	3.4809	3.4897	3.4939	3.4984	3.5018	3.5039	3.5057	3.5076
12	3.1642	3.1839	3.1997	3.2038	3.2078	3.2123	3.2144	3.2188	3.2224	3.2271
13	3.1692	3.1958	3.2126	3.2154	3.2191	3.2224	3.2252	3.2298	3.2302	3.2318
14	3.3102	3.3276	3.3347	3.3366	3.3402	3.3468	3.3509	3.3545	3.3586	3.3607
15	3.4485	3.4775	3.4933	3.499	3.5011	3.5028	3.5075	3.5101	3.5118	3.5123
16	3.092	3.1056	3.1162	3.1192	3.1208	3.1244	3.1286	3.1334	3.1389	3.1417
17	3.5888	3.6003	3.6079	3.6099	3.6154	3.6186	3.6215	3.6252	3.6299	3.6316
18	3.0239	3.0522	3.0637	3.0677	3.0694	3.0709	3.0744	3.0795	3.0832	3.0844
19	3.537	3.5492	3.5583	3.5662	3.5709	3.5752	3.5792	3.5814	3.5819	3.5822
20	3.069	3.081	3.0914	3.0998	3.1031	3.1063	3.1089	3.1121	3.1142	3.1159
21	3.5939	3.6068	3.6133	3.6193	3.6233	3.6288	3.6328	3.6366	3.6386	3.6423
22	3.5331	3.5421	3.5477	3.5519	3.5549	3.5591	3.5617	3.5659	3.5695	3.5732
23	3.5003	3.5142	3.5247	3.5333	3.5423	3.5489	3.5525	3.5568	3.5597	3.5601
24	3.0029	3.0103	3.0203	3.0256	3.0319	3.0392	3.0408	3.0453	3.0461	3.0502
25	3.4451	3.4562	3.4764	3.4876	3.4958	3.5035	3.5047	3.5059	3.5076	3.5092
26	3.4996	3.5096	3.5172	3.522	3.5273	3.5333	3.5347	3.5374	3.5412	3.5451
27	3.4228	3.4386	3.4524	3.461	3.4662	3.4712	3.4746	3.4787	3.4815	3.4851
28	3.4005	3.4158	3.4231	3.4308	3.4351	3.4409	3.4436	3.4472	3.4517	3.4601
29	3.5115	3.5208	3.5299	3.535	3.5387	3.5417	3.5455	3.548	3.5514	3.558
30	2.8917	2.9017	2.9111	2.9189	2.9238	2.9304	2.9333	2.9336	2.9367	2.941
31	3.1918	3.1996	3.2067	3.213	3.2158	3.2204	3.2233	3.226	3.229	3.2331
32	3.4261	3.4362	3.4491	3.4519	3.4561	3.4581	3.4618	3.4646	3.4678	3.4712

Table B.2 Relative Measured Data (Unit: volt)

Group	400	550	700	850	1000	1150	1300	1450	1600
1	0.0151	0.0252	0.0337	0.0403	0.0444	0.0465	0.05	0.0544	0.0579
2	0.0102	0.0312	0.0397	0.0445	0.0472	0.0485	0.0501	0.051	0.0535
3	0.0118	0.025	0.0392	0.0481	0.0529	0.0599	0.0623	0.0638	0.0648
4	0.0218	0.0374	0.0463	0.051	0.0554	0.0575	0.0618	0.0637	0.0654
5	0.0158	0.031	0.0417	0.0441	0.0485	0.05	0.0506	0.0507	0.0508
6	0.0091	0.0197	0.0257	0.031	0.0337	0.035	0.039	0.041	0.0431
7	0.0167	0.0238	0.0317	0.0346	0.0377	0.0399	0.0428	0.0455	0.0459
8	0.0077	0.0192	0.0313	0.0346	0.0389	0.041	0.0461	0.0492	0.0495
9	0.0159	0.0227	0.029	0.0331	0.0358	0.041	0.0442	0.0455	0.0461
10	0.011	0.0233	0.0274	0.0318	0.0363	0.0426	0.0454	0.049	0.0526
11	0.0099	0.0179	0.0267	0.0309	0.0354	0.0388	0.0409	0.0427	0.0446
12	0.0197	0.0355	0.0396	0.0436	0.0481	0.0502	0.0546	0.0582	0.0629
13	0.0266	0.0434	0.0462	0.0499	0.0532	0.056	0.0606	0.061	0.0626
14	0.0174	0.0245	0.0264	0.03	0.0366	0.0407	0.0443	0.0484	0.0505
15	0.029	0.0448	0.0505	0.0526	0.0543	0.059	0.0616	0.0633	0.0638
16	0.0136	0.0242	0.0272	0.0288	0.0324	0.0366	0.0414	0.0469	0.0497
17	0.0115	0.0191	0.0211	0.0266	0.0298	0.0327	0.0364	0.0411	0.0428
18	0.0283	0.0398	0.0438	0.0455	0.047	0.0505	0.0556	0.0593	0.0605
19	0.0122	0.0213	0.0292	0.0339	0.0382	0.0422	0.0444	0.0449	0.0452
20	0.012	0.0224	0.0308	0.0341	0.0373	0.0399	0.0431	0.0452	0.0469
21	0.0129	0.0194	0.0254	0.0294	0.0349	0.0389	0.0427	0.0447	0.0484
22	0.009	0.0146	0.0188	0.0218	0.026	0.0286	0.0328	0.0364	0.0401
23	0.0139	0.0244	0.033	0.042	0.0486	0.0522	0.0565	0.0594	0.0598
24	0.0074	0.0174	0.0227	0.029	0.0363	0.0379	0.0424	0.0432	0.0473
25	0.0111	0.0313	0.0425	0.0507	0.0584	0.0596	0.0608	0.0625	0.0641
26	0.01	0.0176	0.0224	0.0277	0.0337	0.0351	0.0378	0.0416	0.0455
27	0.0158	0.0296	0.0382	0.0434	0.0484	0.0518	0.0559	0.0587	0.0623
28	0.0153	0.0226	0.0303	0.0346	0.0404	0.0431	0.0467	0.0512	0.0596
29	0.0093	0.0184	0.0235	0.0272	0.0302	0.034	0.0365	0.0399	0.0465
30	0.01	0.0194	0.0272	0.0321	0.0387	0.0416	0.0419	0.045	0.0493
31	0.0078	0.0149	0.0212	0.024	0.0286	0.0315	0.0342	0.0372	0.0413
32	0.0101	0.023	0.0258	0.03	0.032	0.0357	0.0385	0.0417	0.0451

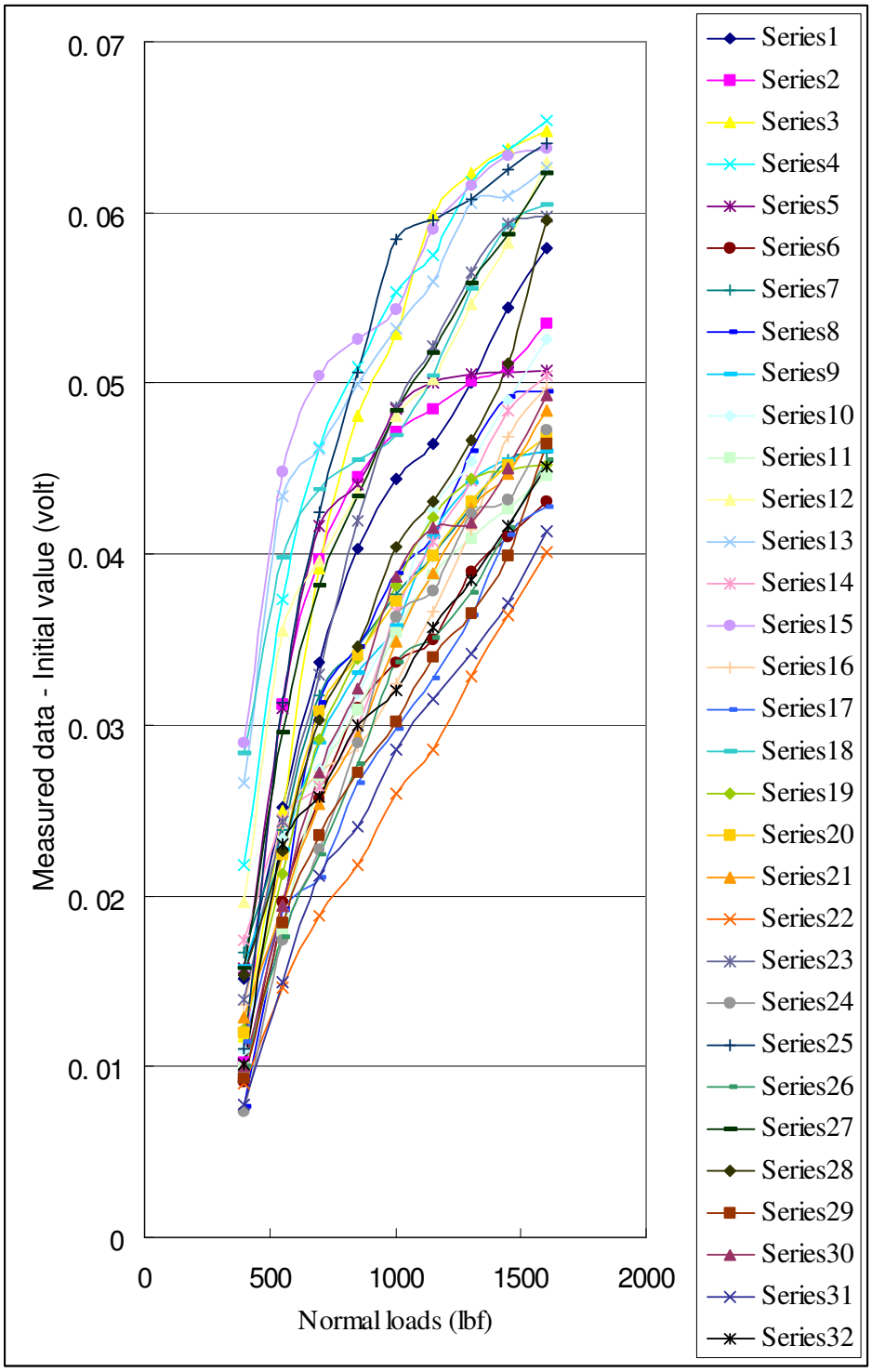

Figure B.1 All Relative Data vs. Normal Loads

Table B.3 All Relative Data vs. Normal Loads

Normal loads (lbf)	400	550	700	850	1000	1150	1300	1450	1600
Mean value (Volt)	1.40E-02	2.51E-02	3.18E-02	3.63E-02	4.06E-02	4.37E-02	4.69E-02	4.96E-02	5.21E-02
Standard Deviation	5.74E-03	7.96E-03	8.49E-03	8.71E-03	8.73E-03	8.77E-03	8.75E-03	8.37E-03	8.01E-03
95% Confidence lever	1.99E-03	2.76E-03	2.94E-03	3.02E-03	3.02E-03	3.04E-03	3.03E-03	2.90E-03	2.78E-03

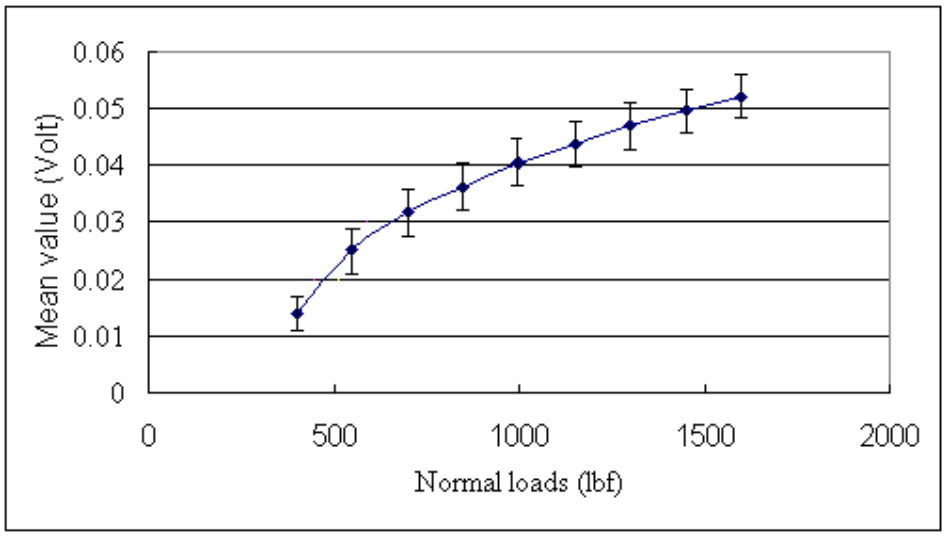

Figure B.2 Mean Values of All Relative Data vs. Normal Loads

Table B.4 Surface Pressure Caused by Normal Loads

Normal Load (lbf)	250	400	550	700	850
Surface Pressure (lbf/in^2)	318.47	509.55	700.64	891.72	1082.80
Normal Load (lbf)	1000	1150	1300	1450	1600
Surface Pressure (lbf/in^2)	1273.89	1464.97	1656.05	1847.13	2038.21

Table B.5 Total Displacement (in)

Group	400	550	700	850	1000	1150	1300	1450	1600
1	7.760E-05	1.290E-04	1.730E-04	2.070E-04	2.280E-04	2.390E-04	2.570E-04	2.800E-04	2.980E-04
2	5.242E-05	1.600E-04	2.040E-04	2.290E-04	2.430E-04	2.490E-04	2.570E-04	2.620E-04	2.750E-04
3	6.064E-05	1.280E-04	2.010E-04	2.470E-04	2.720E-04	3.080E-04	3.200E-04	3.280E-04	3.330E-04
4	1.120E-04	1.920E-04	2.380E-04	2.620E-04	2.850E-04	2.950E-04	3.180E-04	3.270E-04	3.360E-04
5	8.119E-05	1.590E-04	2.140E-04	2.270E-04	2.490E-04	2.570E-04	2.600E-04	2.610E-04	2.610E-04
6	4.676E-05	1.010E-04	1.320E-04	1.590E-04	1.730E-04	1.800E-04	2.000E-04	2.110E-04	2.210E-04
7	8.582E-05	1.220E-04	1.630E-04	1.780E-04	1.940E-04	2.050E-04	2.200E-04	2.340E-04	2.360E-04
8	3.957E-05	9.870E-05	1.610E-04	1.780E-04	2.000E-04	2.110E-04	2.370E-04	2.530E-04	2.540E-04
9	8.171E-05	1.170E-04	1.490E-04	1.700E-04	1.840E-04	2.110E-04	2.270E-04	2.340E-04	2.370E-04
10	5.653E-05	1.200E-04	1.410E-04	1.630E-04	1.870E-04	2.190E-04	2.330E-04	2.520E-04	2.700E-04
11	5.087E-05	9.200E-05	1.370E-04	1.590E-04	1.820E-04	1.990E-04	2.100E-04	2.190E-04	2.290E-04
12	1.012E-04	1.820E-04	2.030E-04	2.240E-04	2.470E-04	2.580E-04	2.810E-04	2.990E-04	3.230E-04
13	1.367E-04	2.230E-04	2.370E-04	2.560E-04	2.730E-04	2.880E-04	3.110E-04	3.130E-04	3.220E-04
14	8.941E-05	1.260E-04	1.360E-04	1.540E-04	1.880E-04	2.090E-04	2.280E-04	2.490E-04	2.600E-04
15	1.490E-04	2.300E-04	2.600E-04	2.700E-04	2.790E-04	3.030E-04	3.170E-04	3.250E-04	3.280E-04
16	6.989E-05	1.240E-04	1.400E-04	1.480E-04	1.660E-04	1.880E-04	2.130E-04	2.410E-04	2.550E-04
17	5.910E-05	9.820E-05	1.080E-04	1.370E-04	1.530E-04	1.680E-04	1.870E-04	2.110E-04	2.200E-04
18	1.454E-04	2.050E-04	2.250E-04	2.340E-04	2.420E-04	2.600E-04	2.860E-04	3.050E-04	3.110E-04
19	6.269E-05	1.090E-04	1.500E-04	1.740E-04	1.960E-04	2.170E-04	2.280E-04	2.310E-04	2.320E-04
20	6.167E-05	1.150E-04	1.580E-04	1.750E-04	1.920E-04	2.050E-04	2.210E-04	2.320E-04	2.410E-04
21	6.629E-05	9.970E-05	1.310E-04	1.510E-04	1.790E-04	2.000E-04	2.190E-04	2.300E-04	2.490E-04
22	4.625E-05	7.500E-05	9.660E-05	1.120E-04	1.340E-04	1.470E-04	1.690E-04	1.870E-04	2.060E-04
23	7.143E-05	1.250E-04	1.700E-04	2.160E-04	2.500E-04	2.680E-04	2.900E-04	3.050E-04	3.070E-04
24	3.803E-05	8.940E-05	1.170E-04	1.490E-04	1.870E-04	1.950E-04	2.180E-04	2.220E-04	2.430E-04
25	5.704E-05	1.610E-04	2.180E-04	2.610E-04	3.000E-04	3.060E-04	3.120E-04	3.210E-04	3.290E-04
26	5.139E-05	9.040E-05	1.150E-04	1.420E-04	1.730E-04	1.800E-04	1.940E-04	2.140E-04	2.340E-04
27	8.119E-05	1.520E-04	1.960E-04	2.230E-04	2.490E-04	2.660E-04	2.870E-04	3.020E-04	3.200E-04
28	7.862E-05	1.160E-04	1.560E-04	1.780E-04	2.080E-04	2.210E-04	2.400E-04	2.630E-04	3.060E-04
29	4.779E-05	9.460E-05	1.210E-04	1.400E-04	1.550E-04	1.750E-04	1.880E-04	2.050E-04	2.390E-04
30	5.139E-05	9.970E-05	1.400E-04	1.650E-04	1.990E-04	2.140E-04	2.150E-04	2.310E-04	2.530E-04
31	4.008E-05	7.660E-05	1.090E-04	1.230E-04	1.470E-04	1.620E-04	1.760E-04	1.910E-04	2.120E-04
32	5.190E-05	1.180E-04	1.330E-04	1.540E-04	1.640E-04	1.830E-04	1.980E-04	2.140E-04	2.320E-04

TableB.6 Contact Displacement (in)

Group	400	550	700	850	1000	1150	1300	1450	1600
1	6.90E-05	1.15E-04	1.51E-04	1.78E-04	1.92E-04	1.95E-04	2.06E-04	2.21E-04	2.32E-04
2	4.38E-05	1.46E-04	1.82E-04	1.99E-04	2.06E-04	2.05E-04	2.06E-04	2.04E-04	2.09E-04
3	5.21E-05	1.14E-04	1.80E-04	2.18E-04	2.35E-04	2.64E-04	2.69E-04	2.69E-04	2.67E-04
4	1.03E-04	1.78E-04	2.16E-04	2.33E-04	2.48E-04	2.52E-04	2.66E-04	2.69E-04	2.70E-04
5	7.26E-05	1.45E-04	1.92E-04	1.97E-04	2.13E-04	2.13E-04	2.09E-04	2.02E-04	1.95E-04
6	3.82E-05	8.66E-05	1.10E-04	1.30E-04	1.37E-04	1.36E-04	1.49E-04	1.52E-04	1.56E-04
7	7.72E-05	1.08E-04	1.41E-04	1.49E-04	1.57E-04	1.61E-04	1.69E-04	1.75E-04	1.70E-04
8	3.10E-05	8.41E-05	1.39E-04	1.49E-04	1.63E-04	1.67E-04	1.86E-04	1.94E-04	1.89E-04
9	7.31E-05	1.02E-04	1.27E-04	1.41E-04	1.47E-04	1.67E-04	1.76E-04	1.75E-04	1.71E-04
10	4.80E-05	1.05E-04	1.19E-04	1.34E-04	1.50E-04	1.75E-04	1.82E-04	1.93E-04	2.05E-04
11	4.23E-05	7.74E-05	1.15E-04	1.30E-04	1.45E-04	1.56E-04	1.59E-04	1.61E-04	1.63E-04
12	9.27E-05	1.68E-04	1.82E-04	1.95E-04	2.11E-04	2.14E-04	2.29E-04	2.41E-04	2.58E-04
13	1.28E-04	2.08E-04	2.16E-04	2.27E-04	2.37E-04	2.44E-04	2.60E-04	2.55E-04	2.56E-04
14	8.08E-05	1.11E-04	1.14E-04	1.25E-04	1.52E-04	1.65E-04	1.77E-04	1.90E-04	1.94E-04
15	1.40E-04	2.16E-04	2.38E-04	2.41E-04	2.43E-04	2.59E-04	2.65E-04	2.67E-04	2.62E-04
16	6.13E-05	1.10E-04	1.18E-04	1.19E-04	1.30E-04	1.44E-04	1.62E-04	1.83E-04	1.90E-04
17	5.05E-05	8.36E-05	8.65E-05	1.07E-04	1.17E-04	1.24E-04	1.36E-04	1.53E-04	1.54E-04
18	1.37E-04	1.90E-04	2.03E-04	2.05E-04	2.05E-04	2.16E-04	2.35E-04	2.46E-04	2.45E-04
19	5.41E-05	9.49E-05	1.28E-04	1.45E-04	1.60E-04	1.73E-04	1.77E-04	1.72E-04	1.67E-04
20	5.31E-05	1.01E-04	1.36E-04	1.46E-04	1.55E-04	1.61E-04	1.70E-04	1.74E-04	1.75E-04
21	5.77E-05	8.51E-05	1.09E-04	1.22E-04	1.43E-04	1.56E-04	1.68E-04	1.71E-04	1.83E-04
22	3.77E-05	6.04E-05	7.47E-05	8.28E-05	9.71E-05	1.03E-04	1.17E-04	1.29E-04	1.40E-04
23	6.29E-05	1.11E-04	1.48E-04	1.87E-04	2.13E-04	2.24E-04	2.39E-04	2.47E-04	2.42E-04
24	2.95E-05	7.48E-05	9.48E-05	1.20E-04	1.50E-04	1.51E-04	1.67E-04	1.64E-04	1.77E-04
25	4.85E-05	1.46E-04	1.96E-04	2.31E-04	2.64E-04	2.62E-04	2.61E-04	2.63E-04	2.64E-04
26	4.28E-05	7.58E-05	9.32E-05	1.13E-04	1.37E-04	1.37E-04	1.43E-04	1.55E-04	1.68E-04
27	7.26E-05	1.38E-04	1.74E-04	1.94E-04	2.12E-04	2.22E-04	2.36E-04	2.43E-04	2.54E-04
28	7.01E-05	1.02E-04	1.34E-04	1.49E-04	1.71E-04	1.78E-04	1.89E-04	2.05E-04	2.41E-04
29	3.92E-05	8.00E-05	9.89E-05	1.11E-04	1.19E-04	1.31E-04	1.36E-04	1.47E-04	1.73E-04
30	4.28E-05	8.51E-05	1.18E-04	1.36E-04	1.62E-04	1.70E-04	1.64E-04	1.73E-04	1.88E-04
31	3.15E-05	6.20E-05	8.70E-05	9.41E-05	1.10E-04	1.18E-04	1.25E-04	1.33E-04	1.47E-04
32	4.33E-05	1.04E-04	1.11E-04	1.25E-04	1.28E-04	1.40E-04	1.47E-04	1.56E-04	1.66E-04

Table B.7 Displacement Analysis

Surface Presure (lbf/in^2)	509.55	700.64	891.72	1082.80	1273.89	1464.97	1656.05	1847.13	2038.22
Total displacement (mean value) in.	7.19E-05	1.29E-04	1.64E-04	1.86E-04	2.09E-04	2.25E-04	2.41E-04	2.55E-04	2.68E-04
Structure displacement of specimen in.	5.62E-06	1.12E-05	1.69E-05	2.25E-05	2.81E-05	3.38E-05	3.94E-05	4.50E-05	5.06E-05
Structure displacement of fixture in.	2.94E-06	3.34E-06	5.01E-06	6.68E-06	8.35E-06	1.00E-05	1.17E-05	1.34E-05	1.50E-05
Contact displacement (mean value) in.	6.34E-05	1.15E-04	1.42E-04	1.57E-04	1.72E-04	1.81E-04	1.90E-04	1.96E-04	2.02E-04

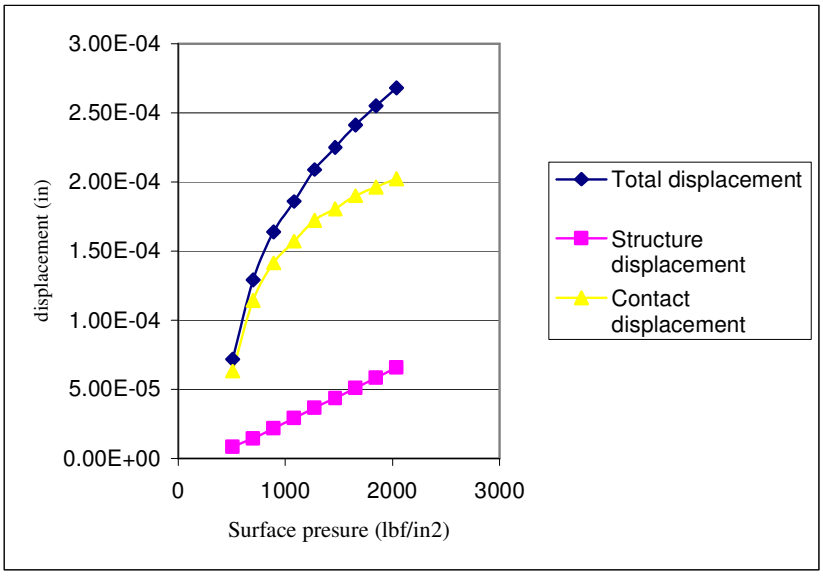

FigureB.3 Displacement vs. Surface Pressure

Table B.8 Contact Stiffness

Group	509.55	700.64	891.72	1082.80	1273.89	1464.97	1656.05	1847.13	2038.22
1	2.77E+06	3.33E+06	3.79E+06	4.30E+06	4.98E+06	5.87E+06	6.50E+06	6.91E+06	7.42E+06
2	4.36E+06	2.62E+06	3.15E+06	3.83E+06	4.64E+06	5.58E+06	6.48E+06	7.51E+06	8.22E+06
3	3.67E+06	3.36E+06	3.19E+06	3.51E+06	4.06E+06	4.34E+06	4.97E+06	5.67E+06	6.43E+06
4	1.85E+06	2.15E+06	2.65E+06	3.28E+06	3.85E+06	4.56E+06	5.02E+06	5.68E+06	6.36E+06
5	2.63E+06	2.64E+06	2.98E+06	3.87E+06	4.49E+06	5.38E+06	6.40E+06	7.56E+06	8.80E+06
6	5.00E+06	4.41E+06	5.20E+06	5.87E+06	6.99E+06	8.43E+06	8.96E+06	1.00E+07	1.10E+07
7	2.47E+06	3.55E+06	4.07E+06	5.14E+06	6.08E+06	7.11E+06	7.92E+06	8.71E+06	1.01E+07
8	6.16E+06	4.55E+06	4.13E+06	5.14E+06	5.85E+06	6.87E+06	7.20E+06	7.86E+06	9.11E+06
9	2.61E+06	3.74E+06	4.51E+06	5.42E+06	6.48E+06	6.87E+06	7.60E+06	8.71E+06	1.00E+07
10	3.98E+06	3.64E+06	4.82E+06	5.69E+06	6.37E+06	6.55E+06	7.34E+06	7.90E+06	8.41E+06
11	4.52E+06	4.94E+06	4.97E+06	5.90E+06	6.57E+06	7.37E+06	8.41E+06	9.49E+06	1.05E+07
12	2.06E+06	2.28E+06	3.16E+06	3.92E+06	4.53E+06	5.35E+06	5.83E+06	6.35E+06	6.68E+06
13	1.49E+06	1.83E+06	2.66E+06	3.36E+06	4.03E+06	4.70E+06	5.14E+06	5.99E+06	6.72E+06
14	2.36E+06	3.43E+06	5.04E+06	6.12E+06	6.30E+06	6.93E+06	7.58E+06	8.03E+06	8.87E+06
15	1.36E+06	1.77E+06	2.41E+06	3.17E+06	3.94E+06	4.42E+06	5.04E+06	5.73E+06	6.56E+06
16	3.12E+06	3.48E+06	4.86E+06	6.43E+06	7.35E+06	7.95E+06	8.27E+06	8.37E+06	9.07E+06
17	3.78E+06	4.57E+06	6.62E+06	7.11E+06	8.19E+06	9.23E+06	9.84E+06	1.00E+07	1.11E+07
18	1.40E+06	2.01E+06	2.82E+06	3.74E+06	4.66E+06	5.31E+06	5.70E+06	6.21E+06	7.01E+06
19	3.53E+06	4.03E+06	4.47E+06	5.27E+06	5.98E+06	6.62E+06	7.55E+06	8.87E+06	1.03E+07
20	3.60E+06	3.80E+06	4.20E+06	5.23E+06	6.16E+06	7.11E+06	7.85E+06	8.79E+06	9.81E+06
21	3.31E+06	4.49E+06	5.28E+06	6.27E+06	6.69E+06	7.34E+06	7.95E+06	8.92E+06	9.40E+06
22	5.07E+06	6.32E+06	7.67E+06	9.23E+06	9.84E+06	1.11E+07	1.14E+07	1.19E+07	1.23E+07
23	3.04E+06	3.45E+06	3.88E+06	4.10E+06	4.48E+06	5.11E+06	5.59E+06	6.19E+06	7.12E+06
24	6.49E+06	5.11E+06	6.05E+06	6.38E+06	6.37E+06	7.59E+06	8.02E+06	9.34E+06	9.70E+06
25	3.94E+06	2.61E+06	2.92E+06	3.30E+06	3.62E+06	4.37E+06	5.12E+06	5.82E+06	6.52E+06
26	4.46E+06	5.04E+06	6.15E+06	6.76E+06	6.99E+06	8.39E+06	9.34E+06	9.84E+06	1.02E+07
27	2.63E+06	2.78E+06	3.29E+06	3.94E+06	4.50E+06	5.16E+06	5.66E+06	6.28E+06	6.76E+06
28	2.73E+06	3.76E+06	4.28E+06	5.14E+06	5.58E+06	6.45E+06	7.08E+06	7.47E+06	7.15E+06
29	4.87E+06	4.78E+06	5.80E+06	6.91E+06	8.05E+06	8.76E+06	9.80E+06	1.04E+07	9.93E+06
30	4.46E+06	4.49E+06	4.86E+06	5.63E+06	5.88E+06	6.75E+06	8.15E+06	8.84E+06	9.16E+06
31	6.06E+06	6.17E+06	6.59E+06	8.12E+06	8.65E+06	9.71E+06	1.07E+07	1.15E+07	1.17E+07
32	4.41E+06	3.69E+06	5.18E+06	6.12E+06	7.47E+06	8.21E+06	9.11E+06	9.81E+06	1.04E+07

Appendix C: Experimental Data (Radius =0.375in)

In order to study the effect of the contact area, the static experiment were conducted for AISI4150 sample with radius 0.375 in. The experiment was repeated 32 times. Table C.1 shows the original measured data. In order to reduce the measured error, Table C.2 lists the relative measured data. Figure C.1 shows the relative measured results. Table C.3 lists the arithmetic mean of the relative measured results. The standard deviation and 95% confidence interval are calculated. Figure C.2 is a plot of the mean values of all relative data versus normal loads. Table C.4 lists the surface pressure on the contact surface. From the relative measured data and Equation 4.3, the total displacement can be obtained, as shown in the Table C.5. According to Equation 4.4, the structure displacement can be computed theoretically. Therefore, contact displacement can be obtained by applying Equation 4.5, as shown in Table C.6. Table C.7 and Figure C.3 show the mean value of all kinds of displacements versus surface pressure. According to the definition of contact stiffness, Equation 4.6 can be used to obtain contact stiffness, as shown in Table C.8.

Table C.1 Original Measured Output Voltage (Unit: volt)

Group	250	400	550	700	850	1000	1150	1300	1450	1600
1	3.7967	3.8117	3.8182	3.824	3.8316	3.8408	3.8466	3.8544	3.8599	3.8673
2	3.1205	3.1359	3.1552	3.1654	3.1698	3.1761	3.1802	3.1831	3.1859	3.1926
3	3.5543	3.5715	3.5848	3.5906	3.5986	3.6044	3.6069	3.6105	3.6114	3.6156
4	3.5602	3.5744	3.5893	3.5963	3.6056	3.6154	3.6219	3.6324	3.6407	3.6488
5	3.6354	3.6468	3.6598	3.668	3.6753	3.6769	3.6777	3.685	3.6866	3.6896
6	3.5539	3.5685	3.5874	3.5961	3.6011	3.6063	3.611	3.6131	3.6194	3.623
7	3.6751	3.6919	3.7005	3.7054	3.7154	3.719	3.7265	3.7289	3.7347	3.736
8	3.439	3.4587	3.4724	3.4783	3.4818	3.4852	3.4889	3.4947	3.4988	3.5007
9	3.6643	3.6785	3.6872	3.6921	3.704	3.7101	3.7101	3.7138	3.7173	3.721
10	3.4862	3.4997	3.5136	3.5203	3.5312	3.5411	3.5467	3.5534	3.5593	3.5637
11	3.6362	3.6487	3.6577	3.6643	3.6704	3.6738	3.677	3.6782	3.6822	3.6847
12	3.5224	3.5353	3.5496	3.5591	3.5713	3.5787	3.5859	3.5929	3.6016	3.6093
13	3.3644	3.3771	3.387	3.3943	3.4002	3.4053	3.4089	3.4132	3.4146	3.4185
14	3.1122	3.1246	3.1362	3.1463	3.1564	3.1682	3.1751	3.1829	3.1906	3.1966
15	3.3572	3.3684	3.379	3.3829	3.3882	3.3933	3.4004	3.4055	3.4115	3.4129
16	3.1579	3.1729	3.1878	3.1961	3.2075	3.2161	3.2247	3.2329	3.2385	3.2462
17	3.2772	3.2883	3.2962	3.303	3.308	3.313	3.3201	3.3247	3.327	3.33
18	3.2284	3.2414	3.2605	3.269	3.2778	3.2845	3.2949	3.3051	3.3123	3.3187
19	3.3256	3.3407	3.3507	3.3595	3.3675	3.3729	3.3785	3.3822	3.3842	3.3861
20	3.1906	3.211	3.2238	3.2327	3.2405	3.2496	3.2576	3.2644	3.2701	3.2751
21	3.2522	3.2635	3.2734	3.2821	3.2901	3.2961	3.3003	3.3028	3.3049	3.3084
22	3.2478	3.2634	3.2765	3.2881	3.2971	3.3071	3.3159	3.3256	3.3312	3.3385
23	3.3334	3.3472	3.3545	3.3622	3.3665	3.3762	3.3799	3.3841	3.3885	3.3917
24	3.1642	3.1809	3.1988	3.2065	3.2169	3.228	3.2383	3.2457	3.2549	3.2629
25	3.1692	3.1817	3.1947	3.2029	3.2112	3.218	3.2239	3.2301	3.2305	3.2348
26	3.3102	3.3318	3.3489	3.3596	3.3681	3.3749	3.382	3.3892	3.395	3.4016
27	3.4485	3.4653	3.4841	3.49	3.4967	3.5018	3.5057	3.5143	3.5199	3.5242
28	3.092	3.1026	3.1128	3.1198	3.1261	3.1344	3.1409	3.1477	3.1535	3.1577
29	3.5888	3.5988	3.6104	3.6159	3.6234	3.6309	3.6376	3.6427	3.6459	3.6469
30	3.0239	3.0441	3.0576	3.0647	3.0736	3.0821	3.0889	3.0962	3.1017	3.1089
31	3.537	3.5529	3.5637	3.5676	3.5729	3.5793	3.5828	3.5869	3.5884	3.5892
32	3.069	3.0793	3.1001	3.1057	3.1161	3.1245	3.1309	3.1415	3.1452	3.1521

Table C.2 Relative Measured Data (Unit: volt)

Group	400	550	700	850	1000	1150	1300	1450	1600
1	0.015	0.0215	0.0273	0.0349	0.0441	0.0499	0.0577	0.0632	0.0706
2	0.0154	0.0347	0.0449	0.0493	0.0556	0.0597	0.0626	0.0654	0.0721
3	0.0172	0.0305	0.0363	0.0443	0.0501	0.0526	0.0562	0.0571	0.0613
4	0.0142	0.0291	0.0361	0.0454	0.0552	0.0617	0.0722	0.0805	0.0886
5	0.0114	0.0244	0.0326	0.0399	0.0415	0.0423	0.0496	0.0512	0.0542
6	0.0146	0.0335	0.0422	0.0472	0.0524	0.0571	0.0592	0.0655	0.0691
7	0.0168	0.0254	0.0303	0.0403	0.0439	0.0514	0.0538	0.0596	0.0609
8	0.0197	0.0334	0.0393	0.0428	0.0462	0.0499	0.0557	0.0598	0.0617
9	0.0142	0.0229	0.0278	0.0397	0.0458	0.0458	0.0495	0.053	0.0567
10	0.0135	0.0274	0.0341	0.045	0.0549	0.0605	0.0672	0.0731	0.0775
11	0.0125	0.0215	0.0281	0.0342	0.0376	0.0408	0.042	0.046	0.0485
12	0.0129	0.0272	0.0367	0.0489	0.0563	0.0635	0.0705	0.0792	0.0869
13	0.0127	0.0226	0.0299	0.0358	0.0409	0.0445	0.0488	0.0502	0.0541
14	0.0124	0.024	0.0341	0.0442	0.056	0.0629	0.0707	0.0784	0.0844
15	0.0112	0.0218	0.0257	0.031	0.0361	0.0432	0.0483	0.0543	0.0557
16	0.015	0.0299	0.0382	0.0496	0.0582	0.0668	0.075	0.0806	0.0883
17	0.0111	0.019	0.0258	0.0308	0.0358	0.0429	0.0475	0.0498	0.0528
18	0.013	0.0321	0.0406	0.0494	0.0561	0.0665	0.0767	0.0839	0.0903
19	0.0151	0.0251	0.0339	0.0419	0.0473	0.0529	0.0566	0.0586	0.0605
20	0.0204	0.0332	0.0421	0.0499	0.059	0.067	0.0738	0.0795	0.0845
21	0.0113	0.0212	0.0299	0.0379	0.0439	0.0481	0.0506	0.0527	0.0562
22	0.0156	0.0287	0.0403	0.0493	0.0593	0.0681	0.0778	0.0834	0.0907
23	0.0138	0.0211	0.0288	0.0331	0.0428	0.0465	0.0507	0.0551	0.0583
24	0.0167	0.0346	0.0423	0.0527	0.0638	0.0741	0.0815	0.0907	0.0987
25	0.0125	0.0255	0.0337	0.042	0.0488	0.0547	0.0609	0.0613	0.0656
26	0.0216	0.0387	0.0494	0.0579	0.0647	0.0718	0.079	0.0848	0.0914
27	0.0168	0.0356	0.0415	0.0482	0.0533	0.0572	0.0658	0.0714	0.0757
28	0.0106	0.0208	0.0278	0.0341	0.0424	0.0489	0.0557	0.0615	0.0657
29	0.01	0.0216	0.0271	0.0346	0.0421	0.0488	0.0539	0.0571	0.0581
30	0.0202	0.0337	0.0408	0.0497	0.0582	0.065	0.0723	0.0778	0.085
31	0.0159	0.0267	0.0306	0.0359	0.0423	0.0458	0.0499	0.0514	0.0522
32	0.0103	0.0311	0.0367	0.0471	0.0555	0.0619	0.0725	0.0762	0.0831

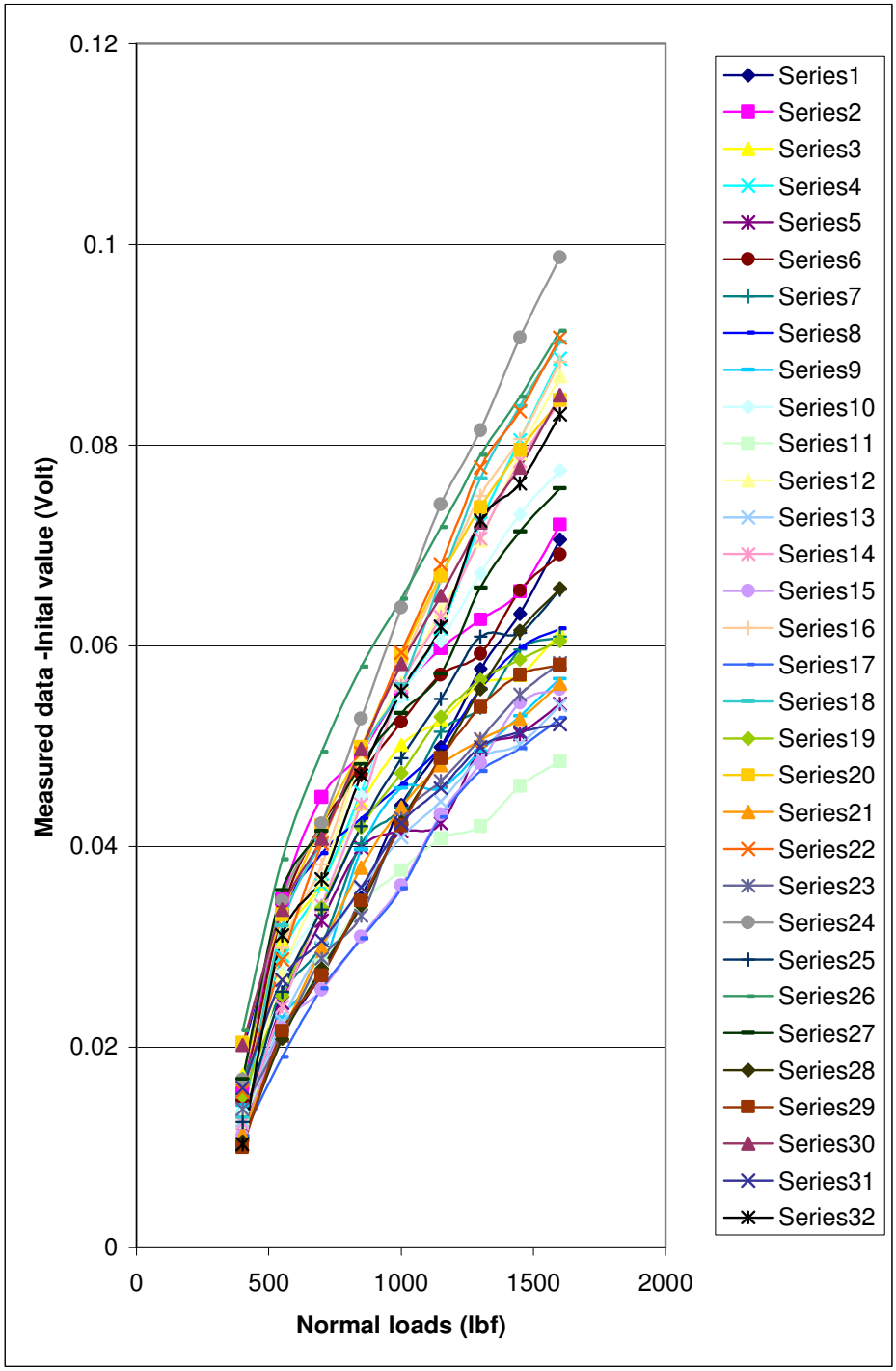

Figure C.1 All Relative Data in Day 1 vs. Normal Loads

Table C.3 All Relative Data vs. Normal Loads

Normal loads (lbf)	400	550	700	850	1000	1150	1300	1450	1600
Mean value (Volt)	1.45E-02	2.75E-02	3.48E-02	4.27E-02	4.97E-02	5.54E-02	6.14E-02	6.60E-02	7.06E-02
Standard Deviation	3.06E-03	5.41E-03	6.27E-03	7.00E-03	8.10E-03	9.53E-03	1.13E-02	1.29E-02	1.48E-02
95% Confidence lever	1.06E-03	1.87E-03	2.17E-03	2.43E-03	2.81E-03	3.30E-03	3.90E-03	4.46E-03	5.12E-03

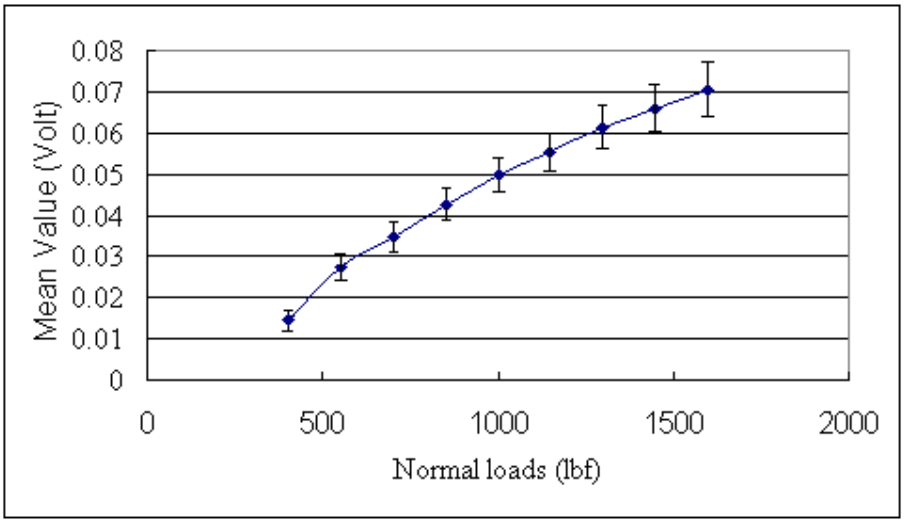

Figure C.2 Mean Values of All Relative Data vs. Normal Loads

Table C.4 Surface Pressure Caused by Normal Loads

Normal Load (lbf)	250	400	550	700	850
Surface Pressure (lbf/in^2)	566.17	905.87	1245.58	1585.28	1924.98
Normal Load (lbf)	1000	1150	1300	1450	1600
Surface Pressure (lbf/in^2)	2264.69	2604.39	2944.09	3283.79	3623.50

Table C.5 Total Displacement (in)

Group	400	550	700	850	1000	1150	1300	1450	1600
1	7.708E-05	1.105E-04	1.400E-04	1.790E-04	2.270E-04	2.560E-04	2.970E-04	3.250E-04	3.630E-04
2	7.914E-05	1.783E-04	2.310E-04	2.530E-04	2.860E-04	3.070E-04	3.220E-04	3.360E-04	3.710E-04
3	8.839E-05	1.567E-04	1.870E-04	2.280E-04	2.570E-04	2.700E-04	2.890E-04	2.930E-04	3.150E-04
4	7.297E-05	1.495E-04	1.860E-04	2.330E-04	2.840E-04	3.170E-04	3.710E-04	4.140E-04	4.550E-04
5	5.858E-05	1.254E-04	1.680E-04	2.050E-04	2.130E-04	2.170E-04	2.550E-04	2.630E-04	2.790E-04
6	7.503E-05	1.721E-04	2.170E-04	2.430E-04	2.690E-04	2.930E-04	3.040E-04	3.370E-04	3.550E-04
7	8.633E-05	1.305E-04	1.560E-04	2.070E-04	2.260E-04	2.640E-04	2.760E-04	3.060E-04	3.130E-04
8	1.012E-04	1.716E-04	2.020E-04	2.200E-04	2.370E-04	2.560E-04	2.860E-04	3.070E-04	3.170E-04
9	7.297E-05	1.177E-04	1.430E-04	2.040E-04	2.350E-04	2.350E-04	2.540E-04	2.720E-04	2.910E-04
10	6.937E-05	1.408E-04	1.750E-04	2.310E-04	2.820E-04	3.110E-04	3.450E-04	3.760E-04	3.980E-04
11	6.423E-05	1.105E-04	1.440E-04	1.760E-04	1.930E-04	2.100E-04	2.160E-04	2.360E-04	2.490E-04
12	6.629E-05	1.398E-04	1.890E-04	2.510E-04	2.890E-04	3.260E-04	3.620E-04	4.070E-04	4.470E-04
13	6.526E-05	1.161E-04	1.540E-04	1.840E-04	2.100E-04	2.290E-04	2.510E-04	2.580E-04	2.780E-04
14	6.372E-05	1.233E-04	1.750E-04	2.270E-04	2.880E-04	3.230E-04	3.630E-04	4.030E-04	4.340E-04
15	5.755E-05	1.120E-04	1.320E-04	1.590E-04	1.860E-04	2.220E-04	2.480E-04	2.790E-04	2.860E-04
16	7.708E-05	1.536E-04	1.960E-04	2.550E-04	2.990E-04	3.430E-04	3.850E-04	4.140E-04	4.540E-04
17	5.704E-05	9.764E-05	1.330E-04	1.580E-04	1.840E-04	2.200E-04	2.440E-04	2.560E-04	2.710E-04
18	6.680E-05	1.650E-04	2.090E-04	2.540E-04	2.880E-04	3.420E-04	3.940E-04	4.310E-04	4.640E-04
19	7.760E-05	1.290E-04	1.740E-04	2.150E-04	2.430E-04	2.720E-04	2.910E-04	3.010E-04	3.110E-04
20	1.048E-04	1.706E-04	2.160E-04	2.560E-04	3.030E-04	3.440E-04	3.790E-04	4.090E-04	4.340E-04
21	5.807E-05	1.089E-04	1.540E-04	1.950E-04	2.260E-04	2.470E-04	2.600E-04	2.710E-04	2.890E-04
22	8.016E-05	1.475E-04	2.070E-04	2.530E-04	3.050E-04	3.500E-04	4.000E-04	4.290E-04	4.660E-04
23	7.091E-05	1.084E-04	1.480E-04	1.700E-04	2.200E-04	2.390E-04	2.610E-04	2.830E-04	3.000E-04
24	8.582E-05	1.778E-04	2.170E-04	2.710E-04	3.280E-04	3.810E-04	4.190E-04	4.660E-04	5.070E-04
25	6.423E-05	1.310E-04	1.730E-04	2.160E-04	2.510E-04	2.810E-04	3.130E-04	3.150E-04	3.370E-04
26	1.110E-04	1.989E-04	2.540E-04	2.980E-04	3.320E-04	3.690E-04	4.060E-04	4.360E-04	4.700E-04
27	8.633E-05	1.829E-04	2.130E-04	2.480E-04	2.740E-04	2.940E-04	3.380E-04	3.670E-04	3.890E-04
28	5.447E-05	1.069E-04	1.430E-04	1.750E-04	2.180E-04	2.510E-04	2.860E-04	3.160E-04	3.380E-04
29	5.139E-05	1.110E-04	1.390E-04	1.780E-04	2.160E-04	2.510E-04	2.770E-04	2.930E-04	2.990E-04
30	8.171E-05	1.372E-04	1.570E-04	1.840E-04	2.170E-04	2.350E-04	2.560E-04	2.640E-04	2.680E-04
31	8.171E-05	1.372E-04	1.570E-04	1.840E-04	2.170E-04	2.350E-04	2.560E-04	2.640E-04	2.680E-04
32	5.293E-05	1.598E-04	1.890E-04	2.420E-04	2.850E-04	3.180E-04	3.730E-04	3.920E-04	4.270E-04

Table C.6 Contact Displacement

Group	400	550	700	850	1000	1150	1300	1450	1600
1	6.41E-05	8.71E-05	1.05E-04	1.33E-04	1.68E-04	1.86E-04	2.15E-04	2.31E-04	2.58E-04
2	6.62E-05	1.55E-04	1.96E-04	2.07E-04	2.27E-04	2.37E-04	2.40E-04	2.43E-04	2.65E-04
3	7.54E-05	1.33E-04	1.52E-04	1.81E-04	1.99E-04	2.00E-04	2.07E-04	2.00E-04	2.10E-04
4	6.00E-05	1.26E-04	1.50E-04	1.87E-04	2.25E-04	2.47E-04	2.89E-04	3.20E-04	3.50E-04
5	4.56E-05	1.02E-04	1.32E-04	1.58E-04	1.55E-04	1.47E-04	1.73E-04	1.70E-04	1.73E-04
6	6.21E-05	1.49E-04	1.82E-04	1.96E-04	2.11E-04	2.23E-04	2.22E-04	2.43E-04	2.50E-04
7	7.34E-05	1.07E-04	1.21E-04	1.60E-04	1.67E-04	1.94E-04	1.95E-04	2.13E-04	2.08E-04
8	8.83E-05	1.48E-04	1.67E-04	1.73E-04	1.79E-04	1.86E-04	2.04E-04	2.14E-04	2.12E-04
9	6.00E-05	9.43E-05	1.08E-04	1.57E-04	1.77E-04	1.65E-04	1.73E-04	1.79E-04	1.86E-04
10	5.64E-05	1.17E-04	1.40E-04	1.85E-04	2.24E-04	2.41E-04	2.64E-04	2.82E-04	2.93E-04
11	5.13E-05	8.71E-05	1.09E-04	1.29E-04	1.35E-04	1.40E-04	1.34E-04	1.43E-04	1.44E-04
12	5.33E-05	1.16E-04	1.54E-04	2.05E-04	2.31E-04	2.56E-04	2.81E-04	3.14E-04	3.41E-04
13	5.23E-05	9.28E-05	1.19E-04	1.37E-04	1.52E-04	1.59E-04	1.69E-04	1.65E-04	1.73E-04
14	5.08E-05	1.00E-04	1.40E-04	1.80E-04	2.29E-04	2.53E-04	2.82E-04	3.09E-04	3.29E-04
15	4.46E-05	8.87E-05	9.70E-05	1.13E-04	1.27E-04	1.52E-04	1.66E-04	1.86E-04	1.81E-04
16	6.41E-05	1.30E-04	1.61E-04	2.08E-04	2.41E-04	2.73E-04	3.04E-04	3.21E-04	3.49E-04
17	4.41E-05	7.43E-05	9.75E-05	1.12E-04	1.26E-04	1.50E-04	1.62E-04	1.62E-04	1.66E-04
18	5.39E-05	1.42E-04	1.74E-04	2.07E-04	2.30E-04	2.72E-04	3.12E-04	3.38E-04	3.59E-04
19	6.47E-05	1.06E-04	1.39E-04	1.69E-04	1.85E-04	2.02E-04	2.09E-04	2.08E-04	2.06E-04
20	9.19E-05	1.47E-04	1.81E-04	2.10E-04	2.45E-04	2.74E-04	2.97E-04	3.15E-04	3.29E-04
21	4.51E-05	8.56E-05	1.19E-04	1.48E-04	1.67E-04	1.77E-04	1.78E-04	1.77E-04	1.84E-04
22	6.72E-05	1.24E-04	1.72E-04	2.07E-04	2.46E-04	2.80E-04	3.18E-04	3.35E-04	3.61E-04
23	5.80E-05	8.51E-05	1.13E-04	1.23E-04	1.62E-04	1.69E-04	1.79E-04	1.90E-04	1.94E-04
24	7.29E-05	1.54E-04	1.82E-04	2.24E-04	2.69E-04	3.11E-04	3.37E-04	3.73E-04	4.02E-04
25	5.13E-05	1.08E-04	1.38E-04	1.69E-04	1.92E-04	2.11E-04	2.31E-04	2.22E-04	2.32E-04
26	9.81E-05	1.76E-04	2.19E-04	2.51E-04	2.74E-04	2.99E-04	3.24E-04	3.42E-04	3.65E-04
27	7.34E-05	1.60E-04	1.78E-04	2.01E-04	2.16E-04	2.24E-04	2.56E-04	2.73E-04	2.84E-04
28	4.15E-05	8.35E-05	1.08E-04	1.29E-04	1.59E-04	1.81E-04	2.04E-04	2.23E-04	2.33E-04
29	3.84E-05	8.76E-05	1.04E-04	1.31E-04	1.58E-04	1.81E-04	1.95E-04	2.00E-04	1.93E-04
30	6.88E-05	1.14E-04	1.22E-04	1.38E-04	1.59E-04	1.65E-04	1.75E-04	1.71E-04	1.63E-04
31	6.88E-05	1.14E-04	1.22E-04	1.38E-04	1.59E-04	1.65E-04	1.75E-04	1.71E-04	1.63E-04
32	4.00E-05	1.36E-04	1.54E-04	1.95E-04	2.27E-04	2.48E-04	2.91E-04	2.98E-04	3.22E-04

Table C.7 Displacement Analysis

Surface Presure (lbf/in^2)	905.87	1245.58	1585.28	1924.98	2264.69	2604.39	2944.09	3283.79	3623.50
Total displacement (mean value) in.	7.38E-05	1.40E-04	1.77E-04	2.17E-04	2.53E-04	2.82E-04	3.12E-04	3.35E-04	3.58E-04
Structure displacement of specimen in.	2.67E-05	3.67E-05	4.67E-05	5.67E-05	6.67E-05	7.67E-05	8.67E-05	9.67E-05	0.000107
Structure displacement of fixture in.	5.72E-06	6.12E-06	7.79E-06	9.46E-06	1.11E-05	1.28E-05	1.45E-05	1.61E-05	1.78E-05
Contact displacement (mean value) in.	6.08E-05	1.17E-04	1.42E-04	1.71E-04	1.94E-04	2.12E-04	2.30E-04	2.42E-04	2.52E-04

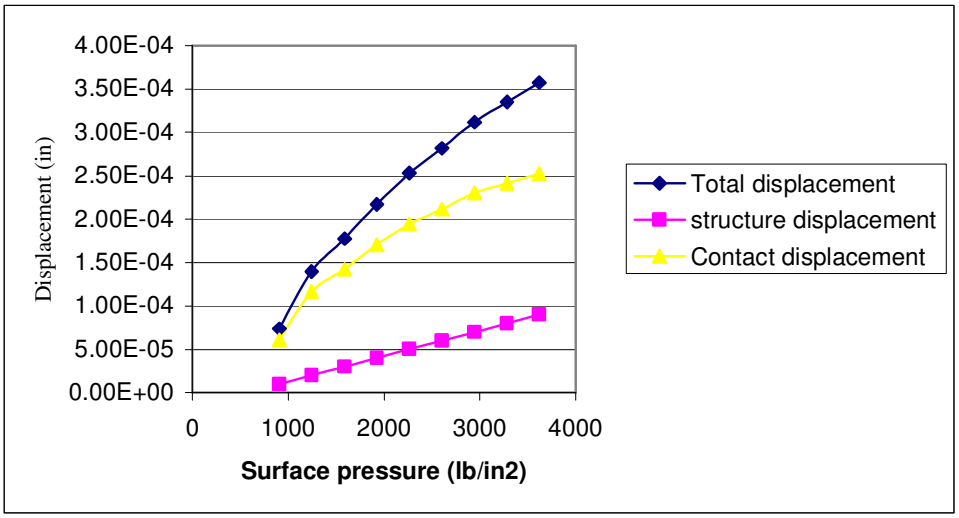

FigureC.3 Displacement vs. Surface Pressure

Table C.8 Contact Stiffness

Group	905.87	1245.58	1585.28	1924.98	2264.69	2604.39	2944.09	3283.79	3623.50
1	5.30E+06	7.80E+06	9.68E+06	1.02E+07	1.01E+07	1.09E+07	1.11E+07	1.17E+07	1.19E+07
2	5.13E+06	4.38E+06	5.21E+06	6.58E+06	7.47E+06	8.61E+06	9.91E+06	1.12E+07	1.15E+07
3	4.50E+06	5.09E+06	6.73E+06	7.51E+06	8.53E+06	1.02E+07	1.15E+07	1.36E+07	1.46E+07
4	5.66E+06	5.38E+06	6.77E+06	7.28E+06	7.54E+06	8.25E+06	8.22E+06	8.49E+06	8.73E+06
5	7.44E+06	6.66E+06	7.69E+06	8.58E+06	1.10E+07	1.38E+07	1.37E+07	1.60E+07	1.76E+07
6	5.47E+06	4.57E+06	5.60E+06	6.94E+06	8.05E+06	9.13E+06	1.07E+07	1.12E+07	1.22E+07
7	4.63E+06	6.34E+06	8.45E+06	8.47E+06	1.02E+07	1.05E+07	1.22E+07	1.28E+07	1.47E+07
8	3.85E+06	4.58E+06	6.11E+06	7.84E+06	9.49E+06	1.09E+07	1.16E+07	1.27E+07	1.44E+07
9	5.66E+06	7.20E+06	9.45E+06	8.64E+06	9.60E+06	1.23E+07	1.38E+07	1.52E+07	1.64E+07
10	6.02E+06	5.78E+06	7.27E+06	7.36E+06	7.59E+06	8.46E+06	9.02E+06	9.63E+06	1.04E+07
11	6.62E+06	7.80E+06	9.32E+06	1.05E+07	1.26E+07	1.46E+07	1.77E+07	1.90E+07	2.12E+07
12	6.37E+06	5.84E+06	6.64E+06	6.64E+06	7.36E+06	7.95E+06	8.48E+06	8.67E+06	8.95E+06
13	6.49E+06	7.32E+06	8.59E+06	9.90E+06	1.12E+07	1.29E+07	1.41E+07	1.65E+07	1.77E+07
14	6.69E+06	6.80E+06	7.27E+06	7.53E+06	7.40E+06	8.05E+06	8.45E+06	8.78E+06	9.30E+06
15	7.61E+06	7.66E+06	1.05E+07	1.21E+07	1.34E+07	1.34E+07	1.43E+07	1.46E+07	1.69E+07
16	5.30E+06	5.21E+06	6.32E+06	6.53E+06	7.06E+06	7.46E+06	7.83E+06	8.47E+06	8.77E+06
17	7.70E+06	9.15E+06	1.04E+07	1.22E+07	1.35E+07	1.36E+07	1.46E+07	1.67E+07	1.84E+07
18	6.31E+06	4.80E+06	5.87E+06	6.56E+06	7.39E+06	7.50E+06	7.61E+06	8.05E+06	8.52E+06
19	5.25E+06	6.43E+06	7.32E+06	8.06E+06	9.20E+06	1.01E+07	1.14E+07	1.31E+07	1.49E+07
20	3.70E+06	4.61E+06	5.62E+06	6.48E+06	6.94E+06	7.43E+06	7.99E+06	8.62E+06	9.29E+06
21	7.53E+06	7.94E+06	8.59E+06	9.18E+06	1.02E+07	1.15E+07	1.33E+07	1.53E+07	1.66E+07
22	5.05E+06	5.47E+06	5.92E+06	6.58E+06	6.90E+06	7.28E+06	7.48E+06	8.11E+06	8.47E+06
23	5.86E+06	7.99E+06	9.02E+06	1.10E+07	1.05E+07	1.21E+07	1.33E+07	1.43E+07	1.57E+07
24	4.66E+06	4.40E+06	5.59E+06	6.06E+06	6.30E+06	6.56E+06	7.05E+06	7.29E+06	7.60E+06
25	6.62E+06	6.31E+06	7.38E+06	8.03E+06	8.83E+06	9.66E+06	1.03E+07	1.23E+07	1.32E+07
26	3.46E+06	3.87E+06	4.66E+06	5.42E+06	6.20E+06	6.82E+06	7.33E+06	7.94E+06	8.39E+06
27	4.63E+06	4.26E+06	5.72E+06	6.76E+06	7.88E+06	9.10E+06	9.27E+06	9.94E+06	1.08E+07
28	8.18E+06	8.13E+06	9.45E+06	1.06E+07	1.06E+07	1.12E+07	1.16E+07	1.22E+07	1.31E+07
29	8.84E+06	7.75E+06	9.78E+06	1.04E+07	1.08E+07	1.13E+07	1.22E+07	1.36E+07	1.58E+07
30	4.94E+06	5.97E+06	8.34E+06	9.86E+06	1.07E+07	1.23E+07	1.36E+07	1.59E+07	1.87E+07
31	4.94E+06	5.97E+06	8.34E+06	9.86E+06	1.07E+07	1.23E+07	1.36E+07	1.59E+07	1.87E+07
32	8.49E+06	4.98E+06	6.64E+06	6.96E+06	7.49E+06	8.22E+06	8.18E+06	9.11E+06	9.50E+06

Appendix D. Experimental Data (Radius =0.5in; Surface Finish Ra =1.44μm)

In order to study the effects of the surface roughness, static experiments were conducted for an AISI4150 sample with different surface finish. The sample radius is 0.5 in, and its surface finish is 1.44μm. The experiment was repeated 32 times. Table D.1 shows the original measured data. In order to reduce the measured error, Table D.2 lists the relative measured data. Figure D.1 shows the relative measured results. Table D.3 lists the arithmetic mean of relative measured results. The standard deviation and 95% confidence interval are calculated. Figure D.2 is a plot of the mean values of all relative data versus normal loads. From the relative measured data and Equation 4.3, the total displacement can be obtained, as shown in the Table D.4. According to Equation 4.4, the structure displacement can be computed theoretically. Therefore, contact displacement can be obtained by applying Equation 4.5, as shown in Table D.5. Table D.6 and Figure D.3 show the mean value of all kinds of displacements versus surface pressure. According to the definition of contact stiffness, Equation 4.6 can be used to obtain contact stiffness, as shown in Table D.7.

Table D.1 Original Measured Output Voltage (Unit: Volt)

Test	250	400	550	700	850	1000	1150	1300	1450	1600
1	4.3281	4.3389	4.3471	4.3575	4.3622	4.3693	4.3732	4.3774	4.3804	4.3834
2	5.0635	5.0748	5.0838	5.0916	5.0948	5.103	5.1068	5.1094	5.1161	5.1197
3	4.3016	4.3109	4.3195	4.3259	4.3295	4.335	4.338	4.342	4.3477	4.3518
4	5.101	5.1121	5.1193	5.1226	5.1289	5.1357	5.1386	5.1441	5.1519	5.1543
5	4.2961	4.3077	4.3138	4.3196	4.3247	4.3299	4.3344	4.3393	4.3434	4.3468
6	5.111	5.125	5.1358	5.1434	5.1465	5.1523	5.1541	5.1571	5.1589	5.1606
7	4.3163	4.3273	4.3352	4.3416	4.3472	4.3515	4.3543	4.3582	4.3621	4.3646
8	5.0972	5.1098	5.1166	5.1253	5.1297	5.1343	5.1417	5.1432	5.1467	5.1497
9	4.3142	4.3265	4.3354	4.3397	4.3437	4.3484	4.3519	4.3555	4.3597	4.3632
10	5.0967	5.1091	5.1156	5.1236	5.1274	5.1289	5.1343	5.1394	5.1432	5.1471
11	4.332	4.3438	4.3558	4.3591	4.3654	4.3684	4.3744	4.3763	4.3794	4.3809
12	5.0877	5.1011	5.1087	5.1152	5.1197	5.1231	5.1268	5.129	5.1333	5.1363
13	4.3812	4.3932	4.4048	4.4096	4.417	4.4186	4.4249	4.4267	4.4297	4.4338
14	5.0179	5.0284	5.0397	5.0488	5.0516	5.0549	5.0574	5.0629	5.0656	5.0698
15	4.3327	4.3474	4.3529	4.3568	4.3614	4.3661	4.3714	4.3757	4.3795	4.3843
16	5.0808	5.0956	5.1058	5.1096	5.1135	5.1168	5.1204	5.1232	5.1265	5.1298
17	4.3506	4.3626	4.3699	4.3741	4.3789	4.3832	4.3866	4.3932	4.3952	4.3966
18	5.0571	5.0707	5.0792	5.0843	5.0892	5.0933	5.0986	5.0995	5.1022	5.1075
19	4.3612	4.3762	4.3822	4.3889	4.393	4.3972	4.3994	4.4045	4.4077	4.4099
20	5.0221	5.0339	5.0419	5.0471	5.0514	5.0573	5.0595	5.0646	5.0662	5.0722
21	4.4004	4.413	4.418	4.4233	4.4271	4.4331	4.4382	4.4415	4.444	4.4472
22	5.0029	5.0158	5.0199	5.0257	5.0294	5.0357	5.0383	5.0434	5.0479	5.0498
23	4.3252	4.337	4.3459	4.3497	4.3558	4.3586	4.3615	4.3647	4.3696	4.3735
24	5.1109	5.1205	5.1297	5.1357	5.1414	5.1448	5.1479	5.1499	5.1537	5.1561
25	4.2789	4.2932	4.2988	4.3055	4.3097	4.3146	4.3201	4.3236	4.3257	4.3284
26	5.113	5.1277	5.136	5.1426	5.1488	5.1517	5.1553	5.1581	5.1608	5.1621
27	4.331	4.3434	4.3497	4.3571	4.3626	4.3681	4.3701	4.3742	4.3764	4.3781
28	5.0725	5.0871	5.0972	5.0997	5.1053	5.1084	5.1095	5.1144	5.1172	5.1193
29	4.0803	4.0923	4.1012	4.1061	4.1094	4.1155	4.1182	4.1208	4.1239	4.1282
30	5.2047	5.2148	5.2238	5.2282	5.2347	5.2383	5.245	5.2486	5.2503	5.2548
31	3.8704	3.8838	3.8916	3.8993	3.9034	3.907	3.9088	3.9142	3.9161	3.9183
32	5.3042	5.3154	5.3273	5.3292	5.3364	5.339	5.3422	5.3456	5.3495	5.3513

Table D.2 Relative Measured Data (Unit: Volt)

Group	400	550	700	850	1000	1150	1300	1450	1600
1	0.0078	0.0137	0.0208	0.0231	0.0278	0.0334	0.0371	0.0421	0.046
2	0.0043	0.0146	0.0202	0.0269	0.0337	0.0365	0.0407	0.043	0.0465
3	0.0077	0.0153	0.0244	0.033	0.0365	0.0416	0.0437	0.0464	0.0491
4	0.0074	0.0164	0.025	0.034	0.0387	0.0419	0.0486	0.0514	0.0525
5	0.011	0.0149	0.0225	0.0285	0.0371	0.0432	0.0444	0.0489	0.0523
6	0.0101	0.0196	0.0221	0.0264	0.0302	0.0321	0.0327	0.0336	0.036
7	0.0076	0.015	0.0198	0.0246	0.0291	0.0361	0.0396	0.043	0.0456
8	0.0088	0.0169	0.0198	0.0245	0.0287	0.036	0.0411	0.0447	0.0476
9	0.008	0.0153	0.0183	0.0226	0.0267	0.0308	0.0383	0.0426	0.0466
10	0.0086	0.0144	0.0198	0.0286	0.03	0.0366	0.0397	0.043	0.046
11	0.0069	0.0134	0.02	0.0253	0.0296	0.033	0.034	0.036	0.0365
12	0.0077	0.0143	0.0217	0.0294	0.032	0.0361	0.0403	0.0438	0.0471
13	0.008	0.0163	0.0201	0.0224	0.0289	0.0311	0.0371	0.0401	0.0432
14	0.0099	0.0151	0.0178	0.0225	0.0268	0.0309	0.0356	0.0382	0.0419
15	0.0105	0.0142	0.0193	0.0233	0.0275	0.032	0.0345	0.0365	0.0388
16	0.0082	0.0177	0.0218	0.0256	0.0296	0.0361	0.0386	0.0416	0.0461
17	0.0114	0.0167	0.0228	0.027	0.0303	0.037	0.0407	0.0428	0.0445
18	0.0095	0.0163	0.0201	0.0227	0.029	0.0332	0.0369	0.0387	0.0398
19	0.0065	0.0158	0.0217	0.0293	0.0322	0.0379	0.0432	0.0463	0.0471
20	0.0094	0.0156	0.0223	0.0294	0.033	0.0344	0.0377	0.0426	0.0445
21	0.0102	0.0167	0.0229	0.0264	0.0277	0.033	0.0371	0.0427	0.0466
22	0.0074	0.0174	0.0208	0.0273	0.0329	0.0349	0.0403	0.0424	0.0459
23	0.0088	0.0145	0.0214	0.0238	0.0285	0.0348	0.0385	0.0404	0.0413
24	0.0095	0.0176	0.0264	0.0321	0.0366	0.0435	0.0448	0.0475	0.0494
25	0.0103	0.0184	0.0231	0.0286	0.0332	0.0382	0.0411	0.0446	0.0465
26	0.0104	0.0165	0.0226	0.0281	0.0291	0.0348	0.0376	0.042	0.0463
27	0.0106	0.0164	0.0203	0.0257	0.028	0.0307	0.0369	0.0398	0.0452
28	0.0101	0.016	0.0259	0.0318	0.0371	0.0405	0.0448	0.0451	0.0497
29	0.0063	0.0141	0.0193	0.0284	0.0324	0.0351	0.0424	0.0485	0.0516
30	0.0083	0.0151	0.0215	0.0295	0.0345	0.038	0.0433	0.0471	0.0531
31	0.0085	0.0133	0.0199	0.0232	0.03	0.0314	0.0354	0.0382	0.044
32	0.0084	0.0139	0.0206	0.0275	0.0335	0.0388	0.0436	0.0488	0.0518

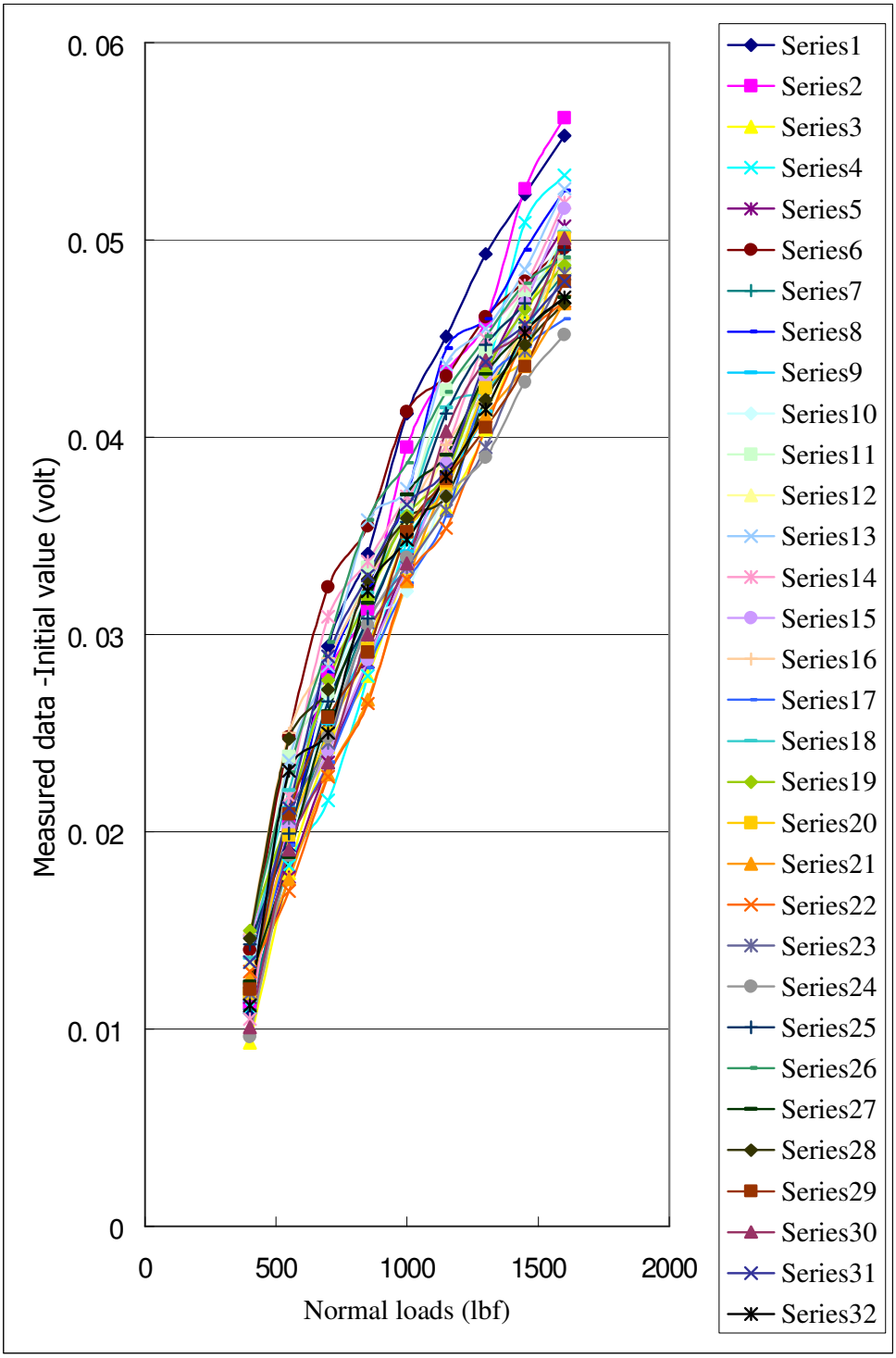

Figure D.1 All Relative Data vs. Normal Loads

Table D.3 All Relative Data vs. Normal Loads

Normal loads (lbf)	400	550	700	850	1000	1150	1300	1450	1600
Mean value (Volt)	1.24E-02	2.06E-02	2.63E-02	3.11E-02	3.56E-02	3.93E-02	4.30E-02	4.65E-02	4.96E-02
Standard Deviation	1.56E-03	2.23E-03	2.53E-03	2.49E-03	2.32E-03	2.64E-03	2.20E-03	2.33E-03	2.54E-03
95% Confidence lever	5.40E-04	7.70E-04	8.80E-04	8.60E-04	8.00E-04	9.10E-04	7.60E-04	8.10E-04	8.80E-04

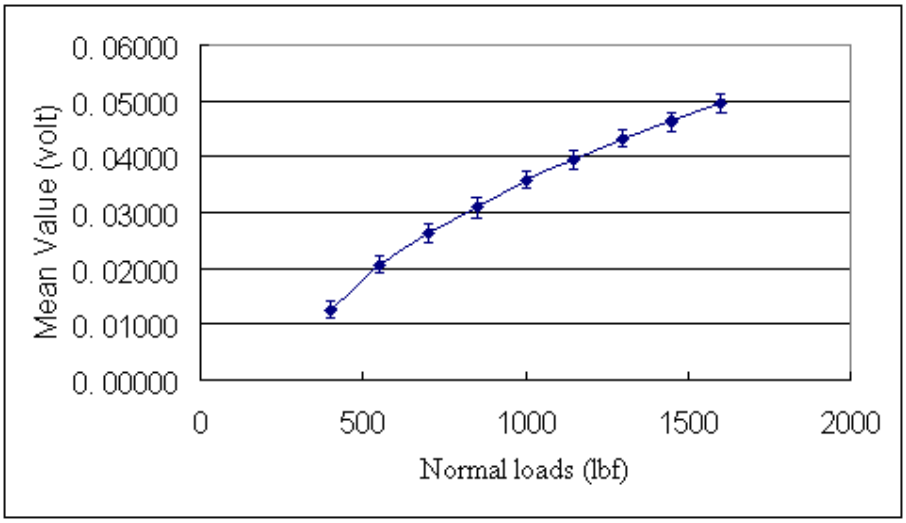

Figure D.2 Mean Values of All Relative Data vs. Normal Loads

Table D.4 Total Displacement (in)

Group	400	550	700	850	1000	1150	1300	1450	1600
1	5.550E-05	9.764E-05	1.511E-04	1.752E-04	2.117E-04	2.318E-04	2.533E-04	2.688E-04	2.842E-04
2	5.807E-05	1.043E-04	1.444E-04	1.608E-04	2.030E-04	2.225E-04	2.359E-04	2.703E-04	2.888E-04
3	4.779E-05	9.198E-05	1.249E-04	1.434E-04	1.716E-04	1.871E-04	2.076E-04	2.369E-04	2.580E-04
4	5.704E-05	9.404E-05	1.110E-04	1.434E-04	1.783E-04	1.932E-04	2.215E-04	2.616E-04	2.739E-04
5	5.961E-05	9.096E-05	1.208E-04	1.470E-04	1.737E-04	1.968E-04	2.220E-04	2.431E-04	2.605E-04
6	7.194E-05	1.274E-04	1.665E-04	1.824E-04	2.122E-04	2.215E-04	2.369E-04	2.462E-04	2.549E-04
7	5.653E-05	9.712E-05	1.300E-04	1.588E-04	1.809E-04	1.953E-04	2.153E-04	2.354E-04	2.482E-04
8	6.475E-05	9.969E-05	1.444E-04	1.670E-04	1.907E-04	2.287E-04	2.364E-04	2.544E-04	2.698E-04
9	6.321E-05	1.089E-04	1.310E-04	1.516E-04	1.758E-04	1.937E-04	2.122E-04	2.338E-04	2.518E-04
10	6.372E-05	9.712E-05	1.382E-04	1.578E-04	1.655E-04	1.932E-04	2.194E-04	2.390E-04	2.590E-04
11	6.064E-05	1.223E-04	1.393E-04	1.716E-04	1.871E-04	2.179E-04	2.277E-04	2.436E-04	2.513E-04
12	6.886E-05	1.079E-04	1.413E-04	1.644E-04	1.819E-04	2.009E-04	2.122E-04	2.343E-04	2.497E-04
13	6.167E-05	1.213E-04	1.459E-04	1.840E-04	1.922E-04	2.246E-04	2.338E-04	2.492E-04	2.703E-04
14	5.396E-05	1.120E-04	1.588E-04	1.732E-04	1.901E-04	2.030E-04	2.312E-04	2.451E-04	2.667E-04
15	7.554E-05	1.038E-04	1.238E-04	1.475E-04	1.716E-04	1.989E-04	2.210E-04	2.405E-04	2.652E-04
16	7.605E-05	1.285E-04	1.480E-04	1.680E-04	1.850E-04	2.035E-04	2.179E-04	2.348E-04	2.518E-04
17	6.167E-05	9.918E-05	1.208E-04	1.454E-04	1.675E-04	1.850E-04	2.189E-04	2.292E-04	2.364E-04
18	6.989E-05	1.136E-04	1.398E-04	1.650E-04	1.860E-04	2.133E-04	2.179E-04	2.318E-04	2.590E-04
19	7.708E-05	1.079E-04	1.423E-04	1.634E-04	1.850E-04	1.963E-04	2.225E-04	2.390E-04	2.503E-04
20	6.064E-05	1.018E-04	1.285E-04	1.506E-04	1.809E-04	1.922E-04	2.184E-04	2.266E-04	2.575E-04
21	6.475E-05	9.044E-05	1.177E-04	1.372E-04	1.680E-04	1.942E-04	2.112E-04	2.241E-04	2.405E-04
22	6.629E-05	8.736E-05	1.172E-04	1.362E-04	1.686E-04	1.819E-04	2.081E-04	2.312E-04	2.410E-04
23	6.064E-05	1.064E-04	1.259E-04	1.573E-04	1.716E-04	1.865E-04	2.030E-04	2.282E-04	2.482E-04
24	4.933E-05	9.661E-05	1.274E-04	1.567E-04	1.742E-04	1.901E-04	2.004E-04	2.199E-04	2.323E-04
25	7.348E-05	1.023E-04	1.367E-04	1.583E-04	1.835E-04	2.117E-04	2.297E-04	2.405E-04	2.544E-04
26	7.554E-05	1.182E-04	1.521E-04	1.840E-04	1.989E-04	2.174E-04	2.318E-04	2.456E-04	2.523E-04
27	6.372E-05	9.610E-05	1.341E-04	1.624E-04	1.907E-04	2.009E-04	2.220E-04	2.333E-04	2.420E-04
28	7.503E-05	1.269E-04	1.398E-04	1.686E-04	1.845E-04	1.901E-04	2.153E-04	2.297E-04	2.405E-04
29	6.167E-05	1.074E-04	1.326E-04	1.495E-04	1.809E-04	1.948E-04	2.081E-04	2.241E-04	2.462E-04
30	5.190E-05	9.815E-05	1.208E-04	1.542E-04	1.727E-04	2.071E-04	2.256E-04	2.343E-04	2.575E-04
31	6.886E-05	1.089E-04	1.485E-04	1.696E-04	1.881E-04	1.973E-04	2.251E-04	2.348E-04	2.462E-04
32	5.755E-05	1.187E-04	1.285E-04	1.655E-04	1.788E-04	1.953E-04	2.127E-04	2.328E-04	2.420E-04

Table D.5 Contact Displacement (in)

Group	400	550	700	850	1000	1150	1300	1450	1600
1	4.693E-05	8.304E-05	1.292E-04	1.460E-04	1.752E-04	1.880E-04	2.022E-04	2.103E-04	2.185E-04
2	4.950E-05	8.972E-05	1.225E-04	1.316E-04	1.665E-04	1.787E-04	1.848E-04	2.119E-04	2.231E-04
3	3.922E-05	7.738E-05	1.030E-04	1.142E-04	1.351E-04	1.433E-04	1.565E-04	1.785E-04	1.923E-04
4	4.847E-05	7.944E-05	8.910E-05	1.142E-04	1.418E-04	1.494E-04	1.704E-04	2.031E-04	2.082E-04
5	5.104E-05	7.636E-05	9.886E-05	1.178E-04	1.372E-04	1.530E-04	1.709E-04	1.846E-04	1.949E-04
6	6.337E-05	1.128E-04	1.446E-04	1.532E-04	1.757E-04	1.777E-04	1.858E-04	1.877E-04	1.892E-04
7	4.796E-05	8.252E-05	1.081E-04	1.296E-04	1.444E-04	1.515E-04	1.642E-04	1.769E-04	1.825E-04
8	5.618E-05	8.509E-05	1.225E-04	1.378E-04	1.542E-04	1.849E-04	1.853E-04	1.959E-04	2.041E-04
9	5.464E-05	9.434E-05	1.091E-04	1.224E-04	1.393E-04	1.500E-04	1.611E-04	1.754E-04	1.861E-04
10	5.515E-05	8.252E-05	1.163E-04	1.286E-04	1.290E-04	1.494E-04	1.683E-04	1.805E-04	1.933E-04
11	5.207E-05	1.077E-04	1.174E-04	1.424E-04	1.506E-04	1.741E-04	1.765E-04	1.851E-04	1.856E-04
12	6.029E-05	9.332E-05	1.194E-04	1.352E-04	1.454E-04	1.572E-04	1.611E-04	1.759E-04	1.841E-04
13	5.310E-05	1.067E-04	1.240E-04	1.548E-04	1.557E-04	1.808E-04	1.827E-04	1.908E-04	2.046E-04
14	4.539E-05	9.743E-05	1.369E-04	1.440E-04	1.536E-04	1.592E-04	1.801E-04	1.867E-04	2.010E-04
15	6.697E-05	8.920E-05	1.020E-04	1.183E-04	1.351E-04	1.551E-04	1.699E-04	1.821E-04	1.995E-04
16	6.748E-05	1.139E-04	1.261E-04	1.388E-04	1.485E-04	1.597E-04	1.668E-04	1.764E-04	1.861E-04
17	5.310E-05	8.458E-05	9.886E-05	1.162E-04	1.310E-04	1.412E-04	1.678E-04	1.708E-04	1.707E-04
18	6.132E-05	9.897E-05	1.179E-04	1.358E-04	1.495E-04	1.695E-04	1.668E-04	1.733E-04	1.933E-04
19	6.851E-05	9.332E-05	1.204E-04	1.342E-04	1.485E-04	1.525E-04	1.714E-04	1.805E-04	1.846E-04
20	5.207E-05	8.715E-05	1.066E-04	1.214E-04	1.444E-04	1.484E-04	1.673E-04	1.682E-04	1.918E-04
21	5.618E-05	7.584E-05	9.578E-05	1.080E-04	1.315E-04	1.505E-04	1.601E-04	1.656E-04	1.748E-04
22	5.772E-05	7.276E-05	9.527E-05	1.070E-04	1.321E-04	1.381E-04	1.570E-04	1.728E-04	1.753E-04
23	5.207E-05	9.177E-05	1.040E-04	1.281E-04	1.351E-04	1.428E-04	1.519E-04	1.697E-04	1.825E-04
24	4.076E-05	8.201E-05	1.055E-04	1.275E-04	1.377E-04	1.464E-04	1.493E-04	1.615E-04	1.666E-04
25	6.491E-05	8.766E-05	1.148E-04	1.291E-04	1.470E-04	1.679E-04	1.786E-04	1.821E-04	1.887E-04
26	6.697E-05	1.036E-04	1.302E-04	1.548E-04	1.624E-04	1.736E-04	1.807E-04	1.872E-04	1.867E-04
27	5.515E-05	8.150E-05	1.122E-04	1.332E-04	1.542E-04	1.572E-04	1.709E-04	1.749E-04	1.764E-04
28	6.646E-05	1.123E-04	1.179E-04	1.394E-04	1.480E-04	1.464E-04	1.642E-04	1.713E-04	1.748E-04
29	5.310E-05	9.280E-05	1.107E-04	1.203E-04	1.444E-04	1.510E-04	1.570E-04	1.656E-04	1.805E-04
30	4.333E-05	8.355E-05	9.886E-05	1.250E-04	1.362E-04	1.633E-04	1.745E-04	1.759E-04	1.918E-04
31	6.029E-05	9.434E-05	1.266E-04	1.404E-04	1.516E-04	1.536E-04	1.740E-04	1.764E-04	1.805E-04
32	4.898E-05	1.041E-04	1.066E-04	1.363E-04	1.423E-04	1.515E-04	1.616E-04	1.744E-04	1.764E-04

Table D.6 Displacements (Mean Value) vs. Surface Pressure

Surface Pressure (lbf/in^2)	509.55	700.64	891.72	1082.80	1273.89	1464.97	1656.05	1847.13	2038.22
Total displacement (mean value) in.	6.35E-05	1.06E-04	1.35E-04	1.60E-04	1.83E-04	2.02E-04	2.21E-04	2.39E-04	2.55E-04
Structure displacement of specimen (in).	5.63E-06	1.13E-05	1.69E-05	2.25E-05	2.81E-05	3.38E-05	3.94E-05	4.50E-05	5.07E-05
Structure displacement of fixture (in).	2.94E-06	3.34E-06	5.01E-06	6.68E-06	8.35E-06	1.00E-05	1.17E-05	1.34E-05	1.50E-05
Contact displacement (mean value) (in)	5.50E-05	9.12E-05	1.13E-04	1.31E-04	1.46E-04	1.58E-04	1.70E-04	1.80E-04	1.89E-04

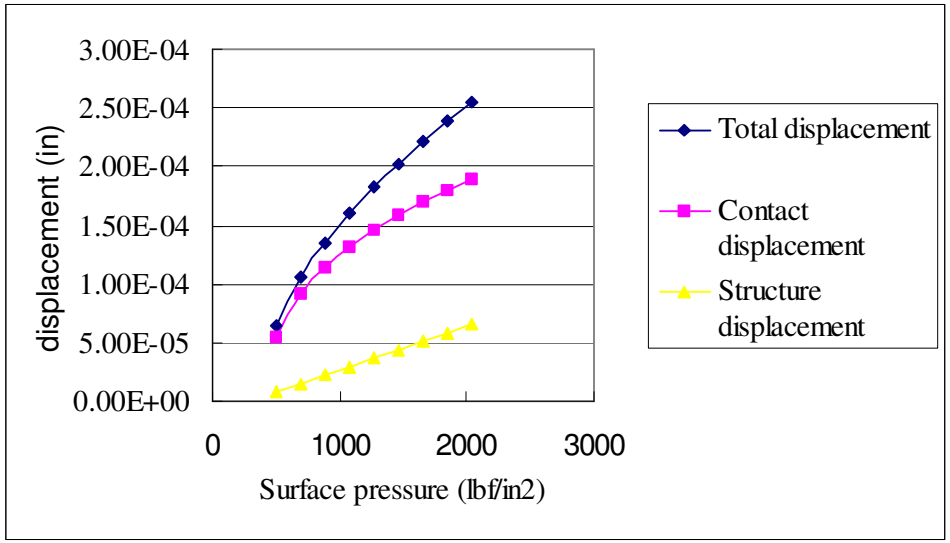

Figure D.3 Displacements (Mean Value) vs. Surface Pressure

TableD.7 Contact Stiffness

Group	509.55	700.64	891.72	1082.80	1273.89	1464.97	1656.05	1847.13	2038.22
1	4.07E+06	4.60E+06	4.44E+06	5.23E+06	5.45E+06	6.10E+06	6.61E+06	7.27E+06	7.87E+06
2	3.86E+06	4.26E+06	4.68E+06	5.81E+06	5.74E+06	6.41E+06	7.24E+06	7.22E+06	7.71E+06
3	4.87E+06	4.94E+06	5.57E+06	6.69E+06	7.07E+06	8.00E+06	8.55E+06	8.57E+06	8.94E+06
4	3.94E+06	4.81E+06	6.43E+06	6.69E+06	6.74E+06	7.67E+06	7.85E+06	7.53E+06	8.26E+06
5	3.74E+06	5.01E+06	5.80E+06	6.49E+06	6.96E+06	7.49E+06	7.83E+06	8.28E+06	8.83E+06
6	3.02E+06	3.39E+06	3.96E+06	4.99E+06	5.44E+06	6.45E+06	7.20E+06	8.14E+06	9.09E+06
7	3.98E+06	4.63E+06	5.30E+06	5.90E+06	6.62E+06	7.57E+06	8.15E+06	8.64E+06	9.42E+06
8	3.40E+06	4.49E+06	4.68E+06	5.55E+06	6.20E+06	6.20E+06	7.22E+06	7.80E+06	8.43E+06
9	3.50E+06	4.05E+06	5.25E+06	6.24E+06	6.86E+06	7.65E+06	8.30E+06	8.72E+06	9.24E+06
10	3.46E+06	4.63E+06	4.93E+06	5.95E+06	7.41E+06	7.67E+06	7.95E+06	8.47E+06	8.90E+06
11	3.67E+06	3.55E+06	4.88E+06	5.37E+06	6.35E+06	6.59E+06	7.58E+06	8.26E+06	9.26E+06
12	3.17E+06	4.10E+06	4.80E+06	5.65E+06	6.57E+06	7.30E+06	8.30E+06	8.69E+06	9.34E+06
13	3.60E+06	3.58E+06	4.62E+06	4.94E+06	6.14E+06	6.34E+06	7.32E+06	8.01E+06	8.40E+06
14	4.21E+06	3.92E+06	4.19E+06	5.31E+06	6.22E+06	7.20E+06	7.43E+06	8.19E+06	8.55E+06
15	2.85E+06	4.28E+06	5.62E+06	6.46E+06	7.07E+06	7.39E+06	7.87E+06	8.40E+06	8.62E+06
16	2.83E+06	3.36E+06	4.55E+06	5.51E+06	6.43E+06	7.18E+06	8.02E+06	8.67E+06	9.24E+06
17	3.60E+06	4.52E+06	5.80E+06	6.58E+06	7.29E+06	8.12E+06	7.97E+06	8.95E+06	1.01E+07
18	3.12E+06	3.86E+06	4.86E+06	5.63E+06	6.39E+06	6.76E+06	8.02E+06	8.82E+06	8.90E+06
19	2.79E+06	4.10E+06	4.76E+06	5.69E+06	6.43E+06	7.52E+06	7.80E+06	8.47E+06	9.32E+06
20	3.67E+06	4.39E+06	5.38E+06	6.30E+06	6.62E+06	7.73E+06	8.00E+06	9.09E+06	8.97E+06
21	3.40E+06	5.04E+06	5.99E+06	7.08E+06	7.26E+06	7.62E+06	8.35E+06	9.23E+06	9.84E+06
22	3.31E+06	5.25E+06	6.02E+06	7.14E+06	7.24E+06	8.30E+06	8.52E+06	8.85E+06	9.81E+06
23	3.67E+06	4.16E+06	5.51E+06	5.97E+06	7.07E+06	8.03E+06	8.81E+06	9.01E+06	9.42E+06
24	4.69E+06	4.66E+06	5.43E+06	5.99E+06	6.94E+06	7.83E+06	8.96E+06	9.47E+06	1.03E+07
25	2.94E+06	4.36E+06	4.99E+06	5.92E+06	6.50E+06	6.83E+06	7.49E+06	8.40E+06	9.11E+06
26	2.85E+06	3.69E+06	4.40E+06	4.94E+06	5.88E+06	6.60E+06	7.40E+06	8.17E+06	9.21E+06
27	3.46E+06	4.69E+06	5.11E+06	5.74E+06	6.20E+06	7.30E+06	7.83E+06	8.74E+06	9.75E+06
28	2.88E+06	3.40E+06	4.86E+06	5.48E+06	6.46E+06	7.83E+06	8.15E+06	8.93E+06	9.84E+06
29	3.60E+06	4.12E+06	5.18E+06	6.35E+06	6.62E+06	7.59E+06	8.52E+06	9.23E+06	9.53E+06
30	4.41E+06	4.57E+06	5.80E+06	6.12E+06	7.02E+06	7.02E+06	7.67E+06	8.69E+06	8.97E+06
31	3.17E+06	4.05E+06	4.53E+06	5.44E+06	6.30E+06	7.47E+06	7.69E+06	8.67E+06	9.53E+06
32	3.90E+06	3.67E+06	5.38E+06	5.61E+06	6.71E+06	7.57E+06	8.28E+06	8.77E+06	9.75E+06

Appendix E: Relationship between Global Contact Stiffness and Local Contact Stiffness

The global contact stiffness is defined as the ratio of the normal load in a unit area over contact displacement.

$$k = \frac{P - P_0}{D_c - D_{c0}} \tag{E.1}$$

The local contact stiffness is defined as the ration of the increment of the normal load in a unit area over the increment of contact displacement.

$$k_l = \frac{\Delta P}{\Delta D_c} \tag{E.2}$$

The relationship between global and local contact stiffness was established.

Set

$$k_i = \frac{P_i - P_0}{D_{ci} - D_{c0}} \tag{E.3}$$

and

$$k_{i+1} = \frac{P_i - P_0 + \Delta P}{D_{ci} - D_{c0} + \Delta D} \tag{E.4}$$

Because P is linearly increased, k_{i+1} can be expressed as

$$k_{i+1} = \frac{P_i - P_0 + \Delta P}{D_{ci} - D_{c0} + \Delta D} = \frac{(i+1)\Delta P}{D_{ci} - D_{c0} + \Delta D} \tag{E.5}$$

Thus,

$$\begin{aligned} \frac{1}{k_{i+1}} &= \frac{D_{ci} - D_{c0} + \Delta D}{(i+1)\Delta P} = \frac{D_{ci} - D_{c0}}{(i+1)\Delta P} + \frac{\Delta D}{(i+1)\Delta P} = \frac{D_{ci} - D_{c0}}{\frac{(i+1)}{i} i\Delta P} + \frac{1}{i+1}\frac{1}{k_l} \\ &= \frac{i}{i+1}\frac{1}{k_i} + \frac{1}{i+1}\frac{1}{k_l} \end{aligned} \tag{E.6}$$

Therefore, the local contact stiffness can be

$$k_l = \frac{k_i k_{i+1}}{(i+1)k_i - ik_{i+1}} \tag{E.7}$$

Appendix F: A Proof of the Orthogonality of the Natural Modes of the Bars

The mode shape functions in Eq. 4.19 for the bar in Figure 4.15 satisfies the following orthogonal relationship:

$$\int_0^l X_i(x)X_j(x)dx = 0 \qquad \forall i \neq j \tag{F.1}$$

A general proof is given as follows:

Assume $X_i(x)$, $X_j(x)$, are two natural modes i and j; λ_i, λ_j are the corresponding eigenvalues; i.e.,

$$\frac{d^2X_i(x)}{dx^2} + \lambda_i^2 X_i(x) = 0 \text{ for mode i} \tag{F.2}$$

$$\frac{d^2X_j(x)}{dx^2} + \lambda_j^2 X_j(x) = 0 \text{ for mode j} \tag{F.3}$$

Multiplying Eq. F.2 by $X_j(x)$, and Eq. F.3 by $X_i(x)$, subtract that second result from the first, then integrate with respect to x from x=0 to l. One obtains

$$\int_0^l [X_j \frac{d^2X_i}{dx^2} - X_i \frac{d^2X_j}{dx^2}]dx + (\lambda_i^2 - \lambda_j^2)\int_0^l X_i X_j dx = 0 \tag{F.4}$$

where

$$\begin{aligned}
&\int_0^l [X_j \frac{d^2X_i}{dx^2} - X_i \frac{d^2X_j}{dx^2}]dx \\
&= X_j \frac{dX_i}{dx}\bigg|_l^0 - \int_0^l \frac{dX_i}{dx}\frac{dX_j}{dx}dx - \left(X_i \frac{dX_j}{dx}\bigg|_l^0 - \int_0^l \frac{dX_i}{dx}\frac{dX_j}{dx}dx \right) \\
&= X_j \frac{dX_i}{dx}\bigg|_l^0 - X_i \frac{dX_j}{dx}\bigg|_l^0
\end{aligned} \tag{F.5}$$

Apply the modal boundary condition equations and substitute them into Eq. F.5. One can get

$$\int_0^l [X_j \frac{d^2 X_i}{dx^2} - X_i \frac{d^2 X_j}{dx^2}] dx = 0 \qquad \text{(F.6)}$$

So substitute Eq. F.6 into Eq. F.4, one can get

$$\int_0^l X_i(x) X_j(x) dx = 0 \qquad i \neq j$$

Note that

$$\int_0^l X^2{}_i(x) = \int_0^l \cos\lambda_i x \cos\lambda_i x = \int_0^l \frac{1}{2}[\cos 2\lambda_i x - 1] = \frac{1}{2}[\frac{1}{2\lambda_i}\sin(2\lambda_i l) - l] \neq 0$$

The above orthogonal relation plays a crucial role in solving vibration problems through modal analysis.

References

[Aliabadi, 1993] Aliabadi, M. H. and C. A. Brebbia, 1993, Computational methods in contact mechanics, Computational Mechanics Publications.

[Amaral, 2001] Amaral, N. "Development of a finite element analysis tool for fixture design integrity verification and optimization," M.S. thesis, Worcester Polytechnic Institute, Worcester, MA, 2001.

[An, 1999] An, Z., S. Huang, J. Li, Y., Rong and S. Jayaram, 1999, "Development of automated fixture design systems with predefined fixture component types: part 1, basic design," Int. J. of Flexible Automation and Integrated Manufg, Vol. 7, No. ¾, pp. 321-341.

[A.R. Mijar, 2000] A.R. Mijar and J.S.Arora, "Review of formulations for elastostatic frictional contact problems", Struct Multidisc Optim, 20, pp.167-189, 2000.

[Asada, 1985] Asada, H. and A. By, 1985, "Kinematics analysis of workpart fixturing for flexible assembly with automatically reconfigurable fixtures", Proc. of IEEE Int Conf on Robotics and Automation, 1985, Vol. RA-1, No. 2, pp. 86-93.

[Bathe, 1996] Bathe, Klaus-Jurgen, "Finite element procedures in engineering analysis", 1996, Merrill Peterson.

[Beards, 1986] Beards, C F, "The damping of structural vibration by controlled inter-facial slip in joints", An ASME publication, 8 l-DET-86, 1986.

[Boyle, 2004] Boyle, I., Y. Rong, and D. Brown. "CAFixD: A case-based reasoning fixture design method, framework, and indexing mechanism," in Proceedings of the 24th

Computers and Information in Engineering (CIE) Conference, Salt Lake City, 28 Sept.–3 Oct., New York: ASME, 2004.

[Brost, 1996] Brost, R.C. and K. Y. Goldberg, 1996, "A complete algorithm for synthesizing modular fixtures for polygonal parts", IEEE Trans. on Robots & Auto., Vol. 12, No. 1, pp. 31-46.

[Cai, 1996] Cai, W. S. J. Hu, and J. X. Yuan. "Deformable sheet metal fixturing: principles, algorithms, and simulations," Journal of Engineering for Industry 118, pp. 318–324, 1996.

[Chou, 1989] Chou, Y. C., V. Chandru, and M. M. Barash, 1989, "A mathematical approach to automatic configuration of machining fixtures: analysis and synthesis," Journal of Engineering for Industry, Vol. 111, pp. 299-306.

[Chou, 1993] Chou, Y. C., 1993, "Automated fixture design for concurrent manufacturing planning", Concurrent Engineering: Res. & Appl., Vol. 1, pp. 219-229.

[Cook, 1989] Cook, R. D., D. S. Malkus, and Michael E. Plesha, 1989, Concepts and applications of finite element analysis, 3rd ed., John Wiley & Sons, NY.

[De Meter, 1993] De Meter EC. Selection of fixture configuration for the maximization of mechanical leverage. In Proc ASME WAM, New Orlens, LA, 1993; PED-4:491-506.

[Fang, 2002] Fang, B., R.E. DeVor, S.G. Kapoor, 2002, "Influence of friction damping on workpiece-fixture system dynamics and machining stability", Journal of Manufacturing Science and Engineering, Vol. 124, pp. 226-233.

[Fuh, 1994] Fuh, J.Y.H, A.Y.C. Nee, 1994, "Verification and optimization of workholding scheme for fixture design", Journal of Design and Manufacturing, No. 4, pp. 307-318.

[Grippo, 1987] Grippo, P. M., M. V. Grandhi, and B. S. Thompson, 1987, "The computer-aided design of modular fixturing systems", The International Journal of Advanced Manufacturing Technology, Vol. 2, No. 2, pp. 75-88.

[Han, 2003] Han, H. and Y. Rong, 2003, "Development of a variation fixture design technique", Research Report, Worcester Polytechnic Institute.

[Hoffman, 1991] Hoffman, E. G, Jig and fixture Design, 3rd Ed., Delmar, New York, 1991.

[Hurtado, 2002] Hurtado, Jose F.and Melkte, Shreyes N., 2002, "Modeling and analysis of the effect of fixture-workpiece conformability on static stability", transactions of the asme, journal of manufacturing science and engineering, May, 2002, Vol. 124, pp234-241.

[Kang, 2003] Kang, Y., Y. Rong, and J-C. Yang, 2003, "Computer-aided fixture design verification, part 1: the framework and modeling; part 2: tolerance analysis; part 3: stability analysis", International Journal of Advanced Manufacturing Technology (to appear).

[Kashyap, 1999] Kashyap, S., and W. R. DeVries. "Finite element analysis and optimization in fixture design," in Structural Optimization, pp. 193–201, Berlin: Springer-Verlag, 1999.

[Kow, 1998] Kow, T. S., A.S. Kumar, J.Y.H. Fuh, 1998, “An integrated computer-aided modular fixture design system for interference free design”, ASME IMECE, Anaheim, CA, Nov. 15-20, Manufacturing Science and Engineering, MED-Vol. 8, pp.909-916.

[Kumar, 1998] Kumar, A. S. and A. Y. C. Nee, 1995, "A framework for a variant fixture design system using case-based reasoning technique," Computer-aided Tooling, ASME WAM, 1995, MED-Vol. 2-1, pp. 763-775.

[Lee,1987] Lee, J. D. and L. S. Haynes, 1987, “Finite element analysis of flexible fixturing systems”, Journal of Engineering for Industry, 109, pp.134-139.

[Li, 1999] Li, B. and S. N. Melkote, 1999, “An elastic contact model for prediction of workpiece-fixture contact forces in clamping”, J. of Manuf. Sci. and Engr., Vol. 121, pp. 485-493.

[Liao, 2001] Liao, Y. G. and S.J. Hu, 2001, “An integrated model of a fixture-workpiece system for surface quality prediction”, Int. J. of Adv. Manufg. Tech., Vol. 17, pp. 810-818.

[Ma, 1998] Ma, W., Z. Lei, and Y. Rong, 1998, “FIX-DES: a computer-aided modular fixture configuration design system,” Int. J. of Adv. Manufacturing Tech., 1998, 14:21-32.

[Ma, 1999] Ma, W., J. Li and Y. Rong, 1999, “Development of automated fixture planning systems,” Int. J. of Advanced Manufacturing Technology, 1999, 15:171-181.

[Mani,1988] Mani M, Wilson WRD, “Automated design of workholding fixtures using kinematic constraint systhesis”, In Proc. ASME WAM, Dallas, TX, 1990; PED-47:203-18.

[Marin, 2002] Marin, R. A. and P. M. Ferreira, 2002b, “Optimal placement of fixture clamps: part 1, maintaining form closure and independent regions of form closure; part 2, minimizing the maximum clamping forces”, J. of Manuf. Sci. and Engr., Vol. 124, pp. 676-694.

[Markus, 1988] Markus, A., 1988, "Strategies for the automated generation of modular fixtures", Proc. Manufacturing Internal, 1988, pp. 97-103.

[Marsh, 1997] Marsh, E.R. and Yantek, D.S., 1997, "Experimental measurement of precision bearing dynamic stiffness," Journal of Sound and Vibration, Vol.202, No.1, pp. 55-66.

[Mazurkiewicz M, 1983] Mazurkiewicz M, W. Ostachowicz, 1983, “Theory of finite element method for elastic contact problems of solid bodies”, Computer Structure, Vol. 17, pp51-59.

[Menassa, 1990] Menassa RJ, DeVries, W. “A design synthesis and optimization method for fixtures with compliant elements”, In Proc 16th NAMRC, 1988; 437-44.

[Nee, 1991] Nee, A. Y. C. and A. Senthil Kumar, 1991, "A framework for an object/rule-based automated fixture design system", Annals of the CIRP, Vol. 40/1/1991. pp. 147-151.

[Nnaji, 1990] Nnaji, B. O., S. Alladin, and P. Lyu, 1990, "Rules for an expert fixturing system on a cad screen using flexible fixtures", J. of Intelligent Manuf. Vol. 1, pp. 31-48.

[Patricia, 1999] Patricia, J., W. Becker, and R. H. Wynn. “Using rigid-body dynamics to measure joint stiffness,” Mechanical Systems and Signal Processing 13:5, pp. 789–801, 1999.

[Pham, 1990] Pham, D. T. and A de Sam Lazaro, 1990, "AUTOFIX-an expert CAD system for jigs and fixtures", Int. J. of Machine Tools and Manufacture Vol. 30, No.3, pp. 403-411.

[Pong, 1993] Pong, P. C., R. R. Barton, and P. H. Cohen. “Optimum fixture design,” in Proceedings of the Second Industrial Engineering Research Conference, May 26–28, Los Angeles, CA, pp. 6–10, Norcross, GA: IIE, 1993.

[P. Wriggers, 1996] P. Wriggers, “Finite element methods for contact problems with friction”, Tribology International, 29(8), pp.651-658, 1996.

[Ren, 1995] Ren, Y., and C. F. Beards. “On substructure synthesis with FRF data,” Journal of Sound and Vibration, pp. 845–866, 1995.

[Rong, 1992] Rong, Y., Y. Zhu, 1992, "An application of group technology in computer-aided fixture design," Int. J. Systems Automation: Res. & Appl., Vol. 2, No. 4, pp. 395-405.

[Rong, 1997] Rong, Y. and Y. Bai, 1997, "Automated generation of modular fixture configuration design," Journal of Manufacturing Science and Engineering, Vol. 119, pp. 208-219.

[Rong, 1999] Rong, Y. and Y. Zhu, 1999, Computer-Aided Fixture Design, New York, NY, Dekker.

[Rong, 2003] Rong, Y., 2003, “Four generations of computer-aided fixture design”, Research Report, Worcester Polytechnic Insititute.

[Roy, 2002] Roy, U. and J. Liao, 2002, “Fixturing analysis for stability consideration in an automated fixture design system”, J. of Manuf. Science and Engineering, Vol. 124, pp. 98-104.

[Sen, 1990] Sen, A., and M. Srivastava, “Regression analysis: theory, methods, and applications”, New York: Springer-Verlag, 1990.

[Shigley, 1989] Shigley, J. E., and C. R. Mischke, “Mechanical engineering design”, New York: McGraw-Hill, 1989.

[Sun, 1995] Sun, S. H. and J. L. Chen, 1995, "A modular fixture design system based on case-based reasoning,” Int. J. of Advanced Manufg. Tech, Vol. 10, 1995, pp. 389-395.

[Thomposon, 1986] Thomposon, B. S. and M. V. Gandhi, “Commentary on flexible fixturing, applied mechanics review”, Vol. 39, No. 9, pp. 1365-1369.

[Trappey, 1995] Trappey, A. J. C., C. S. Su, J. L. Hou, 1995, “Computer-aided fixture analysis using finite element analysis and mathematical optimization modeling,” ASME INECE, MED v 2-1, Nov. 12-17, 1995, pp 777-787.

[Tsai, 1988] Tsai, J. S., and Y. F. Chou. “The Identification of Dynamic Characteristics of a Single Bolt Joint,” Journal of Sound and Vibration 125:3, pp. 487–502, 1988.

[Tzou, 1991] Tzou, H. S. and Y. Rong, 1991, "Contact dynamics of a spherical joint and a jointed truss-cell unit system: theory and stochastic simulation," AIAA Journal, Vol. 29, No. 1, 1991, pp. 81-88.

[Wang, 1990] Wang, J., and C. M. Liou,. “identification of parameters of structural joints by use of noise-contaminated FRFs,” Journal of Sound and Vibration Vol. 141, pp. 261-277, 1990.

[Wang, 1999] Wang, J. H., and M. J. Yang. "Problems and solutions in the parameters of mechanical joints," in the 3rd International Conference in Inverse Problem in Engineering: Theory and Practice, June 13-18, 1999, Port Ludlow, WA, U.S.A., ASME Paper No. ME 03.

[Wardak, 2001] Wardak et al, 2001, "Optimal fixture design for drilling through deformable plate workpieces – part 1: model formulation", Journal of Manufacturing Systems, Vol 20, No.1, pp23-21.

[Whitney, 1999] Whitney, D. E., R. Mantripragada, J. D. Adams and S. J. Rhee, 1999, "Designing assemblies", Research in Engineering Design, Vol. 11, pp. 229-253.

[Wu, 1997] Wu, Y., Y. Rong, T. Chu, 1997, "Automated generation of dedicated fixture configura-tion," Int. J. Computer Application in Tech., Vol. 10, No. 3/4, pp. 213-235.

[Wu, 1998] Wu, Y., Y. Rong, W. Ma, and S. LeClair, 1998, "Automated modular fixture design: part 1, geometric analysis; part 2, accuracy, clamping, and accessibility analysis," Robotics and Computer-integrated Manufacturing, 14:1-26, 1998.

[Xiong, 1998] Xiong, C. and Y. Xiong, 1998, "Stability index and contact configuration planning for multifingered grasp", Journal of Robotic Systems, Vol. 15, No. 4, pp. 183-190.

[Yang, 1998] Yang, B. D., M. L. Chu, and C. H. Menq. "Stick-slip-separation analysis and non-linear stiffness and damping characterization of friction contacts having variable normal load," Journal of Sound and Vibration 210:4, pp. 461–481, 1998.

[Yang, 2003] Yang, T., S.-H. Fan, and C.-S. Lin. "Joint stiffness identification using FRF measurements," Computers and Structures 81, pp. 2459–2566, 2003.

[Yeh, 1999] Yeh, J. H., F. W. Liou, 1999, “Contact condition modeling for machining fixture setup processes”, Int. Journal of machine tools & manufacture, Vol. 39, pp. 787-803.

[Zhu, 1993] Zhu, Y., S. Zhang, Y. Rong, 1993, "Experimental study on fixturing stiffness of T-slot based modular fixtures," NAMRI Transactions XXI, NAMRC, Stillwater, OK, May 19-21, pp. 231-235.

[Tao, 1999] Z.J. Tao, A.S. Kumar and A.Y.C. Nee, “Automatic generation of dynamic clamping forces for machining fixtures”, International Journal of Production Research, vol.37, No. 12, pp. 2755-2776,1999.